Editorial Board

PUBLISHER & EDITORIAL OFFICE
University of Oradea Editing House,
Str. Universitatii Nr. 1, Oradea, jud. Bihor, România, Zip code: 410087, Tel.: 00-40-259-408171, Fax: 00-40-259-408404
ISSN: 2067-5534 (print version)

The Journal of Sustainable Energy (JSE) had its first appearance under this name in 2010. The history of JSE is the following: is formed in 2010 by transforming of 1993-2009 Analele Universitatii din Oradea. Fascicula de Energetica, 1224-1261. Which superseded in part (1991-1992): Analele Universitatii din Oradea. Fascicula Electrotehnica si Energetica (1221-1311); Which superseded in part (1976-1990): Lucrari Stiintifice - Institutul de Invatamant Superior Oradea. Seria A, Stiinte Tehnice, Matematica, Fizica, Chimie, Geografie (0254-8593);

The Journal of Sustainable Energy (JSE) publishes original contributions in the field of the following topics:

- Energy engineering education
- System reliability and power service quality
- Generation of electric and thermal power
- Energy policy and economics
- Energy development (solar power, renewable energy, waste-to-energy systems)
- Energy systems operation
- Energy efficiency, reducing consumption for conservation of energy
- Energy sustainability as related to energy and power production, distribution and usage
- Waste management and environmental issues
- Energy infrastructure issues (power plant safety, security of infrastructure network)
- Energetic equipments

The articles quality increases with every issue. Apart from its improved technical contents, a special care is given to its structure. The guidelines for preparing and submitting an article were modified and developed in order to meet high quality standards requirements. With every passing issue the peer-review process was developed too, being now a double-blinded peer-review process.

Authors who wish to submit a manuscript to the Journal of Sustainable Energy (JSE) are kindly asked to send their manuscripts as DOC and PDF format to JSEoradea@yahoo.com, according to the formatting instructions. Once the manuscript is submitted, the authors will shortly receive a feedback regarding the status of their submission. As the review process is completed, the author will be informed about the reviewers' comments and the changes the paper should suffer in order to satisfy the journal quality requirements.

Journal of Sustainable Energy JSE is covered/indexed/abstracted in:

- Index Copernicus
- Ulrich's Update - Periodicals Directory
- DOAJ - Directory of Open Access Journals
- EBSCO Publishing - EBSCOhost Online Research Databases
- Engineering village (Pending)

The JSE may be purchased based on annual subscription (4 issues) at the following prices: paper – 50 □ , electronic – 20 □, or individually (each number) at the following prices: paper - 20 □, electronic – 8 □. To purchase the complete "control" standard (www.energy-cie.ro) and submitted electronically or by fax. In order to generate the invoice (www.energy-cie.ro) is transmitted to the applicant. After payment of the amount stated in the bill the applicant receives and invoice numbers ordered JSE.

Publishing House name/address:
University of Oradea Editing House
Universitatea din Oradea, Universitatii Str., No. 1, 410087, Oradea, Bihor, Romania

- ISSN: 2067-5534
- Tel.: 00-40-259-408171 (231, 288)
- Fax: 00-40-259-408404
- Place of publishing: Oradea, Romania
- Year of the foundation of publication in domain of power engineering: 1976
- Releasing frequency: 4 / year
- Language: English

CONTENTS

RELIABILITY AND SYSTEMS ENERGY QUALITY SERVICES

RENEWABLE SOURCES OF ENERGY. SUSTAINABLE ENERGY TECHNOLOGIES

EVOLUTION OF POWER ELECTRIC SYSTEMS TRANSPORT AND DISTRIBUTION. ENERGY SYSTEM'S PERFORMANCE

MARKET AND STOCK-MARKET OF POWER. MANAGEMENT OF POWER SYSTEMS

VIRTUAL INSTRUMENT FOR POWER QUALITY ASSESSMENT

GHEORGHE D., CHINDRIS M., CZIKER A., VASILIU R.
Technical University of Cluj – Napoca, C. Daicoviciu no.15, Cluj – Napoca
Daniel.Gheorghe@eps.utcluj.ro

Abstract - The paper presents a Virtual Instrument (VI) for Power Quality (PQ) events monitoring and analysis designed in LabView. The instrument is designed to detect harmonics, interharmonics, dips, swells and unbalance and it also performs a distortion classification prior to the identification step. The harmonics and interharmonics are detected with high accuracy using a time domain technique based on linear algebra. Dips and swells are identified using the wavelet technique and the unbalance analysis is based on the symmetrical components method. Time-frequency representations (TFR) are obtained for distortion classification by performing the Stockwell Transform (ST) and they are fed to a pattern recognition system.
The normal operation limit is previously established on empirical expert knowledge and then a few measurements are performed on an experimental rig. The measurements reveal the accuracy of the instrument and its high online analysis performance.

Keywords: distortions analysis, time-frequency representations, self organising maps.

1. INTRODUCTION

Electric power quality is a term that has gained more importance over the years. The increasing use of sensitive and non-linear loads, the deregulation of utilities, and the increased interconnections in power systems has led to an increased need to solve and prevent power quality problems [1]. Dugan [2] defined power quality as "Any power problem manifested in voltage, current, or frequency deviations that results in failure or malfunction of customer equipment." Power quality results in equipment malfunction and premature failure and has financial consequences on utilities grids, their customers and suppliers of load equipment. Thus, monitoring power quality has become a necessity for fast identification and correction power quality problems. Signal processing methods for power quality analysis comprise Fourier Transform (FT), Park's Vector Approach, Kalman filters and time-frequency analysis methods such as Short Time Fourier Transform (STFT), Wavelet Transform (WT) and Stockwell Transform (ST).

Stationary signals are those whose statistical properties do not change with time while the characteristics of non-stationary signals vary with time [3]. Fourier Transform (FT) determines the spectral components of a signal without providing the times at which the different frequency components occurred. FT produces a time-averaged spectrum which is inadequate to track the changes in signal magnitude, frequency and phase with time. Thus, non-stationary signals are better processed in the time-frequency plane by using techniques like STFT, WT and ST.

For non-stationary signals like power quality disturbance signals, where the frequency content change with time, STFT has got a fixed resolution over the time-frequency plane and does not recognize the signal dynamics properly due to the limitation of a fixed window width chosen a priory [4,5].

WT is incapable of providing accurate results under noise conditions [5]. Moreover, if an important disturbance frequency component is not precisely extracted by the WT, the classification accuracy using artificial intelligence techniques may be limited [4]. Also, there is an absence of phase information in WT and the time-scale plots provided by WT are difficult to interpret [3].

Therefore ST which combines the elements of STFT and WT and which performs multiresolution time-frequency analysis is a better candidate for power quality distortion classification.

Time-frequency representations are then analysed with a self-organising map that extracts key features for each distortions.

The paper continues to describe the power quality analysing system where the harmonics and interharmonics are studied with a novel time-based parametric method.

Voltage dips are monitored by the means of the WT and the RMS method for dip amplitude computation.

The paper also analysis the flicker effect and transients. The first is studied with a method that extracts the modulating component parameters from the spectral estimation algorithm used for interharmonics estimation and the second is extracted from the ST time-frequency representations.

In the last decades power quality analysis became a very important issue in power systems so the necessity of accurate parameters measurement has grown in importance too [6]. Virtual instrumentation will play an important role among the power quality monitoring systems. The main advantage is that it is much cheaper than the standard equipment and it is much more flexible.

2. VIRTUAL INSTRUMENTATION

In the recent years, analysis of electromagnetic distortions in power systems requires a significant volume of data and knowledge. Therefore, using computers, new analysis methods and artificial intelligence techniques became a necessity.

The virtual instrument developed in this paper was designed in LabView and it drives a PCMCIA data acquisition board (DAQ-NI-6008). Fig. 1 shows the instrument organization where part a describes the input options followed a sampling action (Fig. 1. b.).

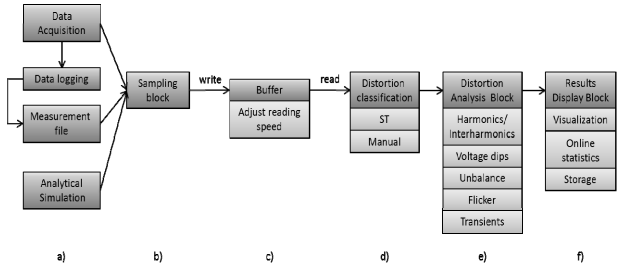

Fig. 1 - Virtual instrument structure

The influx of data can be inserted either in an analytic way, for testing purposes, from the acquisition card (Fig. 2.) or from a previously made recording.

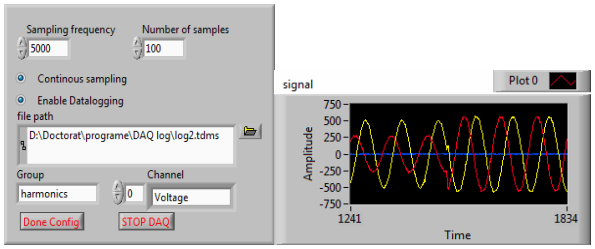

Fig. 2 - Data aquisition subroutine

LabView environment is very efficient for data aquisition. It offers all the necessary functions to develop a data aquisition virtual routine.

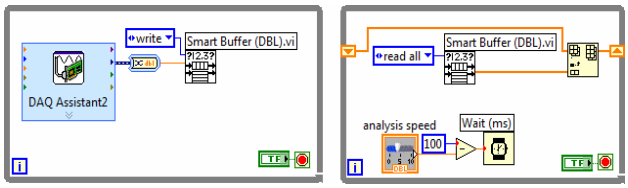

Fig. 3 - Virtual buffer

First, a smart buffer was programmed (Fig. 3). This buffer performs a very accurate data synchronization (Fig. 1.c.) with the acquisition card and the desired reading speed can also be adjusted.

A brief description of the block d performs a distortion classification based on the Stockwell transform and self-organizing maps prior to the distortion analysis found in block e. The last block (Fig. 1.f.) is the user interface of the instrument where the results and statistical data can be visualized.

3. DISTORTION CLASSIFICATION

At present more and more power electronic elements and nonlinear load are used in industry application which brings heavy pollution to power network. The correct classification of power disturbance is the premise and basis of the power quality analysis and evaluation.

3.1. Time-frequency analysis

S Transform, developed by Stockwell, is a powerful time-frequency multi-resolution analysis signal processing tool. ST provides a time-frequency representation (TFR) with a frequency dependent resolution. The window width varies inversely with frequency and thus, ST produces high time resolution at high frequency and high frequency resolution at low frequency as presented in Fig. 4.

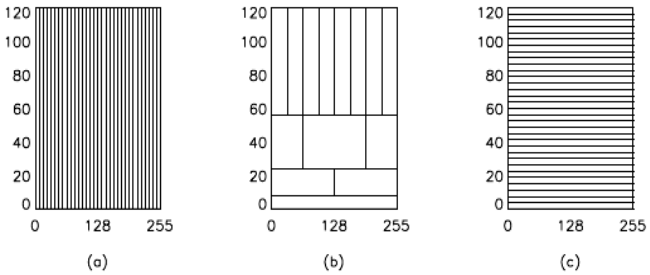

Fig. 4 - The resolution of time frequency space when the signal is viewed: a) as a time series, having precise time resolution, and no frequency resolution. b) in the ST representation, having frequency dependent resolution. c) as a spectrum, having no time resolution, and precise frequency resolution.

The ST of a discrete time series *h[kT]* is given by:

$$S\left[jT, \frac{n}{NT}\right] = \sum_{m=0}^{N-1} H\left[\frac{m+n}{NT}\right] e^{-\frac{2\pi^2 m^2}{n^2}} e^{\frac{i2\pi mj}{N}} \qquad (1)$$

where *j, m* and *n = 0,1,...,N-1* [7].

In this work, four single commonly occurring PQ disturbances namely voltage dip, harmonics, transient and flicker, as well as the pure sinusoidal waveform are considered. The following plots show some of the essential information that can be obtained from the modified ST.

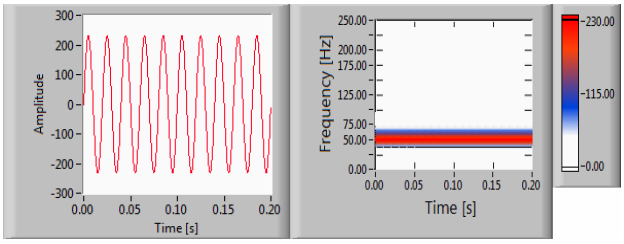

Fig. 5 - Pure sine wave and its feature waveforms

ISSN 2067-5534 © 2012 JSE

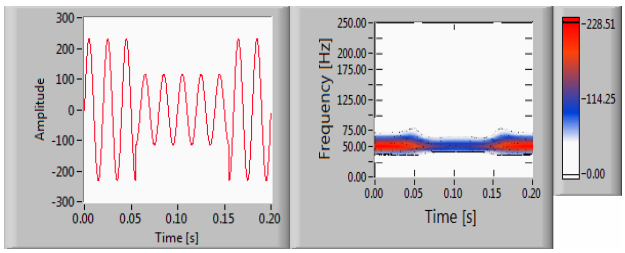

Fig. 6 - Instantaneous voltage dip and its ST

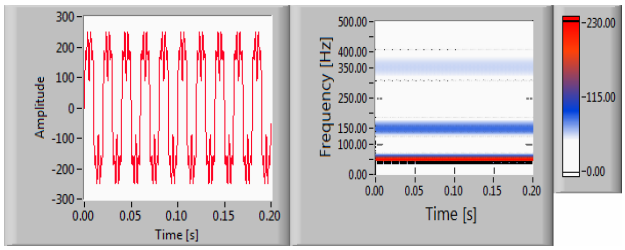

Fig. 7 - Voltage harmonics and its ST

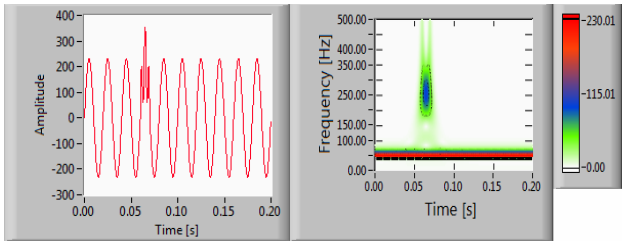

Fig. 8 - Low frequency transient and its ST

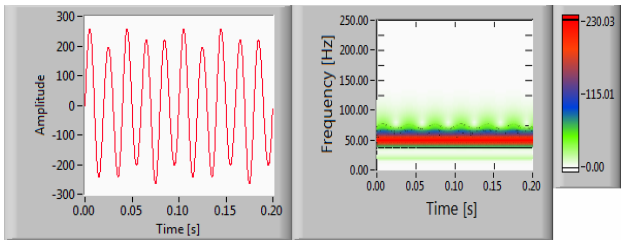

Fig. 9 - Voltage flicker and its ST

From the ST, the time-frequency, time-amplitude and frequency-amplitude plots can easily be obtained. These plots enable the detection, localization and visual classification of PQ disturbances.

3.2. Self-organising maps (SOM)

The features required for PQ disturbance classification are extracted from the S-matrix. The features extracted are used to train a self-organizing map that allows automatic distortion classification. In this work, three features are extracted and they are:

1) Standard deviation (SD) of the data set comprising the elements of maximum magnitude from each column of the S-matrix.

2) Energy of the data set comprising the elements of maximum magnitude from each column of the S-matrix.

3) Mean of the data set constituting the elements of maximum magnitude from each row of the S-matrix.

Clustering techniques come under the concept of competitive learning. Clustering is one of the most important unsupervised training techniques. Basically it is a process by which objects that are closely related to each other are grouped. Similar objects form groups and they are dissimilar from other groups.

a) SOM architecture

In this paper the topology of the SOM network is a 40x40 neurons lattice and 3 input vector space as shown in Fig. 10

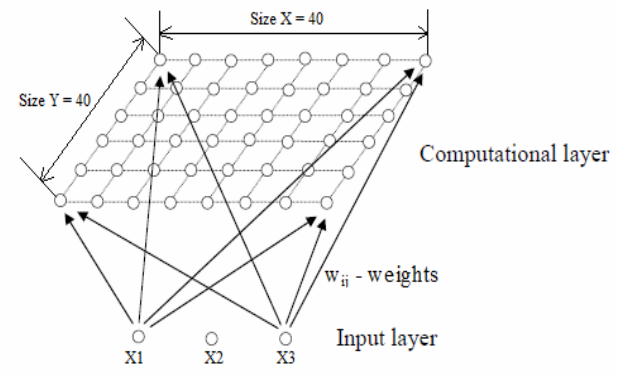

Fig. 10 - SOM topology

b) SOM algorithm

The self-organization process involves four major components:

Initialization: All the connection weights are initialized with random values scaled between 0 and 1. Fig. 11 rescales the weights on the interval 0-255 and plots them on an RGB color map for better visualization.

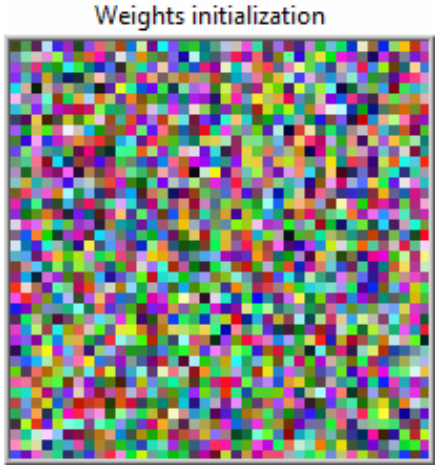

Fig. 11 - 40x40 weight initialization lattice

Competition: For each input pattern the neurons compute their respective values of a *discriminant function* which provides the basis for competition. The particular neuron with the smallest value of the discriminant function is declared the winner.

Cooperation: The winning neuron determines the spatial location of a topological neighborhood of excited neurons, thereby providing the basis for cooperation among neighboring neurons.

Adaptation: The excited neurons decrease their individual values of the discriminant function in relation to the input pattern through suitable adjustment of the associated connection weights, such that the response of the winning neuron to the subsequent application of a similar input pattern is enhanced.

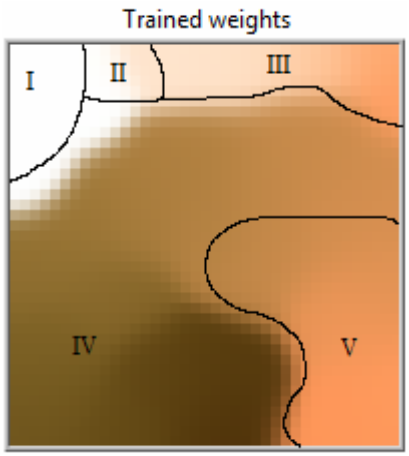

Fig. 12 - SOM weights after 1000 cycles

Cycle by cycle the weights are updated until an optimum distribution is reached. This distribution (Fig. 12.) delimitates separate areas corresponding to each distortion:

Zone I – pure signal
Zone II – subharmonic region
Zone III – harmonics region
Zone IV – changes in RMS (dips)
Zone V – transients region

c) SOM testing

Once an optimum distribution map was achieved, testing can be performed using analytically created distortions.

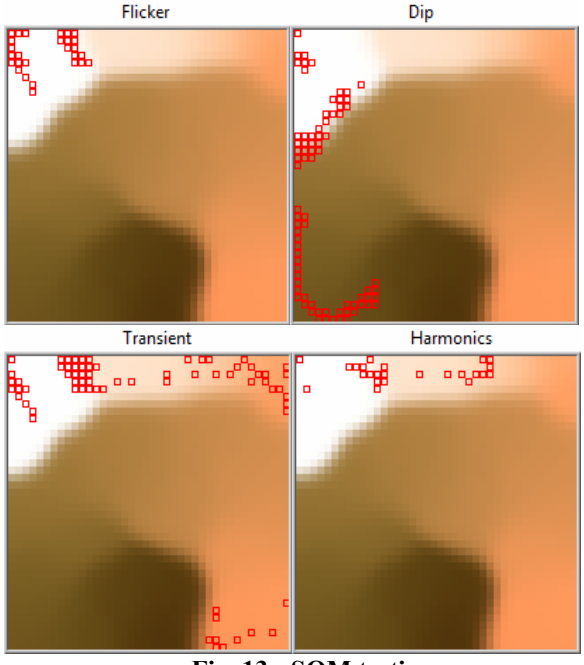

Fig. 13 - SOM testing

The signal considered in this paper has 10 fundamental cycles sampled at 5000Hz, therefore, the total length of the analysis window is 1000 samples. Computing the S-matrix and extracting the three corresponding features, the input vector size will be 3x500 so it will plot 500 hits on the SOM map.

Signals shown in Fig. 5-9 were used and since they contain different distortions, they correspond to different regions on the map (Fig. 13). This feature allows accurate distortion classification.

4. DISTORTIONS ANALYSIS

As soon as the distortions are classified by the self-organizing maps, the instrument triggers the corresponding analysis subroutine.

4.1. Harmonics and interharmonics analysis

The real-time performance of a spectral estimation algorithm depends not only on its computational efficiency but also on its ability to obtain accurate estimates from short signal segments. Here, the system estimates harmonics and interharmonics with a time based method, assessing a parametric model of the signal as in equation (1) where *y(t)* represents the sampled signal and *n(t)* the noise.

$$y(t) = \sum_{i=1}^{M} A_i \exp(j\omega_i t) + n(t);\ 0 \le t \le T \qquad (2)$$

The parametric model of is written in matrix form and following a strict linear algebra algorithm, the instrument performs spectral estimation.

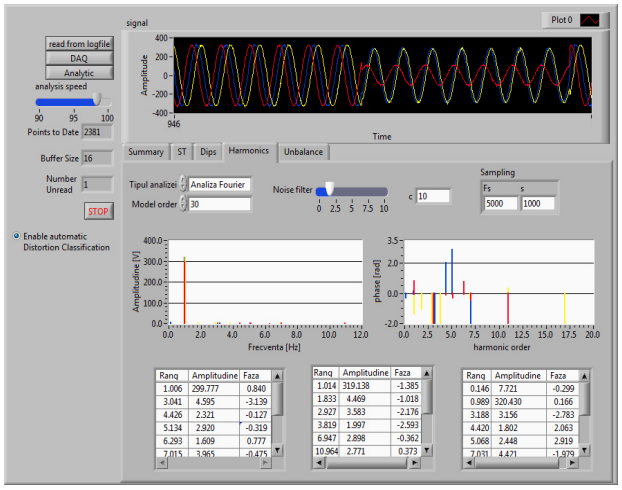

Fig. 14 - Online harmonics/interharmonics analysis subroutine

The instrument approximates the frequency, magnitude and phase of the harmonics/interharmonics, on each phase, every 10 cycles of fundamental. The front panel of the online subroutine in presented in Fig. 14.

4.2. Dips analysis

There are various methods of dips analysis in the current literature. The classic method is based on a RMS plot of the signals every half-cycle, other methods require a high amount of computational time as the recursive methods like the Kalman filters. However, these methods seem to have problems in noisy conditions and long response times for control purposed. The subroutine developed implements the wavelet transform for fast initial and final time of dip computation while the amplitude of the sag is computed according to the classic RMS method.

ISSN 2067-5534 © 2012 JSE

The wavelet transform is described as:

$$W(\tau,d)=\int_{-\infty}^{\infty}h(t)w(t-\tau,d)dt \qquad (3)$$

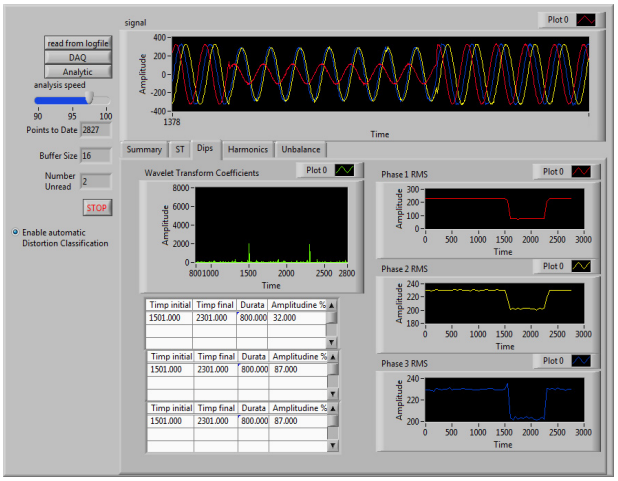

Fig. 15 - Online dips analysis subroutine

Fig. 15. shows the front panel of the online dips analyser subroutine under real operation conditions. It displays the three phase sampled signal acquired from the power systems, a plot of the wavelet coefficients and the dips parameters on each phase.

4.3. Flicker effect analysis

Current standards present the flicker analysis implying a filter cascade that extracts the modulating waveform frequency and amplitude. The last two blocks in Fig. 16. compute the flicker parameters, respectively the long and short term flicker.

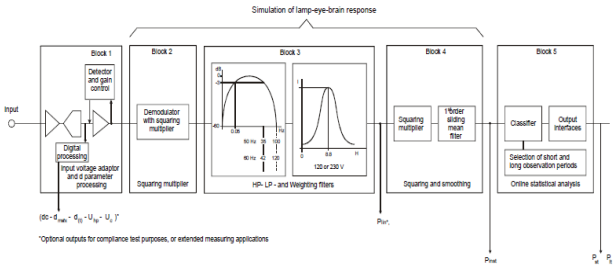

Fig. 16 - Flicker meter functional scheme - IEC 61000-4-15

The drawback of the method imposed by the IEC standard is the wide analysis window that it requires. Signals in power systems are time-variable and a stationary requirement of 500 cycles is almost impossible to achieve in real operation conditions. The method proposed here replaces the filter cascade method with a spectral pairing method. It has been observed that the flicker effect produces a particular spectral pattern. The modulating component lies around the fundamental, seen as a pair of subharmonics – interharmonics components (Fig. 17.).

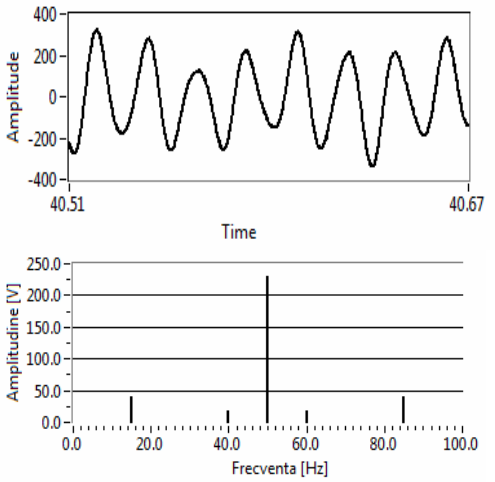

Fig. 17 - Two components flicker signal and spectrum

Using the method developed under the interharmonics analysis block, these components can be carefully extracted from the 10 cycles.

4.4. Transients analysis

Transient analysis has been an issue for a very long time as the phenomena is very short and hard to accurately detect and measure. Classic methods like the ones implying the Fourier transform fail due to severe spectral leakage and therefore, time-frequency analysis is the best tool to locate such distortions in frequency and time.

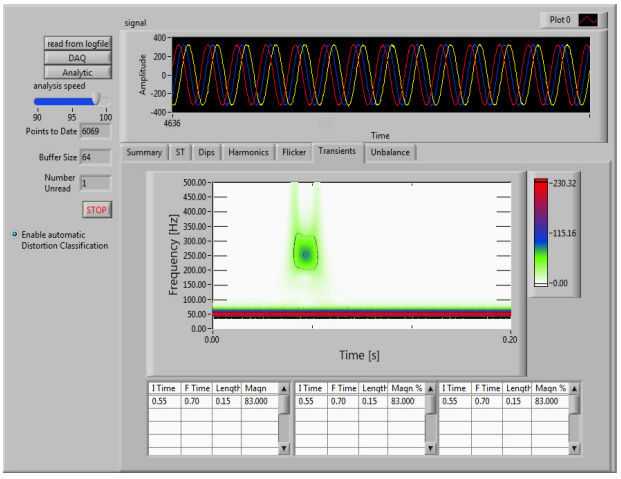

Fig. 18 - Online transients analysis subroutine

The LabView system developed (Fig. 18.) collects the transient's information from the ST's time-frequency representations since the transform provides a very good time-frequency resolution and it is computed in the distortions classification step anyway.

5. CONCLUSION

This paper describes a virtual instrument designed to analyse the most common power quality disturbances.

In this work, an S-Transform based process is proposed for power quality disturbances recognition. Thus it is suitable for an online power quality disturbance

classification system where a very large number of waveforms can be captured and analysed in a very short time interval.

The S-transform performs multiresolution analysis on a time varying signal as its window width varies inversely with frequency. This gives high time resolution at high frequency and high frequency resolution at low frequency. Since power quality disturbances make the power signal a nonstationary one, the S-Transform can be applied effectively. Together with the self-organising maps, the system performs a distortion classification in just a few milliseconds. This preidentification reduces the computational effort since the whole system doesn't analyse the signal for distortions that are not present.

Harmonics and interharmonics are computed with a model based algorithm in time. It can approximate with high accuracy the real harmonics or interharmonics even if their frequencies are very close. Based on simple principle, the same algorithm is effectively used to extract the flicker modulation waveform frequency and amplitude parameters.

In the last part, the ST is used again for transient analysis.

6. ACKNOLEDGEMENT

This paper was supported by the project "Doctoral studies in engineering sciences for developing the knowledge based society-SIDOC" contract no. POSDRU/88/1.5/S/60078, project co-funded from European Social Fund through Sectorial Operational Program Human Resources 2007-2013.

REFERENCES

[1]. Kennedy, B.W., *Power Quality Primer*. New York: McGraw-Hill, 2000.
[2]. Dugan, R.C. et al., *Electrical Power Systems Quality*. 2nd ed. USA: McGraw-Hill, 1996.
[3]. George, N.V., *S transform: Time Frequency Analysis and Filtering*. Thesis (MTech). National Institute of Technology Rourkela, 2009.
[4]. Chikuri, M.V. and Dash, P.K. *Multiresolution S-Transform-Based Fuzzy Recognition System for Power Quality Events*. IEEE Transactions on Power Delivery, 19(1), pp. 323-330, 2004.
[5]. Samantaray, S.R., *Power System Events Classification using Pattern Recognition Approach.* International Journal of Emerging Electric Power Systems, 6(1), pp. 1-16, 2006.
[6]. Gheorghe, D., Chindriş, M., Cziker, A., Vasiliu, R. B., *Online Power Systems Harmonics/Interarmonics Analysis* , Conferința Internațională MPS 2011, editția a IV-a, 17-20 Mai, Cluj-Napoca, România
[7]. Stockwell, R.G., *S-Transform Analysis of Gravity Wave Activity from a Small Scale Network of Airglow Imagers*. Thesis (PhD). The University of Western Ontario, 1999.
[8]. Stockwell, R.G., Mansinha, L., *Localization of the Complex Spectrum: The S Transform*. IEEE Transactions on Signal Processing. 44(4), pp. 998-1001, 1996.
[9]. Reddy, J.B., Power System Disturbance Recognition Using Wavelet and S-Transform Techniques. International Journal of Emerging Electric Power Systems. 1(2), pp. 1-14., 2004.
[10]. Gheorghe, D., .a., *Signal Analysis in Polluted Power Networks*, CIE 2010, 27-28 May 2010, Oradea, Romania.
[11]. Portnoff, M.R., *Time-frequency representation of digital signals and systems based on short-time fourier analysis.* IEEE Transactions on Acoustics, Speech, and Signal Processing, 1980.
[12]. Bollen, M., *Signal Processing of Power Quality Disturbances*, IEEE Press Series on Power Engineering, ISBN-13 978-0-471-73168-9, United States, 2006.
[13]. Neumann, T., Feltes, C., Erlich, I. *Development of an Experimental Rig for Doubly-Fed Induction Generator based Wind Turbine,* IEEE Transactions on Signal Processing, MEPS, September 20 - 22, 2010, Wroclaw, Poland
[14]. Ouibrahim, H., *Matrix pencil approach to direction finding*, IEEE Transactions on Acoustics, Speech and Signal Processing, Aprilie 1988, pp. 610-612.
[15]. Gantmacher, F.R., *Theory of Matrices,* Vol. 1, New York, 1960.
[16]. Hanzelka, Z., Bien, A., *Perturbații de tensiune: Măsurarea nivelului de flicker,* AGH University of Science and Technology, Octombrie 2005
[17]. Gheorghe, Şt., ş.a. Monitorizarea calității energiei electrice, Editura Macarie, Târgovişte, 2001
[18]. ***IEC 61000-4-15 Ed.1: Electromagnetic compatibility (EMC) - Part 4- 15: *Testing and measurement techniques - Flickermeter - Functional and design specifications*, Noiembrie 2002.
[19]. *** Ghid de Aplicare – Calitatea Energiei Electrice, *Armonici Interarmonici*, http://www.sier.ro/
[20]. Barros, J., *A virtual measurement instrument for electrical power quality analysis using wavelets,* Measurement 42, 2009, pp. 298–307.
[21]. Gheorghe, D., Cziker, A., Vasiliu, R. B., *Estimarea semnalelor interarmonice în sisteme electroenergetice*, Masa Rotundă – Calitatea Energiei Electrice, 30 Noiembrie, Bucureşti, România.

 ISSN 2067-5534

SYNTHESIS STUDY ON THE OPERATIONAL RELIABILITY OF AN URBAN TRANSPORT SYSTEM USING ELECTRICALLY DRIVEN TRAMS

FELEA I.[*], CSUZI I.[**], SECUI C.D.[*], BENDEA G.[*]
[*]University of Oradea, University Street, No. 1, Oradea
[**]Oradea Public Transport Company, (OTL S.A.)
ifelea@uoradea.ro

Abstract - The paper is structured in five parts. The first part is a brief presentation of the structure and the functioning of the urban transport systems using electrically driven trams (EUTS), based on which, the equivalent reliability diagrams of these systems are presented. Further on, based on the analysis of operational reliability, one can identify and there are defined the time characteristics and the transport capacity of EUTS. In the third part there are defined and analytically determined the safety and the availability of EUTS. The paper also contains results of a comprehensive study of case on EUTS from Oradea, results on which one can calculate, in the end, the availability indicators of the system. The last part of the paper contains the results and conclusions of the carried out analysis.

Key words: operational reliability, electric traction, indicators, trams.

1. INTRODUCTION

Applying the concept of sustainable development [1] is one of the most important priorities of modern society. In this context, in large urban areas, urban transport of people - in all its aspects - is a priority area of great importance and implications. Outstanding contribution to transport in general, especially of urban public transport (UPT), environmental pollution, especially of the atmosphere by greenhouse gases is well known [2]. Sharpening pollution in big cities is a major problem, which may decide even the fate of transport strategies, implicitly the UPT. In these circumstances, in the perspective of sustainable development, it is essential that local city fathers to consider:

- Priority development of UPT, which will reduce car traffic with all their implications;
- The developing, especially of the urban public transport with electric traction, the transport system that does not pollute, is relatively quiet and increases the safety in circulation.

Specific problems of urban public transport systems are largely reflected in the literature. Much of the work aimed at the UPT systems performance measured by efficiency, service quality and environmental impact. In [3] one can identify the factors that influence the demand for UPT insisting mainly on service quality, and in [4] a methodology for development is proposed and exemplified to elaborate the quality studies of the UPT system. Detailed methodology for assessing the quality of transport service is in [5], applying decisive impact factors such as availability, comfort and convenience. Availability of transport is exanimate in terms of service frequency and service coverage zone. One analyzed the comfort and convenience level for an UPT system using busses. The effectiveness of a specific UPT system is analyzed in [6,7]. Thus, in [6] the effectiveness of the UPT systems of 12 cities from Europe are analyzed, and 7 from Brazil. Based on these results the authors conclude for the UPT systems efficiency of only nine cities in Europe and one in Brazil, the inefficiency is due mainly to social interference. Using recorded data from 15 European UPT systems in [7] one aims to answer three questions identifying the essential performance of transport systems: the impact of design methodology, the impact of organization and the UPT system performance.

This paper is part of the concerns mentioned above, but stands firmly by these, being dedicated to determine the availability of an urban public transport system using electrically driven trams (EUTS) and to exemplify how to illustrate the evaluation of a specific EUTS.

2. SHORT PRESENTATION OF EUTS

EUTS functional aspect can be regarded and treated as a result of the interconnection of three subsystems (Fig.1), [8,9].

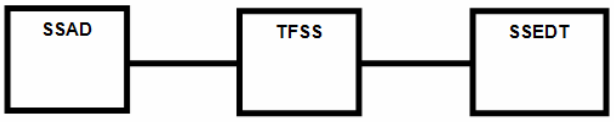

Fig. 1 - Structural block diagram of EUTS

Where:
SSAD - subsystem of electrical values adaptation of the electro-energetic system level (EES), the electrically driven trams (EDT) need;
TFSS - transfer subsystem (distribution) of electric energy (EE) between SSAD and EDT, including: bars of recovery stations (RS) and DC power supply grid from RS, including sections of the injection (SI), the contact sections (CS) and rails (R);

SSEDT- subsystem of powered trams covering the entire vehicle, actuators, with the transfer of EE (pantograph), with speed control equipment (controller, inverter, converter), with own facilities (lighting, thermal comfort) and other specific equipment and facilities.

UPT using EDT in Oradea started in 1906. EUTS of Oradea, operated by SC "Oradea Local Transport SA" (OTL), has the following features:

- Double rail length divided into five zones (Fig. 2): 39.86 km.
- The installed capacity in the five recovery substations: 5550 kVA.
- The total EDT: 73 of which, for maximum carrying capacity is required 44 pieces.
- Types of EDT used:
  → Produced by TATRA (Czech Republic), with DC motors without energy recovery, type KT4D (20 pieces) and T4D + B4D (43 pieces) in circulation, and two pieces of T4D processed for snow cleaning, as so in circulation a total of: 20 + 43 = 63 pieces

→ Produced by SIEMENS (Austria) 151 ULF (Ultra Low Floor): 10 pieces.

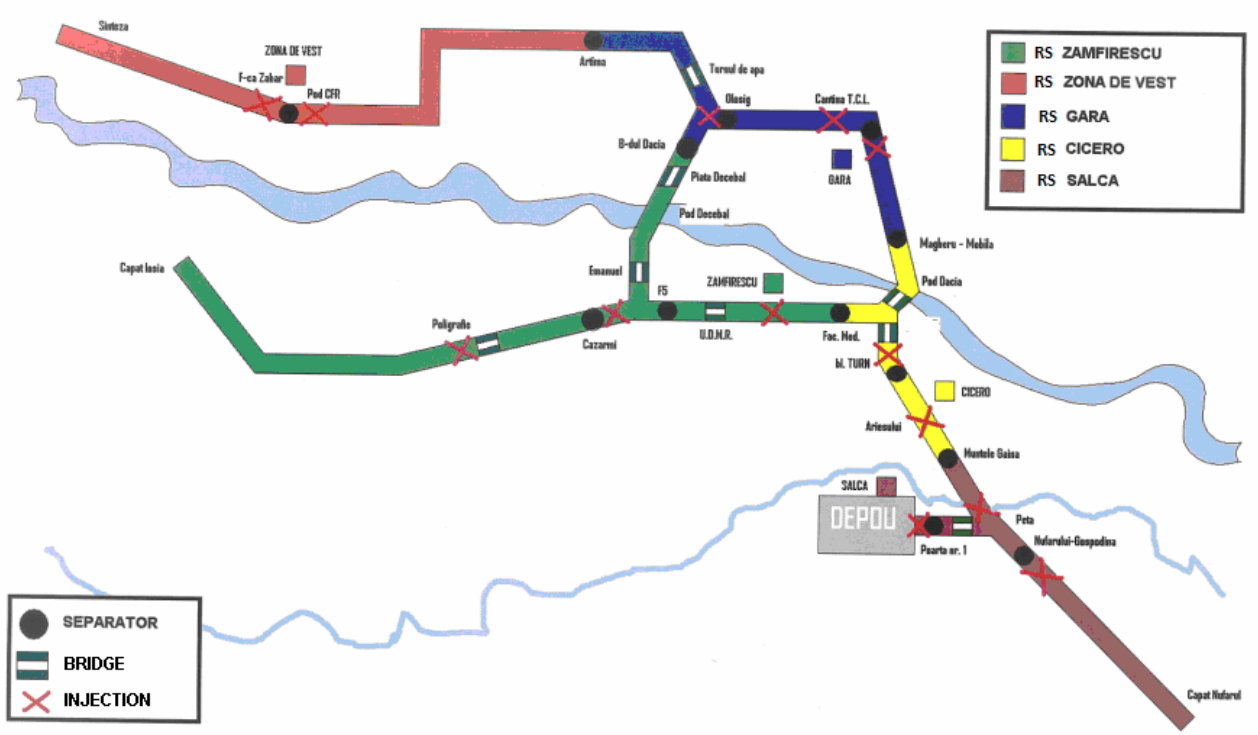

Fig. 2 – The zoning of TFSS at OTL

→ Average number of passengers served daily: 22,761.

- Average distance travelled 2,405,000 km a year;
- Average daily consumption of EE: 8759.8 MWh;
- Average cost per passenger and km EE: 0.055 LEI / passenger x km = 0.012 Euro/passenger x km;
- Average cost of operation: 22,715 thousand lei;
- Average profitability index: 1,128.

3. THE STUDYS OBJECTIVE AND WORKING METHOD

Operational reliability is determined in actual operating conditions [10,11,12,13]. In some cases, such as those of EUTS specific power equipment, laboratory testing and tracking are wasteful exploitation that remain the only source of information on reliability. Information on equipment reliability is useful both for users (maintenance optimization) and for producers (the purpose of corrections in design and manufacture).

The study has as main objective:

- Determine of EUTS equipment and installations operational reliability (OR);
- Hierarchy of equipment and facilities according to their reliability;
- Identify causes and typical modes of failure;
- Determining values for basic indicators of reliability;
- Identify laws that shape the distribution of random variables "for proper functioning time" and "for maintenance".

The applied working methodology was that, typical for such studies [7,8,9] and is based on careful monitoring of operational behaviour of the equipment, recording and event characterization, processing and interpretation of results. At OTL - EUTS, events recorded after equipment failure and during daily maintenance activities (DM), technical maintenance (TM) and prophylactic measurements.

Maintenance and operation staff of EUTS recorded in the books and records specific events, set in the OTL. Going through these documents held, first, information of

ISSN 2067-5534 © 2012 JSE

interest to characterize EUTS - OR components in tables with the following structure [9]:

Table 1 – Synoptic events recorded EUTS components

Nr. crt.	Component of EUTS structure	Date and time of the produced event	Event description [fault element, fault method, causes]	Type and work sheet number	Maintenance time [minutes]
1	2	3	4	5	6
1	.		.		.
2	.		.		.

Systematization array of events was recorded on the three subsystems of EUTS: SSAD, TFSS and SSEDT. Please note that the number of events recorded with reference to SSAD and TFSS components is much lower than for SSEDT, where the level of information details is greater. This situation derives from the legal provisions [9], which are more stringent on monitoring the operation of EDT. Since January 2011, for an analysis of the maintenance of EDT, the internal decision OTL was to increase the detail of the EDT operation behaviour records, realizing, in addition to card occurrences (Table 1) and monthly summary, the following documents:

- Report maintenance activities;
- Synoptic situation of repeated failure for EDT;
- States for EDT;
- Failure for EDT;

In [9] one can find examples of summary tables above documents, which are intermediate between the books and records established and operating maintenance, charts and indicators that has been obtained by statistical processing of events based on statistical data recorded in the [2005 - 2010] period and the first half of 2011 for EDT.

Assessment results are presented in the following levels:

- Interpretation of data concerning events;
- Distribution of random variables and fundamental indicators of reliability of EDT;
- Global indicators of reliability of EDT.

4. STATISTICAL DATA INTERPRETATION ON RECORDED EVENTS AT OTL UTSUED.

Results were obtained by processing primary information is presented successively, with reference to three of EUTS - SS.

4.1. Results obtained on SSAD level

SSAD components are subject to the preventive maintenance (PM) works (technical revision) at intervals of about six months. From existing records in the OTL results a few unwanted events, followed by corrective maintenance work on the elements of SSAD structure. Summary of events is shown in table 2.

For comparison, the number of occurrences of lack of power supply in the national energetic system (NES) "unwanted event is given in table 2, which estimates the level of safety associated with the NES on the connection points of the five RS.

Table 2 – Summary of events followed by corrective maintenance (CM) on SSAD components

Nr. Crt.	The name of the unwanted event	YEAR/ Number of events [υ(T_A)]					TOTAL on 5 years
		2006	2007	2008	2009	2010	
1.	Shutdown due to overload or wagon fault	57	65	52	43	922	1139
2.	Lack of communication (computer modem)	24	35	17	14	166	256
3.	No voltage supply of the NES (6kV)	7	18	16	13	11	65
4.	Switch coil lock	14	7	6	3	-	30
5.	Injection Cable Fault	5	7	3	1	7	23
6.	Advanced wear of switch contacts	4	5	4	2	-	16
7.	Diode protection burnout	4	-	4	2	1	11
8.	Switch coil burnout	3	1	2	2	-	8
9.	Pierced diode	-	-	2	2	-	4

Number of events recorded and incomplete information on the characterization of events allows us to make a more complete statistical processing, to determine OR indicators such as total length of defects

during the analysis [$\beta(T_A)$], the average time of proper operation [MTBF], average corrective maintenance time [MTCM(MTTR)], λ, μ.

4.2. Results obtained on TFSS level

TFSS components are very important both for security and availability EUTS, especially since there are no reservations in this subsystem. Therefore, TFSS components are subject to rigorous periodic inspections. In [9] provides detailed results of deep checks on the roadworthiness of TFSS. Statistically speaking, the main synthesis of unwanted events at EUTS rail structure (RS) for the 2006-2010 period are presented in table 3.

Table 3 - Unwanted events at EUTS rail structure at OTL

Nr. crt.	The name of the unwanted event	YEAR				
		2006	2007	2008	2009	2010
1.	Rail crossings faults (wear, tear, expansion)	205	230	215	220	159
2.	Rail Fractures (joints coupons, coupling different track)	395	380	175	162	155
3.	Switch crossing faults (mobile arms, connection bars, bolts, springs)	55	70	73	67	39
4.	Over widening (track changed, weakened grip)	7	9	4	6	6
5.	TOTAL [$\upsilon(T_A)$]	662	689	467	455	359

4.3. Results obtained on SSEDT level

SSEDT is equipped with a high degree of reservation. However, EDT actions are subject to systematic and targeted PM, based on strict rules [15,16,17]. Database events recorded with reference to SSEDT is much wider than the other two EUTS-SS of OTL and contains findings during the CM and the PM. Results are presented both separately and compared, on all EDT types. In tables 4 to 6 one can find the main components of EDT which recorded undesirable events (faults) in the 2005-2010 period.

Table 4. - List of components with the highest number of defects [$\upsilon(T_A)$] for T4D - EDT type

Nr. crt.	Subsystem or component	YEAR						TOTAL
		2005	2006	2007	2008	2009	2010	
1.	**2.**	**3.**	**4.**	**5.**	**6.**	**7.**	**8.**	**9.**
1.	Electric cables	21	61	25	29	22	12	**170**
2.	Solenoids	32	49	52	46	41	22	**242**
3.	Validators	21	130	42	15	45	11	**264**
4.	Oil pumps	40	55	49	77	81	30	**332**
5.	Motor	25	126	55	70	51	38	**365**
6.	Caseing screws	35	89	64	102	77	3	**370**
7.	Pantographs	67	119	111	93	47	20	**457**
8.	Chassis/bogie	80	104	197	85	10	10	**486**
9.	Contactors/contacts	64	133	230	64	58	65	**614**
10.	Accelerator	127	88	246	105	94	40	**700**
11.	Lighting/signallings	54	225	47	271	263	24	**884**
12.	Doors	40	46	71	536	343	17	**1053**
13.	Breaking Systems	620	969	871	286	209	320	**3275**
14.	Others	795	812	1357	1198	1056	320	**5538**
15.	**TOTAL per year [$\upsilon(T_A)$]**	**2021**	**3006**	**3417**	**2977**	**2397**	**932**	**14750**

ISSN 2067-5534 © 2012 JSE

Table 5. List of components with the highest number of defects [$\upsilon(T_A)$] for kT4D - EDT type

Nr	Subsystem or component	YEAR						TOTAL
		2005	2006	2007	2008	2009	2010	
1.	Oil pump	25	5	1	13	9	1	**54**
2.	Validator	10	17	8	11	9	2	**57**
3.	Electric cables	20	43	12	26	15	4	**120**
4.	Motor	35	14	27	49	24	12	**161**
5.	Pantographs	25	26	40	45	21	13	**170**
6.	Solenoid	30	38	44	66	20	10	**208**
7.	Chassis/bogie	46	51	68	53	39	30	**287**
8.	Contactors/contacts	72	89	112	52	28	25	**378**
9.	Accelerator	70	74	146	75	45	11	**421**
10.	Caseing screw	72	92	143	86	47	8	**448**
11.	Doors	20	35	29	233	136	6	**459**
12.	Lighting/signallings	45	112	47	111	151	44	**510**
13.	Breaking Systems	192	247	249	96	47	104	**935**
14.	Others	423	563	736	615	299	74	**2710**
15.	**TOTAL per year [$\upsilon(T_A)$]**	**1085**	**1406**	**1662**	**1531**	**890**	**344**	**6918**

Tabel 6. - List of components with the highest number of defects [$\upsilon(T_A)$] for ULF - EDT type

Nr.crt.	Subsystem or component	YEAR			TOTAL
		2008	2009	2010	
1.	**2.**	**3.**	**4.**	**5.**	**6.**
1.	Motor	0	0	1	**1**
2.	Pantographs	0	0	4	**4**
3.	Contactors/contacts	0	2	3	**5**
4.	Chassis/bogie	0	0	6	**6**
5.	Electric cables	0	2	5	**7**
6.	Caseing screw	0	1	7	**8**
7.	Solenoid	0	0	10	**10**
8.	Accelerator	0	3	10	**13**
9.	Validator	3	5	7	**15**
10.	Lighting/signallings	2	1	19	**22**
11.	Breaking Systems	4	3	20	**27**
12.	Doors	6	4	22	**32**
13.	Others	26	128	132	**286**
14.	**TOTAL per year [$\upsilon(T_A)$]**	**41**	**149**	**246**	**436**

Fig. 3 shows a comparison of the variable values for the most vulnerable components of the three EDT types[$\upsilon(T_A)$].

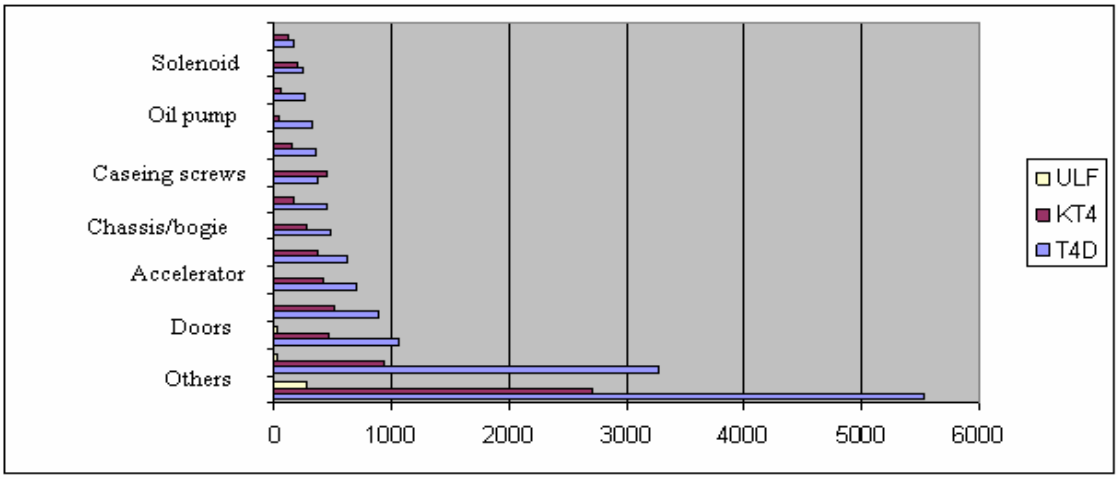

Fig. 3. – Values of [$\upsilon(T_A)$] variable during the analysis time on EDT components

For comparative analysis of EDT, for each EDT type, one calculated the "number of relative fails" indicator for the studied period:

$$v_r(T_A) = \frac{v(T_A)}{n} \qquad (1)$$

n – the number of a certain type of EDT
Results are presented in table 7.

In Fig.4 and 5, three types of EDT evolutions are compared during the analysis of the "number of relative fails" indicator [$\upsilon_r(T_A)$].

Table 7. – Annual relative number of fails on EDT types

EDT Type	Nr.EDT [n]	Year	Fails per year [$\upsilon(T_A)$]	Relative Fails [$\upsilon_r(T_A)$]
1	**2**	**3**	**4**	**5**
ULF	5	2008	39	7.8
ULF	10	2009	149	14.9
ULF	10	2010	59	5.9
Average/year	8.33		82.33	9.53
KT4D	25	2005	1085	43.4
KT4D	24	2006	1416	59
KT4D	25	2007	1662	66.48
KT4D	30	2008	1511	50.36
KT4D	21	2009	867	41.28
KT4D	20	2010	344	24.57
Average/year	23.83		1147.5	47.51
T4D	44	2005	2021	45.93
T4D	44	2006	3006	68.32
T4D	45	2007	3417	75.93
T4D	42	2008	2898	69
T4D	45	2009	2452	54.48
T4D	43	2010	932	20.71
Average/year	43.83		2379.33	55.72

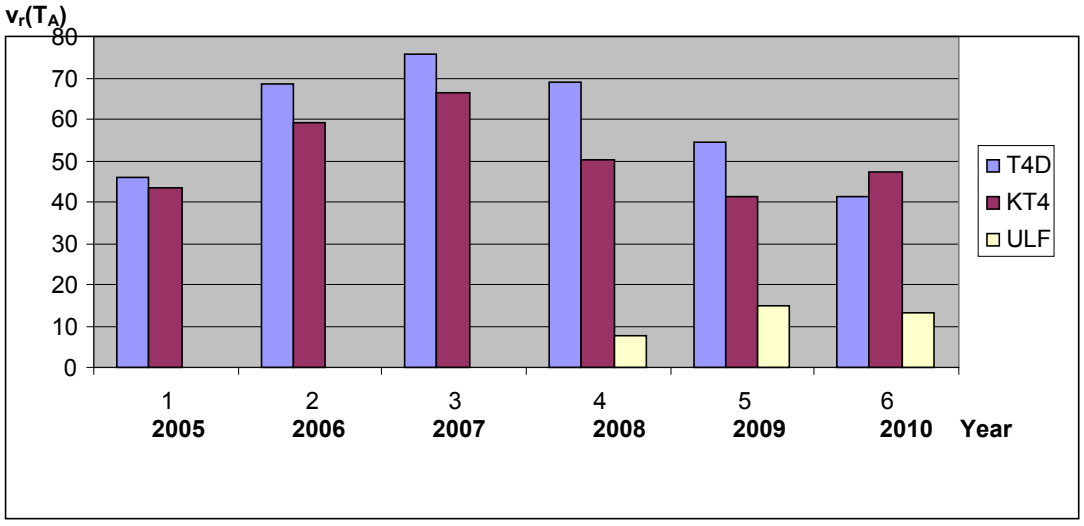

Fig. 4 – The evolution of $\upsilon_r(T_A)$ indicator for EDT of TL

ISSN 2067-5534 © 2012 JSE

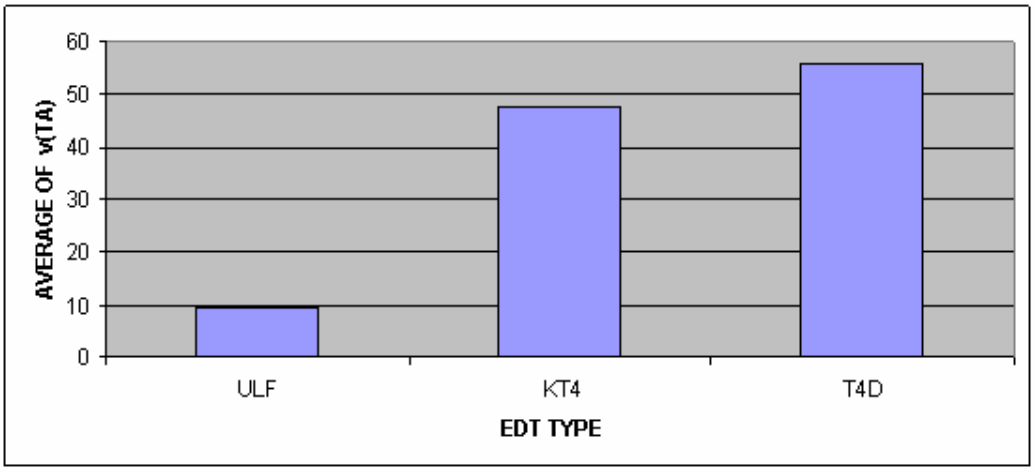

Fig. 5 – The comparison of average values of fails / year $v_r(T_A)$ for EDT of OTL

5. IDENTIFICATION OF DISTRIBUTION LAWS OF RANDOM VARIABLES THAT CHARACTERIZE THE OPERATIONAL RELIABILITY OF EUTS

Based on detailed EDT records, variation form strings of random variables (RV) can be made:

- Good operation time (T_F)
- Corrective maintenance time (T_{CM})
- Preventive maintenance time (T_{PM}).

T_{PM} variable is, in fact, a quasi-random one. Variation strings were calculated for all EDT types, and they are fully given in [9]. Processing of the 9 sets of values by running the program FRVA [18,19], we obtain parameter values of the tested theoretical distribution functions (E, W, N) and maximum deviation values from the empirical distribution [D_{max}], in table 8.

Table 8. – Parameter values of the tested theoretical tested distributions referring on RV specific to EDT of OTL

EDT Type	Distribution function		T_F (R)		T_{CM}(CM)		T_{PM}(PM)	
			Parameter values	D_{max}	Parameter values	D_{max}	Parameter values	D_{max}
T4D	Exponential		λ =0.037	0.097	μ_{CM} =0.067	0.152	μ_{PM} =0.134	0.43
	Weibull	η	23.897	0.075	1.578	0.102	2.885	0.114
		β	1.157		14.164		1.075	
	Normal	m	24.428	35.136	13.319	0.269	3.161	0.41
		σ	35.136		19.68		13.82	
KT4D	Exponential		λ =0.031	0.109	μ_{CM} =0.058	0.202	μ_{PM} =0.325	0.154
	Weibull	η	33.29	0.076	13.587	0.105	2.522	0.102
		β	1.194		1.332		1.223	
	Normal	m	32.045	0.184	13.473	0.304	2.628	0.335
		σ	35.393		24.281		5.573	
ULF	Exponential		λ =0.002	0.486	μ_{CM} =0.255	0.291	μ_{PM} =0.119	0.212
	Weibull	η	143.233	0.101	9.305	0.164	2.484	0.151
		β	0.964		1.431		1.052	
	Normal	m	163.702	0.422	8.455	0.212	2.628	0.335
		σ	810.104		8.065		5.573	

Where the units of measuring are: (λ, μ) - [h^{-1}] ; η – [h]; m – [h] ; σ – [h]

Given the D_{max} values, one recommends the following distribution functions for modelling the reliability and maintainability of EDT:

a.) For KT4D type of EDT:

- Random T_F variable:

$$R(t) = e^{-\left(\frac{t}{33.3}\right)^{1.19}} \quad (2)$$

- Random T_{CM} variable:

$$M_{CM}(t_{CM}) = 1 - e^{-\left(\frac{t_{CM}}{13.59}\right)^{1.33}} \quad (3)$$

Random T_{PM} variable:

$$M_{PM}(t_{PM}) = 1 - e^{-\left(\frac{t_{PM}}{2.52}\right)^{1.22}} \quad (4)$$

b.) For T4D+B4D type of EDT:

- Random T_F variable:

$$R(t) = e^{-\left(\frac{t}{23.9}\right)^{1.16}} \quad (5)$$

- Random T_{CM} variable:

$$M_{CM}(t_{CM}) = 1 - e^{-\left(\frac{t_{CM}}{14.16}\right)^{1.58}} \quad (6)$$

- Random T_{PM} variable:

$$M_{PM}(t_{PM}) = 1 - e^{-\left(\frac{t_{PM}}{2.89}\right)^{1.08}} \quad (7)$$

c.) For ULF type of EDT:

- Random T_F variable:

$$R(t) = e^{-\left(\frac{t}{143.2}\right)^{0.96}} \quad (8)$$

- Random T_{CM} variable:

$$M_{CM}(t_{CM}) = 1 - e^{-\left(\frac{t_{CM}}{9.31}\right)^{1.43}} \quad (9)$$

- Random T_{PM} variable:

$$M_{PM}(t_{PM}) = 1 - e^{-\left(\frac{t_{PM}}{2.48}\right)^{1.05}} \quad (10)$$

Values of fundamental reliability indicators for EDT are presented in table 9.

Table 9. – Values of fundamental reliability indicators for EDT of OTL

EDT Type	**MTBF [hours]**	**MTCM (MTTR) [hours]**	**MTPM [hours]**	**λ [h^{-1}]**	**μ_{CM} [h^{-1}]**	**μ_{PM} [h^{-1}]**
KT4D	32.3	17.24	3.08	0.031	0.058	0.325
T4D+B4D	27.03	14.93	7.46	0.037	0.067	0.143
ULF	500	3.92	8.4	0.002	0.255	0.119

5. CONCLUSIONS

Database operational reliability of the components of OTL - EUTS structure is consistent with respect to EDT and inconsistent with respect to components of SSAD and TFSS structure. The data was organized and completed substantially in the last two years.

Analysis of operational reliability, on the extended five years [2006 ÷ 2010], reflects the following hierarchy of events with the greatest impact on the SSAD structures unavailability of OTL - UTSUEDT:

→ Shutdown due to overload or wagon fault;
→ Lack of communication (computer modem);
→ No voltage supply of the NES (6kV);
→ Switch coil lock;
→ Injection Cable Fault.

The operational reliability analyzes of TFSS networks of OTL - EUTS made for a period of 5 years [2006 ÷ 2010], reflect the following hierarchy of events with the greatest impact on availability of this subsystem:

→ Rail Fractures (joints coupons, coupling different track);
→ Over widening (track changed, weakened grip);
→ Rail crossings faults (wear, tear, expansion);
→ Switch crossing faults (mobile arms, connection bars, bolts, springs).

From the database established for EDT at OTL, during the six years [2005 ÷ 2010], one obtained the following hierarchy of components in terms of impact on EDT operational reliability:

- EDT type T4D + B4D: braking system, lighting system / signal, doors, screw housing and accelerator;
- EDT type KT4D: brakes, doors, lighting / signalling, accelerator and contactors / contacts;
- EDT type ULF: type doors, brake systems, lighting / signalling, validation and acceleration system.

Summary of events registered at OTL database reflects the following increases in the relative number of falls (number of falls / number of copies in use) over 6 years [2005 ÷ 2010] on the endowment EDT of OTL

- for type T4D and KT4D of EDT increased from [2005 ÷ 2008] and decreases in [2008 ÷ 2010] period;
- for type ULF of EDT increased in 2009 and decreased in 2010 compared to 2009;
- the 3 types of EDT of OTL administration, rank in the terms of average value ν_r indicator (relative number of defects per year) as follows: T4D (55.7), KT4D (47.5); ULF (9.5).

Database on the events recorded in the OTL EDT is suitable to statistical analysis of identifying laws that reflect the true empiric distributions of random variables. Application of statistical processing model using the FRVA computer program, concluded that for the three types of EDT and with reference to the three random variables (T_F, T_{CM}, T_{PM}), Weibull distribution law most closely reflects the empirical distribution. The value

 ISSN 2067-5534 © 2012 JSE

obtained for the parameter β of the random variable T_F distribution law, reflects the fact that during the analysis, reliability improves for ULF type of EDT compared to the other two types of EDT (KT4D and T4D) which are worse.

The values for EDT fundamental reliability indicators of OTL reflect the followings:

- The reliability of EDT type ULF is much higher than the level of reliability of EDT type kT4D and T4D that have similar values for MTBF indicator;
- Time spent on preventive maintenance for EDT type ULF is greater than EDT type T4D and much higher than type KT4D;
- Corrective maintenance time for EDT type T4D and kT4D is much higher than EDT type ULF;
- CM time for old EDT (KT4D and T4D) is more than PM time of these EDT types; for EDT type ULF this is vice versa.

REFERENCES

[1] ***: *Strategy of sustainable development for EU, Bruxelles*, 10117/06;
[2]***: *Politics of energy for EU*, Phare RO 0006/18.02.2003;
[3] Paulley N. – *The demand for public transport: the effects of fares, quality of service, income and car ownership,* Elsevier Ltd, 2006
[4] L Dell'ollio, A. Ibeas, P. Cecin, *The quality of services desired by transport users*, Elsevier Ltd, 2010
[5] P. Yaliniz, S. Bilgic, Y. Vitosoglu, C. Turan, Evaluation of urban public transportation efficiency in Kutahya, Turkey;
[6] B.R. Sampanio, O.L. Neto, Y. Sampanio, Efficiency analyzes of public transport systems. Lessons for institutional planning, Elsevier Ltd, 2008;
[7] M.G. Karlaftis, D. Tsamboulas, Efficiency measurement in public transport: Are findings specification sensitive? Elsevier Ltd, 2011;
[8] Felea I. - *Reliability in electro-energetics,* Bucureşti, 1996;
[9] Csuzi I., *"Contributions to evaluating and optimizing the energetic and availability performance of the urban electrical traction system ", Thesis for PhD,* University of Oradea, 2011
[10] Birolini A., - *Quality and Reliability of Technical Systems*, Springer–Verlag, Berlin, 1994*;*
[11] O'Connor, P., - *Practical Reliability Engineering*, Editura John Wiley & Sons, England, 1991;
[12] Felea I, Coroiu N., - *Fiabilitatea şi mentenanţa echipamentelor electrice, Editura Tehnică Bucureşti, 2001;*
[13] Ivas D., Munteanu F., - *Fiabilitate, mentenanţă, disponibilitate, performabilitate în hidroenergetică*, Editura Prisma, Râmnicu Vâlcea 2000;
[14] Nitu V.I., - *Fiabilitatea instalaţiilor energetice – Culegere de problema pentru energeticieni,* Ed.Tehnică, Bucuresti 1979;
[15]***: SR EN 50119-2001, *Railway aplications.Fixed instalations.Electric traction overhead contact lines*;
[16]***: *Service guide for tram SiemensULF151,* Oradea 2008;
[17]*** *Documentation of tram Tatra T4D+B4D,* Praga,1974;
[18] Felea I. Secui C., - *Algoritm si program pentru stabilirea functiilor de distributie ale variabilelor aleatoare*, Lucrarile conferintei de electroenergetica, Timisoara,1994;
[19] Felea I., Secui C, Dzitac S., - *Indrumar de aplicatii in fiabilitate,* Editura Universitatii din Oradea, 2008

ASSESSMENT OF THE ELECTRIC HYDRO GENERATOR STATOR INSULATION CONDITION BY MEANS OF ON-LINE PARTIAL DISCHARGE MEASUREMENT

ZLATANOVICI D. , DUMITRESCU S.
ICEMENERG Bucuresti
danz@icemenerg.ro

Abstract - The paper presents the principle of the measurement method, the quantities characterizing the partial discharges and the criteria utilized for the evaluation of the insulation condition. Further, the results of the measurements of several hydro generators and the variation with time of the quantities that characterize the partial discharges, Qmax magnitude and the normalized quantity NQN, over a period of about 10 years are presented. A synthetic presentation of the conclusions of the insulation condition annual evaluation and of the decisions that have been taken relating to the hydro generator maintenance has been made. The paper ends with several considerations on the method and evaluation criteria efficiency

Keywords: partial discharges, hydrogenerators, measurement, magnitude, normalized quantity

1. GENERALITIES

In general, partial discharges (PD) are small non-disruptive electrical discharges that occur in the micro cavities existing in the insulation. The discharges are partial due to the fact that in series with the micro cavity where the discharges occur there is also an area with solid insulation.

The pulses of partial discharge are very rapid phenomena that last only for a few nanoseconds. The insulations, especially the stratified ones, cannot be considered as perfectly homogenous. There are always small size micro cavities filled with gas resulting from the different contractions of the insulation constituents or even from the technological execution process itself. The occurrence of such micro cavities and cracks is favored by the intermittent action of the thermal and mechanical stresses to which the insulation is subjected during operation, as well as to the action of the pollutant factors (moisture, dust, oil) from the insulation operational environment.

In the conditions of an electrical field, these micro cavities get ionized and, when the voltage between two opposed surfaces attains the disruptive gradient of the gases contained in the micro cavity, partial discharges (ionizations) occur.

The occurrence and development of internal PDs has a negative impact on the insulation, leading to the formation of micro cavities that increase with time, forming channels when several such cavities unite, and finally resulting in craters; thus, the insulation is weakened and breakthroughs that ruin the insulation may occur.

The PD are measured as voltage pulses; that is why, during the positive alternation of the voltage wave form a discharge or a partial short circuit lead to a negative pulse oriented downwards. These pulses are called negative polarity PD and occur during the first quarter of the period, during period of increase in the amplitude of positive alternation of the voltage applied to the cavity. During the third quarter of the period a partial short circuit leads to the occurrence of a positive impulse, oriented upwards. These pulses are called positive polarity PD s and occur during the increase in the negative alternation amplitude.

2. METHOD OF MEASUREMENT

The on – line measurement can be carried out only on generators previously fitted with couplers. The method consists in previously mounting several couplers on the terminals or even the stator bus bars, taking out the wires to a terminal block, exterior, and the measurement of the PD during generator operation by means of an analyzer connected to the respective connection terminals. The couplers are usually insulator type capacitors, having a capacity of about 80-100 pF and operating voltages of 25-30 kV.

According to the type of the generator and of the stator winding, two coupler mounting systems are used:
- The differential mounting (PDA) with a coupler on each current path of each phase, at about 1 m from the connection point of the current paths;
- The directional mounting (BUS) with two couplers at each phase outlet, at about 2 m one against the other and 1 m from the terminal outlet of the machine .

The coupler that is the nearest to the winding is called machine coupler, and the other one is called system coupler.

 ISSN 2067-5534

These systems enable the elimination of the electric noise occurring inside and in the proximity of the machine that interferes with the partial discharges from the machine. It is possible to discriminate the partial discharges by comparing the signals from the two associated couplers, situated on two current paths of a phase (for the differential system), or to the outlet of the same phase (for the directional system) and considering the time difference of nanoseconds with which they get to the analyzer due to the electrical distance between the associated couplers. The partial discharges originate in the stator winding as compared to the noise signals that come from the outside the winding.

The couplers are connected to the terminal box, to which the measurement system made up of a partial discharge analyzer and a laptop with specialized software is connected

Measurement system calculates and displays the following quantities and diagrams (fig. 1):

- The maximum magnitude (peak) of partial discharge, noted with the symbol ±Qmax, which is the magnitude corresponding to a repetition rate (P_w) of 10 pulses per second and window (negative and positive), expressed in mV:
-

$$Q_{max} = \max [M = f(P_w)] \qquad (1)$$

$$P_{win} \geq 10 \text{ p/sw}, \quad w \in (0\text{-}N)$$

where:

P_w - number of pulses per second and magnitude window (p/sw)

M - magnitude of partial discharge (mV)

- The normalized quantity (also named "total activity") of PD, noted by ±NQN that is a relative quantity, equal to the ratio between the area under the curve of the number of pulses versus the amplitude (from the 2D diagram) and the area of the normal range of 10000 pulses per second at 800 mV (negative and positive);

$$NQN = \sum_{w=0}^{N} A_w = \frac{M}{N} \sum_{w=0}^{N} \frac{p_w - p_{w+1}}{2} \qquad (2)$$

$$p_w = \log_{10}(P_w) \qquad P_w \in (0,1,2 \ldots .N) \qquad (3)$$

$$NQN = \frac{M}{NG}\left[\frac{\log_{10}(P_0)}{2} + \sum_{w=1}^{N-1} \log_{10}(P_w) + \frac{\log_{10}(P_N)}{2}\right] \qquad (4)$$

where:

A_w – surface under the curve $M=f(P_w)$ for each window

N - number of magnitude windows,

p_w - logarithm of the pulse counts

G - gain of the partial discharge detector (arithmetic, not decibels)

- The bi-dimensional diagrams 2D: the number of pulses per second and window (the rate of pulses) versus the amplitudes that define the windows;
- The tri-dimensional diagrams 3D: the pulse rate versus the phase angle of the sinusoidal voltage at which they occur and the magnitude of the window;

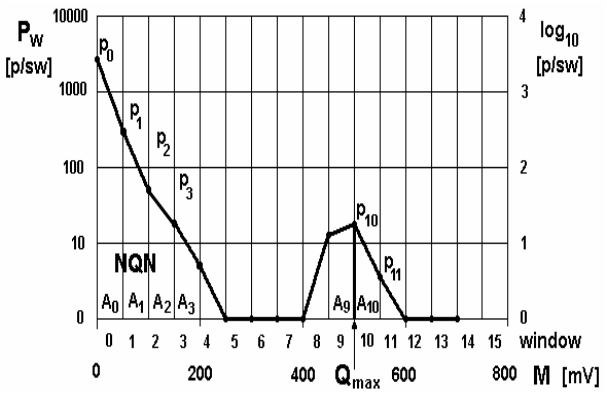

Fig. 1 - Definition of the normalized quantity NQN and maximum magnitude Q_{max}

3. CRITERIA FOR THE EVALUATION OF THE STATOR WINDING CONDITION

Based on the research and experience in measurements and the analysis of events and maintenance works in the field of electrical generator insulations [4], three main and two intermediary categories of insulation conditions have been defined:

Table 1 -Categories of insulation condition

Category	Condition description	Level of risk
I	Very good condition (new insulation), good, normal	operation without risks
I-II	Acceptable condition, slow , normal, small scale deteriorations	operation without risks
II	Slow, normal deteriorations	average breakdown risk
II -III	Slow, normal, average scale deteriorations with a tendency towards becoming more severe	average breakdown risk
III	Severe deteriorations	high breakdown risk

Based on the experience from the literature in the field [5,6,7], on the utilization instructions of the IRIS type analyzer [8] and on authors' experience, the limit values of the maximum magnitude and the normalized quantity have been established according to the level of the hydro generator rated voltage and the condition of insulation (table 2). Also, qualitative criteria for the assessment of the insulation condition on the basis of the 2D and 3D diagram analysis, presented in table 3, have been developed.

Table 2 - Quantitative criteria

Cat.	Insulation condition	± NQN (p.u.)		± Qmax (mV)		
		<15 kV	> 15 kV	< 7 kV	10 ÷ 15 kV	> 15 kV
I	Good	<100	<250	< 60	< 170	<300
II	Slow, normal deteriorations	100-250	250-450	60-140	170 - 400	300-600
III	Severe deteriorations	>250	>450	> 140	> 400	>600

Note

The maximum amplitude Qmax indicates the level of insulation deterioration in the worst affected point in the winding. The normalized quantity NQN is proportional to the total extent of the overall insulation deterioration.

Table 3 - Qualitative criteria

Assessed parameter	Assessment criterion	Insulation condition
1.Variation of arameters ±Qmax and ±NQN with time	increase < 25 %	Category I – Good condition
	Constant increase	Category II – Slow, normal deteriorations
	increase > 100 %	Category III – Severe deteriorations
2. Curve aspect in 2D diagrams	Polarity equality Ratio R = -Qmax / +Qmax =1 Curves overlapping / knitting p/sf = f(mV) in 2D	Volume PD in the slot area due to separation between layers (delaminations) and empty spaces (voids) in the insulation mass (thermal effect). Cat. II
	Mainly negative polarity Ratio R =-Qmax/ +Qmax > 2 Curves position ± p/sf =f(mV) in 2D	Volume PD, due to the voids between the insulation and the copper conductor (cyclic load effect) R= 1-2 cat. I, R >2 cat. II, R>> 2 cat. III
	Mainly positive polarity Ratio R=+Qmax/ -Qmax > 2 Curves position ± p/sf =f(mV) in 2D	Surface PD in the slot area between the insulation and the slot wall due to the deterioration of the conductive lacquer coating R= 1-2 cat. I, R >2 cat. II, R>> 2 cat. III
3. PD presence in the 3D diagrams, on the sinusoid	Presence of negative PD at α between 0^0 and 90^0 , centered on 45^0	Volume PD due to separation (voids) between insulation and the copper conductor (cyclic load effect)
	Presence of positive PD at α between 180^0 and 270^0, centered on 225^0	Surface PD in the slot area between the insulation and the slot wall due to the deterioration of the conductive lacquer coating
4. Aspect of the 3D and 2D diagrams relating to the PD in the frontal area (ZF)	In 3D, PD occurrence at $\alpha = 15^0, 75^0, 195^0, 255^0$ In 2D, curve humps ± p/fs =f(mV) at high magnitudes and low p/sf	Surface PD in the area of the frontal ends due to dust, oil, etc., pollution and / or of their consolidation weakening and/or deterioration of the conductive lacquer on the surface of the insulation
5. Extent of the PD occurrence in the 3D diagrams (p/sf and mV)	0-20 p/sf	Category I – Good condition
	20-50 p/sf	Category II – Slow deteriorations, normal
	>50 p/sf	Category III – Severe deteriorations

4. MEASUREMENTS RESULTS

Further, the results of the on-line PD measurements and analysis for the evaluation of the insulation condition of 4 hydro generators selected out of the 13 with a measurement history are presented. All these generators have mica-epoxy type stator winding insulation.

At **HG 2 HPS Mărişelu**, 75 MW, 15.75 kV (fig. 2) during the entire period 1999 – 2010 the values of ±NQN and ±Qmax on all the phases had a practically constant evolution. The ±NQN parameters surpassed the maximum reference value of 450 p.u., varying around the value of 800 for all the phases. This has indicated an expanded extent of the deterioration (category III).

The ±Qmax parameters remained within the reference range (300-600 mV) indicating a slow and normal deterioration of the insulation (category II). The zigzag aspect of the PD variation curves was due to the maintenance works, simple or more complex. The effect of these works on the stator winding resulted in a certain improvement in the PD parameters.

In the 2D diagrams (fig.3), on all the phases, for all the measurements, a quasi-equality between polarities with the overlapping of the p/sf =f(mV) curves, or their knitting, indicating the occurrence of volume PDs within the slot area (category II) was noticed.

In the 3D diagrams (fig.4), on all the phases, the occurrence of the negative and positive PDs at the electric angles of α=0°-90° and α=180°- 270°, respectively, was very dense, indicating the occurrence of volume and surface PDs in the slot area. In 2007, the repetition frequencies were of 80-100 p/sf with low magnitudes and 10 p/sf with high magnitudes and in 2010, of about 60 -80 p/sf with low magnitudes and 10 p/sf with high magnitudes, (category III).

At the same time, for all the phases, the occurrence of PD at $\alpha = 15^0, 75^0, 195^0, 255^0$ with frequency values of about 40-50 p/sf on phase A and B and over 50 p/sf on phase C and relatively high magnitudes were noticed, indicating surface PD in the area of the frontal ends (categories II-III)

At an overall evaluation, there results that the insulation presents volume PD in the slot area due to delaminations and voids in the insulation (thermal effect) between the insulation and the copper conductor (effect of the cyclic load) and surface ones in the frontal area due to their consolidation and the deterioration of the conducting lacquer on the insulation surface. Thus, the insulation on its whole can be included in category II-III with normal, slow deteriorations of medium extent in the entire mass of the insulation having the tendency to worsen. Maintenance works (re-wedging, repainting in the frontal area) and the continuation of periodic PD measurements were recommended. At the same time, a set of supplementary measurements (tan δ, increased voltage, local PD measurement with corona probe) to check the opportunity of the generator re-winding were recommended.

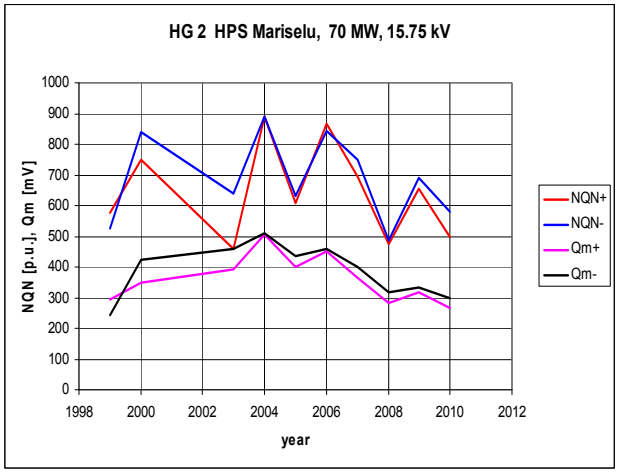

Fig. 2 - HG2 HPS Mărişelu NQN, Qmax =f (time)

ISSN 2067-5534 © 2012 JSE

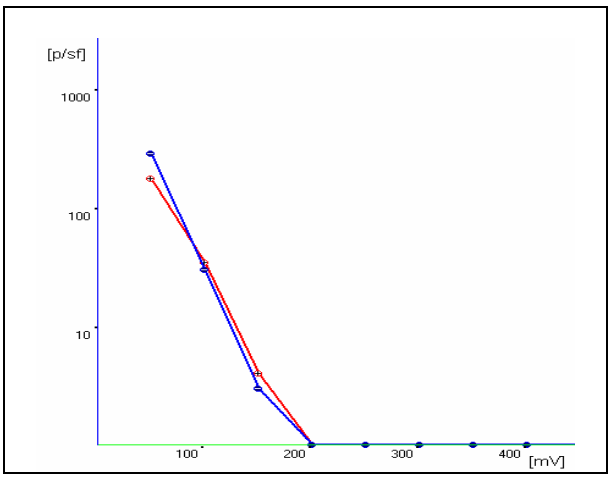

Fig. 3 - HG2 HPS Mărişelu, 2D - 2008

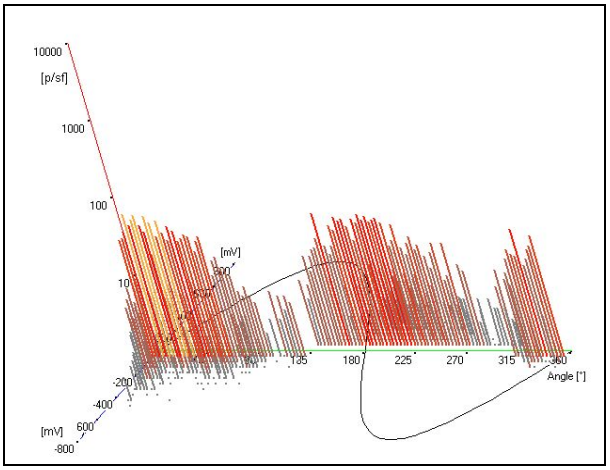

Fig. 4 - HG2 HPS Mărişelu, 3D - 2010

At **HG 2 HPS Vidraru**, 50 MW, 10.5 kV, (fig.5) in 2003 and 2010 extensive maintenance works were carried out: the stator bars were replaced (2003), the stator bars were re-wedged, the stator iron was repaired (2010) and the frontal winding ends were re-varnished with semi-conducting lacquer. The PD measurements after all these works showed an obvious improvement in the values of the PD parameters. In between the two extensive maintenance works the evolution of the PD parameters was monotonously increasing (the insulation is of the mica-epoxy type and is about 24 years old).

Thus, the ±NQN values increased from approximately 110-250 p.u (category I-II) to approximately 320 p.u. (category III) and the ±Qmax values of about 120 mV (category I) to 270 mV (category II). After the maintenance works of 2010, the ±NQN values decrease to about 200 p.u. (category II) and the values ±Qmax decrease to 120 mV (category I).

In 2D diagrams, all the phases, for all the measurements, had quasi-equal values of the positive and negative pulses, the ratio +Qmax/-Qmax ≈ 1 and the p/sf=f(mV) curves are knitted in all the operating conditions, or presented a slight preponderance of the negative polarity. This has indicated the occurrence of volume PD in the slot area due to delaminations between the layers and the voids in the insulation, as a result of the thermal effect, (category II).

In the 3D diagrams, in 2009, the occurrence of negative PD on all the phases in the angle range of $\alpha = 0^{\circ} - 90^{\circ}$ was noted with a repetition frequency ranging between 40 and 100 p/sf (category III) but of low magnitudes of 8-12 p/sf and higher magnitudes. At the same time, the occurrence of positive PD in the angle range of $\alpha = 180^{\circ} - 270^{\circ}$, with the repetition frequency of 80-100p/sf (cat. III), but of low magnitudes was noticed. At the same time, the occurrence of PD in the frontal area, respectively, at angles $\alpha = 15^{0}, 75^{0}, 195^{0}, 255^{0}$ with repetition frequencies of 30-100 p/sf and low magnitudes (category III) were noticed.

After the measurements carried out since 2009 the re-wedging of the entire stator winding, injection of conducting lacquer in the slot part and re-varnishing with semi-conducting lacquer of the frontal coil ends have been recommended.

In 2010, in the 3D diagrams (fig.6), the decrease in the repetition frequency to 10 - 40 p/sf (category II) on all the phases for the negative PD in the angle range $\alpha = 0^{\circ} - 90^{\circ}$, with low magnitudes and to 5 p/sf with higher magnitudes wad noticed. The persistence of negative PD indicates the occurrence of volume PD especially between the insulation and the copper conductor. At the same time, a decrease in all the phases of the repetition frequency to 10 - 40 p/sf (cat. II) for the positive PD in the angle range of $\alpha = 180^{\circ} - 270^{\circ}$ is noted. The persistence of positive PD indicates the surface PD occurrence in the slots. The decrease in the frequency of repetition at 10 - 40 p/sf (category II) of PD in the frontal area is also noticed, which indicates an improvement in the condition of the surface at the ends of the frontal coils.

Therefore, the maintenance works carried out in 2010 resulted in the reduction of the PD parameter values and in the reduction of the pulse repetition frequency and, therefore the overall insulation condition was improved, especially relating to its surface. Thus, the insulation passed from category III in 2009 into category II in 2010 . Continuation of periodic PD measurements was recommended. A set of supplementary measurements (tan δ, increased voltage, local measurement of PD with corona probe) were also recommended.

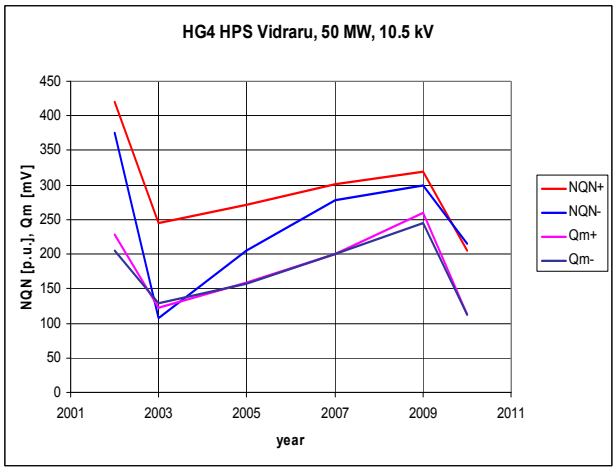

Fig. 5 - HG 4 HPS Vidraru , NQN, Qmax =f (time)

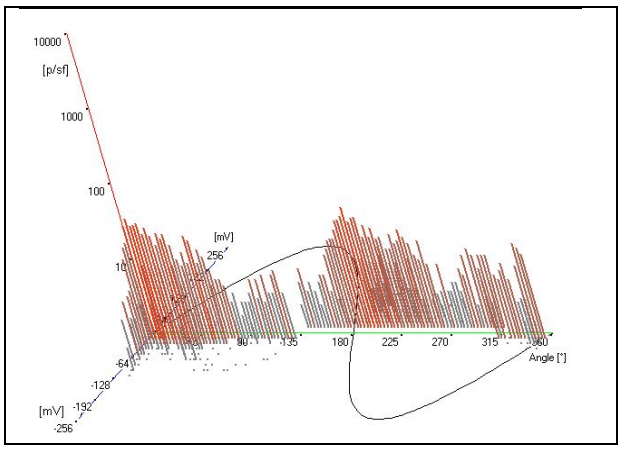

Fig. 6 - HG 4 HPS Vidraru 3D - 2010

At **HG 2 HPS Remeți**, 45 MW, 10.5 kV, (fig.7) during the entire period 2000 – 2010, the ±NQN and ±Qmax values on all phases had a monotonous increasing evolution. Thus, the ±NQN parameters increased from 150 p.u. to 450 p.u. (surpassing the maximum limit) indicating an expansion with time of the deteriorations of the entire insulation (category III). The ±Qmax parameters increased from 50 ...100 mV to 270 ... 350 mV nevertheless remaining within the reference range (170-400 mV) thus indicating the development of slow, normal deteriorations (category II) in the course of time. In the period 2004-2005 maintenance works were carried out (radial re-wedging, re-varnishing of the frontal part) that led to the temporary diminishing in the ±NQN and ±Qmax values.

In the 2D diagrams, all the phases, all the measurements presented values almost equal of the positive and negative pulses, the ratio +Qmax/-Qmax ≈ 1 and the curves p/sf=f(mV) knitted, in all the operating conditions. This indicated the occurrence of volume PD in the slot area due to the delaminations between the layers and the voids in the insulation as a result of the thermal effect, (category II).

In the 3D diagrams (fig. 7), the occurrence of positive PD at α= 180° -270° that evolved with time from the repetition frequency of about 10-20 p/sf in 2007 to the repetition frequency of 30 -50 p/sf in 2010 with low magnitudes and the development with time of negative PD in the α= 0° -90° range with the repetition frequency of 10-15 p/sf and low magnitudes and frequencies of 5 p/sf and higher magnitudes was noticed. These evolutions indicated an expansion of the volume PD due to the cavities (voids) between the insulation and the copper conductor (effect of the cyclic load), of medium extent (category II -III) and the surface PD development in the slot area, between the insulation and the slot wall due to the deterioration of the conducting lacquer.

It was also noted the expansion with time of PD, from electric angles of α=195° to electric angles of α =15°, α=195° and α=255°, indicating the occurrence of surface PD in the frontal end area, with frequencies up to 0-30 p/fs and low magnitudes (category II). After the maintenance works carried out in the period 2004-2005, the occurrence of these DP diminished, but in 2010 they re-occurred.

Therefore, the insulation on its whole was included in the category II –III, with normal, slow deteriorations in the entire insulation, tending to expand in the entire insulation.

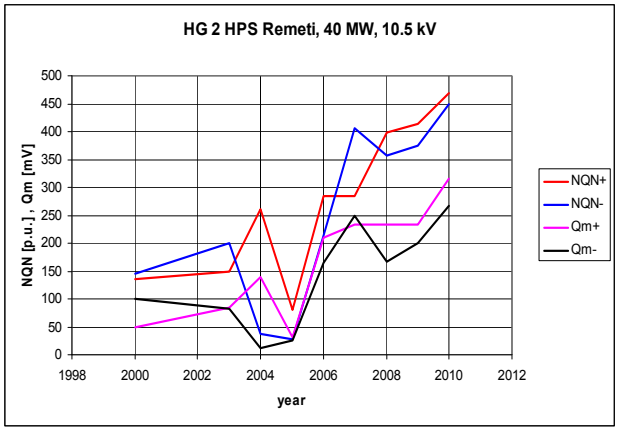

Fig. 7 - HG2 HPS Remeti, NQN, Qmax =f (time)

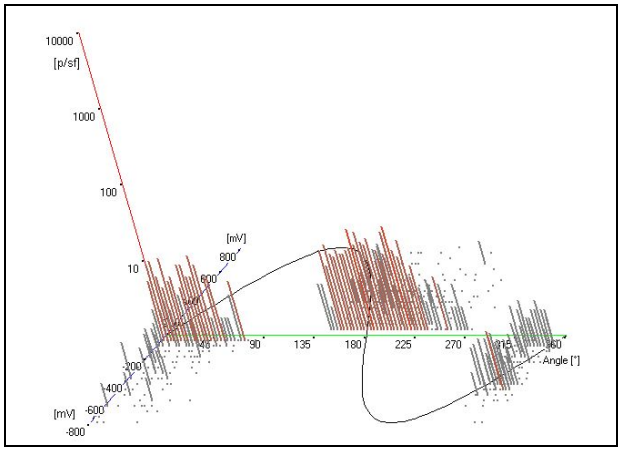

Fig. 8 - HG 2 HPS Remeti 3D - 2010

The insulation was affected in its entirety as volume PD were noticed in the slot area due to delaminations between layers and voids in the entire insulation as a result of the thermal effect and the delaminations (voids) between the insulation and the copper conductor (cyclic load effect), of medium value with worsening tendencies. At the same time, the deterioration of the conducting lacquer in the slot area and of the semi-conducting lacquer at the ends of frontal terminal ends was noticed.

At **HG 2 HPS Munteni**, 31 MW, 10.5 kV, (fig. 9) there are results only for the period 2007-2010. In 2006, the generator was rewound. In the period 2007 – 2010 the ±NQN and ±Qmax values, on all phases, registered a slightly monotonous increase. Thus the ±NQN values increased from about 20 p.u. to about 70-80 p.u. and the ±Qmax values increased from about 10-15 mV to about 35 mV. These values are below the minimum reference limits (100 p.u. for ±NQN and 170 mV for ±Qmax), the insulation being included in category I, very good condition, for both criteria.

In 2D diagrams (fig.10), on all the phases an equality between the polarities with the overlapping or knitting of

ISSN 2067-5534 © 2012 JSE

the curves p/sf =f(mV) was noticed, the presence of the PD being of very low intensity (cat. I)

In 3D diagrams (fig. 11), on all the phases, under all operating conditions and for all the measurements, the PD occurrence on the sinusoid is rare, being insignificant in general, having low magnitudes and low frequencies of 5-10 p/fs (category I)

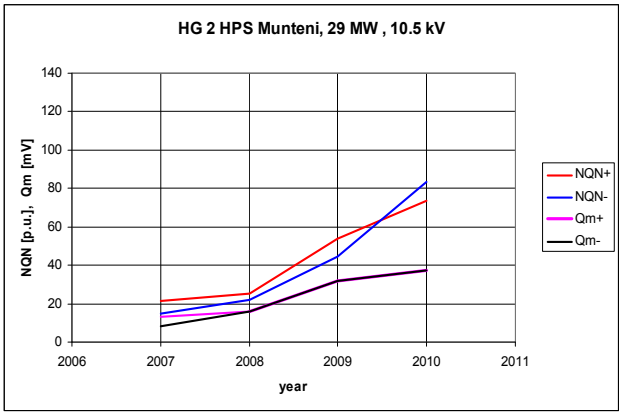

Fig. 9 - HG 2 HPS Munteni NQN, Qmax =f (time)

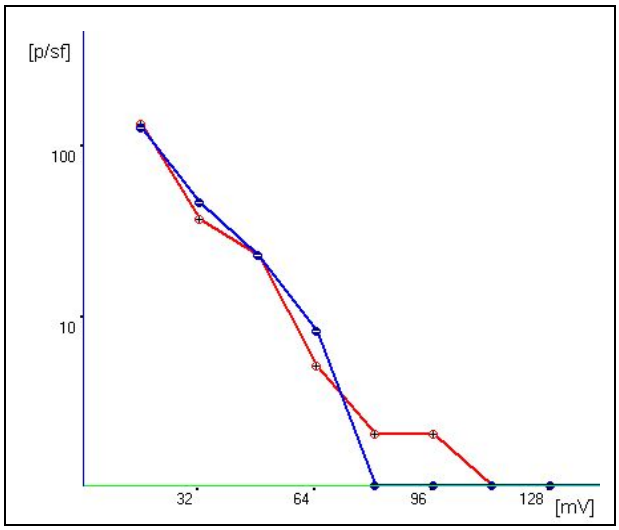

Fig. 10 - HG2 HPS Munteni 2D - 2010

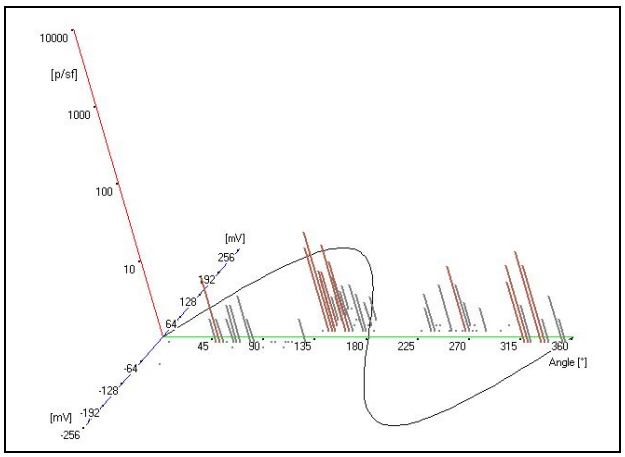

Fig. 11 - HG 2 HPS Munteni 3D – 2010

To conclude, after 4 years of operation, the insulation is in very good condition, the PDs having insignificant values (category I). It was recommended to continue the annual PD measurements paying special attention to the condition of the semi-conducting lacquer coating from the frontal area during the maintenance works.

5. CONCLUSIONS

The PD measurements and the careful analysis of the results have enabled the assessment of the stator winding insulation condition, their classification and recommendations for the maintenance works.

The criteria can be improved by monitoring the evolution of the PD parameters with time and the correlation with the maintenance works carried out. It would be ideal to perform a set of measurements before and after maintenance works.

In the case of the generators analyzed in this report, the periodic measurements and the utilized evaluation have enabled the correct assessments of the condition of the respective insulations and substantiated decisions for the maintenance works. In general, these works have had the expected result and improved the insulation condition.

REFERENCES

[1] IEEE 1434-2000 IEEE Trial-"Use Guide to the Measurement of Partial Discharges in Rotating Machinery" (Converted to a full-use standard. June 1, 2005)

[2] SR 9385-1: 2008 Synchronous Hydro Generators. Part 1: General Technical Conditions

[3] SR 9385-1: 2008 Part 2: Rules and methods for quality verification

[4] Zlatanovici D., Engster F. "Method for the Assessment of residual life time for stator winding Insulation", Proceedings of the CIGRE / IEE Japan Joint Colloquium.Rotating Electric Machine Life Extension Yokohama,Japan, 1997, rapp. 1-9 , 6 p)

[5] V.Warren and P. Kantardziski, „On-line partial discharge monitoring: where we stand and wat next", Prodceedings of conference Modeling, Testing & monitoring for Hydro Powerpants –III, Aix-en-Provence, France, 1989

[6] C.J. Azuaje, W.J.Torres, "Experiences in identification of partial discharge patterns in large hydrogenerators", IEEE PES Transmission and distribution conference and exposition latin America , Venesuela,2006)

[7] J.F.Lyles, G.C.Stone, M.Kurtz. „Experience with PDA Diagnostic. Testing on Hydraulic Generators", IEEE Transactions on Energy Conversion, vol. 3, no. 4, dec. 1988)

[8] *** IRIS Power Engineering inc „Operating Manual PDA IV LITE"

[9] G.Stone, E.Boulter, I.Culbert, H.Dhirani, "Electrical Insulation for rotating machines" (IEE Press, SUA,2004)

[10] D. Zlatanovici, V.Kahle, M. Park "Methods for determining the Condition of Stator Windings Insulation", Romanian Rev. Energy Technologies, no.7, 2008, p. 7-19

[11] D. Zlatanovici. **"**Partial discharges in the insulation of the stator windings of the electric generators and methods for their measurement" (Romanian Rev. Energy Technologies , no 11-12, 2006, p.36)

EXPERIMENTAL STUDY ON THE INCREASE OF THE EFFICIENCY OF VERTICAL AXIS WIND TURBINES BY EQUIPPING THEM WITH WIND CONCENTRATORS

RUS L.F.
Technical University of Cluj-Napoca, Faculty of Building Services, 21 Decembrie no. 128-130, Cluj-Napoca, lucian.rus@insta.utcluj.ro

Abstract – The vertical axis wind turbines, which are operating on the principle of aerodynamic drag, have relatively low efficiency of about 20 to 30%, but they have the great advantage that they can operate at full capacity and produce energy in areas with low wind potential or with turbulent winds. There are several ways one can improve the power coefficient of this type of wind turbine, such as establishing the ideal shape of the rotor blades or by choosing the optimal number of stages of the rotor. In this study, for the improvement of the power coefficient of the wind turbine, a concentrator (curtain) was used in order to cancel the negative moments that affect the rotational movement of the rotor and to increase the speed of the airflow at the entry into the rotor. By analyzing the behavior of the rotors without a concentrator and equipped with various types of wind concentrators one could determine the optimal configuration of the concentrator and the influence that it has on the operation of the wind turbines.

Keywords: wind turbine, rotor, blades, concentrator, wind tunnel, rotational speed.

1. INTRODUCTION

Wind energy is one of the most important sources of clean energy and the generation of electricity by converting this type of energy has become increasingly important in recent years. The installed capacity of wind farms is strongly increasing from year to year, this increase being accentuated also by the support programs granted to the investors in green energy technologies, existing in most developed countries. There are many types of wind turbines that are currently used to produce electricity, which can be divided into two categories depending on the orientation of their axis of rotation [1,2]: horizontal axis wind turbines, HAWT's and vertical axis wind turbines, VAWT's (Fig. 1).

The wind turbines that have the axis of rotation in a horizontal position are performed almost exclusively based on the principle of operation of the propeller and they work based on the effect of aerodynamic lift. The superiority of this design over other solutions developed so far is based on the following characteristics:

- the rotor speed and the amount of energy produced can be controlled by pitching the rotor blades in relation to their longitudinal axes;
- the shape of rotor blades can be aerodynamically optimized;
- the technological advances in the design of the propeller blade type, favored by the development of the aeronautic industry, constitute a decisive factor.

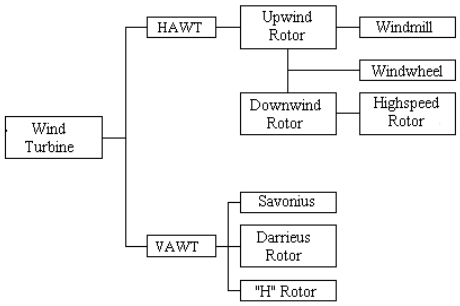

Fig. 1 - Classification of wind turbines after their constructive form

In general, the performance coefficient of modern turbines has values between 0.4 and 0.5, values that are approximately 70 to 80% of the theoretical limit of this coefficient, which is 0593 [3].

Vertical axis wind turbines can operate both on the principle of aerodynamic lift, such as Darrieus turbine and the „H" rotor, and based on the effect of aerodynamic drag, such as Savonius wind turbines and their different variants. Although these turbines do not meet the performances of the horizontal axis wind turbines, having performance coefficients, *Cp* between 0.25 and 0.4 (Fig. 2), the turbines in this category have several important advantages compared to the others [4]:

- they do not require yaw mechanisms, having the ability to accept wind from any direction;
- the orientation of their axis of rotation allows the generator to be located at the bottom of the tower.

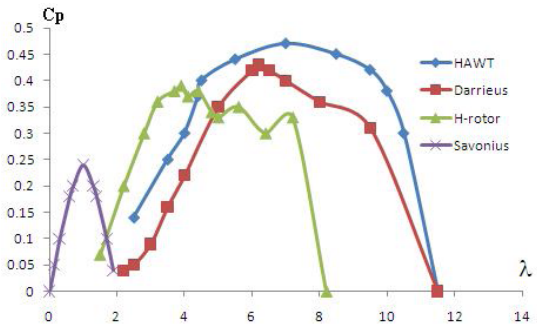

Fig. 2 - Power curves for different turbine types

ISSN 2067-5534 © 2012 JSE

Also, Savonius type wind turbines, which operate based on the principle of the aerodynamic drag, can provide high starting torque, can operate in areas with low wind potential or turbulent wind, and the manufacturing costs of the rotor blades can be very low, because they can be made, in many cases, by recycling other items such as metal and plastic drums or other similar cylindrical objects, aspects which makes them very attractive for low power electricity generation facilities.

2. VERTICAL AXIS WIND TURBINES

Vertical axis wind turbines may be divided, as was shown before, in two categories, depending on their operating principle: wind turbines that operate under the effect of aerodynamic lift and wind turbines that are operating under the principle of aerodynamic drag. The wind turbines from the first category need, in order to operate at full capacity, high wind speeds, similar with those needed in the case of horizontal axis wind turbines, this, combined with their lower power coefficient, makes this type of wind turbine to be less attractive for use at the expense of conventional wind turbines, with propeller type rotor. The turbines from the second category, because they are using the aerodynamic drag in order to get a rotational move, can operate in low wind conditions, at air speeds of about 2 to 4 m/s, and they are very suitable to be located in areas with low wind potential, how, as a matter of fact, most areas of our country are, areas where horizontal axis wind turbines are totally inefficient.

One of the main wind turbine from this category is the turbine invented by the Finnish researcher S.J. Savonius, which is composed of two semi-cylindrical or semi-elliptical blades placed in the shape of the letter "S", as shown in Figure 3, the convex and the concave side of the rotor being under the influence of the wind at the same time [5, 6].

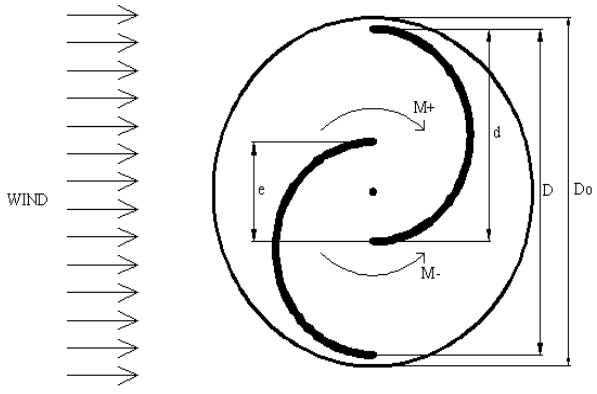

Fig. 3 - Principle scheme of the Savonius rotor D0 – endplate diameter; D – rotor diameter; e – gap distance; d – blade diameter

The operation of the Savonius rotor is based exclusively on the effect of aerodynamic drag and the rotational motion is possible because the coefficient of friction of the concave surface of the blade is greater than the one corresponding for the convex surface so that the force acting on the first surface is greater than the force acting on the second surface, generating a higher torque which moves the rotor. Because the torque which generates the rotational motion is the result of the difference between the torque provided by the force that is acting on the concave surface and the one that is acting on the convex side of the blade, the Savonius wind rotor has a relatively low performance coefficient of about 0.2 - 0.3. A very adequate solution for improving this power coefficient is to install a concentrator nozzle to the Savonius rotor (Fig. 4), in order to increase the speed of the air at the entry into the rotor and to direct the airflow only over the concave blade, thus providing the cancellation of the negative moment produced by the action of the wind on the convex side of the blades and to offer the possibility that the movement of the rotor to take place only under the action of the positive momentum, which leads to an increase of the rotor efficiency [7]. However, it should be noted that, by equipping the Savonius wind rotors with a wind concentrator, the possibility of the vertical axis wind turbines to receive wind from any direction, i.e. their omni-directional nature, will be cancelled.

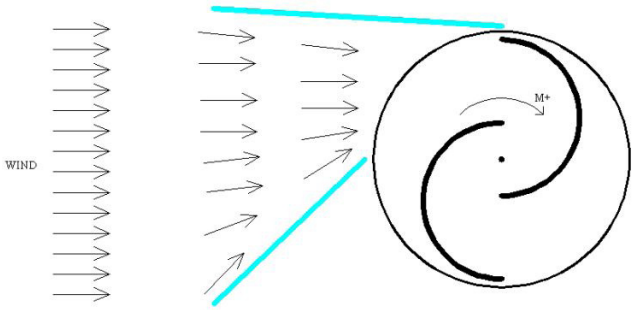

Fig. 4 - Savonius wind turbine equipped with a wind concentrator

3. EXPERIMENT SET-UP

Experimental studies were held in the Research Laboratory of the Faculty of Building Services of the Technical University of Cluj-Napoca. For the proper conduct of the experiments it was necessary to build an open subsonic wind tunnel, which can generate speeds o the air masses of 0 to 13 m/s, the manufacture of three types and configurations of vertical axis wind turbines based on the Savonius principle and the design of three wind concentrators with different constructive sizes.

3.1. Vertical axis wind turbines

All the rotors used in the experiments have the same constructive sizes, i.e. the diameter of the rotor, D=18 cm and height of the rotor, H=18 cm, so that the swept area of the rotors would be the same and all the wind rotors would benefit from the same amount of wind energy. The rotor blades were made of plastic materials (PET) and the endplates of the rotor of comatex, and they were placed on a metal frame by means of axial bearings [8]. The rotors were chosen so that the experimental study can cover the most common configurations of vertical axis wind turbines, namely:

- a simple Savonius rotor, with two semi-cylindrical blades and one stage of the rotor, with an overlap ratio of the blades, e/D=0.2 (Fig. 5);
- a double Savonius rotor, with two semi-cylindrical blades and two stages of the rotor (Fig. 6);
- a Savonius rotor, with two blades placed in the shape of the letter “Z”, design that offers a much

simpler design than the one in the case of the Savonius rotor, with semi-cylindrical blades (Fig. 7).

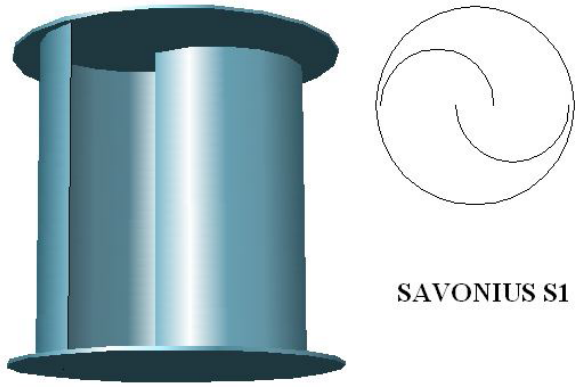

Fig. 5 - Single-stage Savonius wind rotor

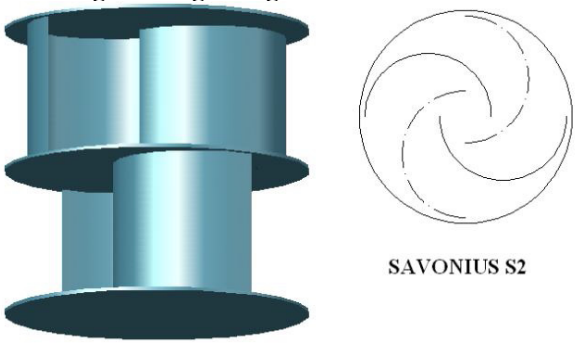

Fig. 6 - Double-stage Savonius wind rotor

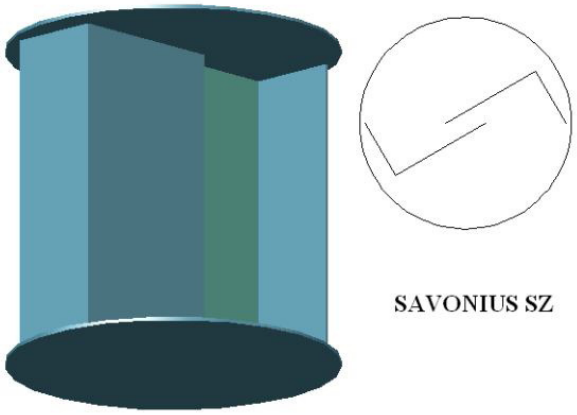

Fig.7 - Type "Z" Savonius wind rotor

3.2. Wind concentrators

In this experimental study three wind concentrators were used, which have been designed so that their central side have the same size as the rotor diameter, in order to exist a correlation between the overall sizes of the two components, i.e. concentrator and rotor, of the wind turbine [7]. The wind concentrators were made of comatex, their scheme and design principle are shown in Figure 8, and their constructive sizes, are summarized in Table 1.

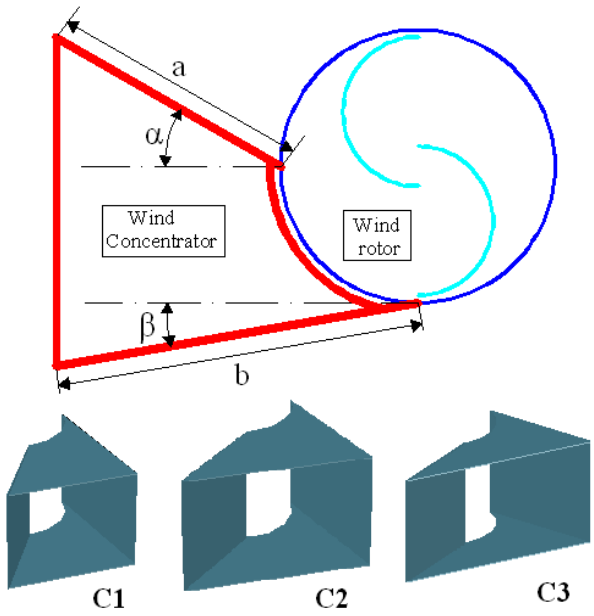

Fig. 8 - The constructive scheme of the concentrators used in the experimental study

Table 1 - The constructive sizes of the used wind concentrators

Type	Dimensions			
	a	b	α	β
C1	18 cm	25 cm	30°	10°
C2	18 cm	23 cm	45°	15°
C3	18 cm	21 cm	60°	25°

3.3. Aerodynamic wind tunnel

Uniform main flow is produced by an open-circuit subsonic wind tunnel [9, 10], presented in Figure 9, which has a rectangular exit section with dimensions of 300x300 mm. Airflow is provided with an axial fan that can deliver a maximum flow of 4300 m³/h.

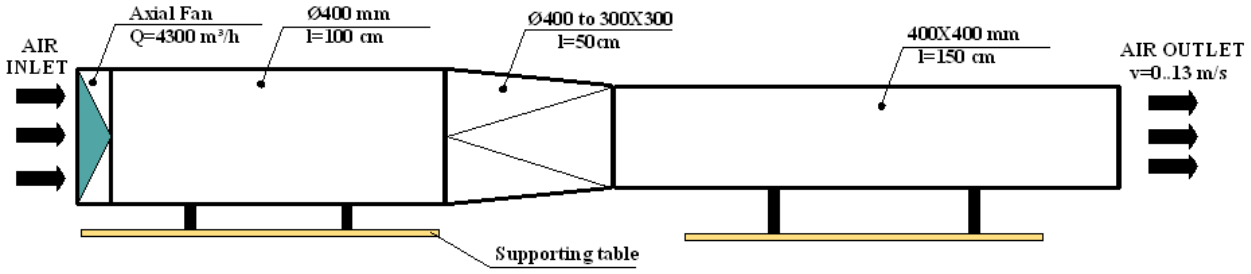

Fig. 9 - Aerodynamic subsonic wind tunnel

ISSN 2067-5534 © 2012 JSE

In terms of existing size of the exit section of the wind tunnel and the air flow circulated by the axial fan, the wind tunnel can provide air speeds, *v* up to 13 m/s. Figure 10 presents a single-stage Savonius wind rotor equipped with a wind concentrator, and the schematic diagram of the experimental installation is shown in Figure 11.

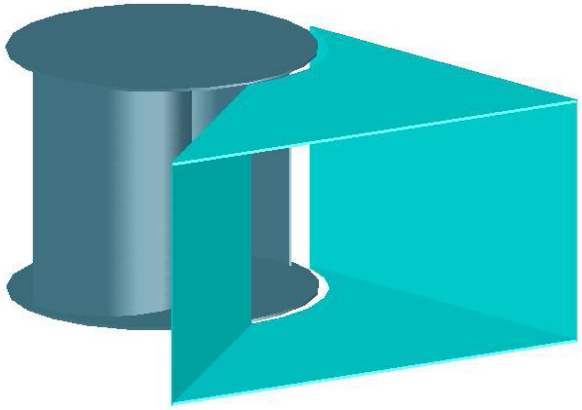

Fig. 10 - Savonius wind rotor equipped with a wind concentrator

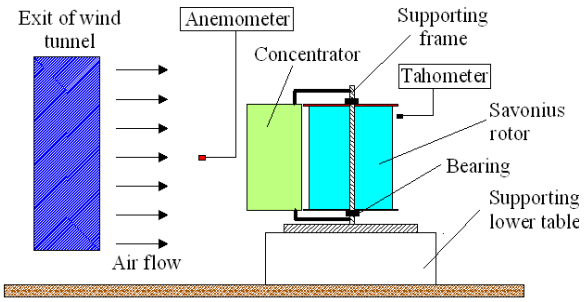

Fig. 11 - Schematic diagram of experimental set-up

4. RESULTS AND DISCUSSION

Although the wind tunnel that was available for the tests offers the possibility that the measurements to be made for winds speeds between 0 and 13 m/s, as vertical axis wind turbines, which are operating on the principle of aerodynamic drag, are of interest only in the case of low wind speeds, the measurements were performed for airflow speeds between 0 and 7 m/s. The air flow speed was monitored using a propeller anemometer placed at the exit of the wind tunnel and the rotational speed of the turbine, corresponding to different wind speeds, was recorded with a digital tachometer.

In the first part of the experiment, the three wind rotors have been subject to the same test conditions, the airflow speed was increased from 0 to7 m/s, with the aid of a speed controller mounted on the motor of the axial fan, and the correlation between the wind speed and the rotational speed of the rotor, unequipped with a wind concentrator, was monitored. The results obtained from the measurements were synthesized through the graphs presented in Figure 12, that show the correlation between the rotational speed (rpm) of the wind rotors and the speed of the air flow (or the wind speed, v).

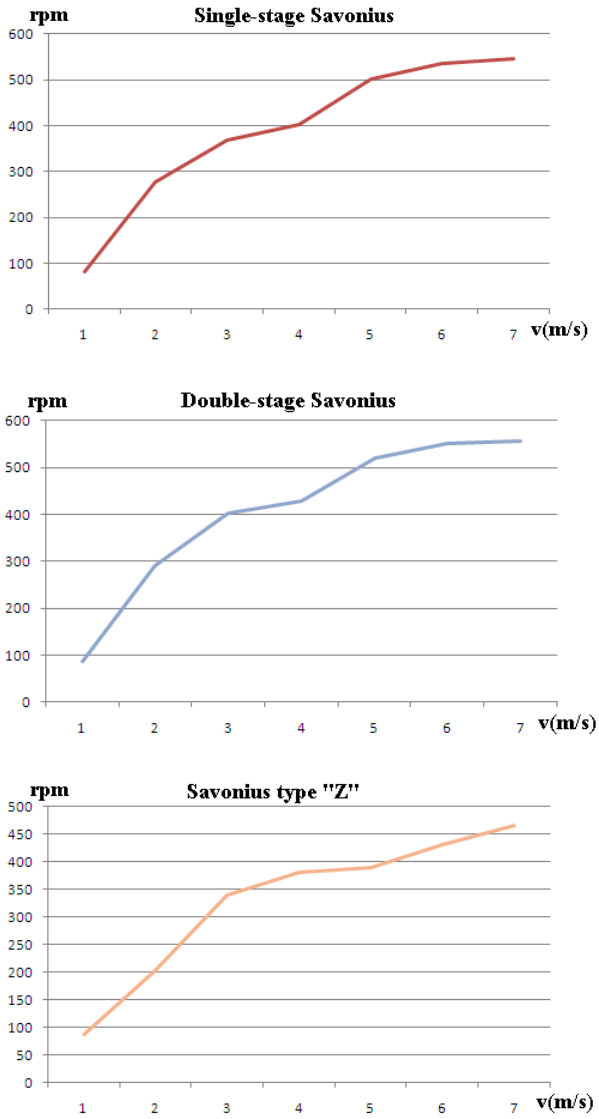

Fig. 12 - The *rpm-v* curves of the vertical axis wind turbines, VAWT's

In the second part of the experiment, the wind rotors were fitted in turn with each of the three wind concentrators and were subject to the same test conditions as those in the first phase of testing. Based on the data obtained from the measurements, the comparative charts (Fig. 13a, b, c) which are presenting the variation curves of the rotor speed depending on the speed of the air flow for all three configurations of the wind concentrators, as well as if the rotors were not equipped with a concentrator were made.

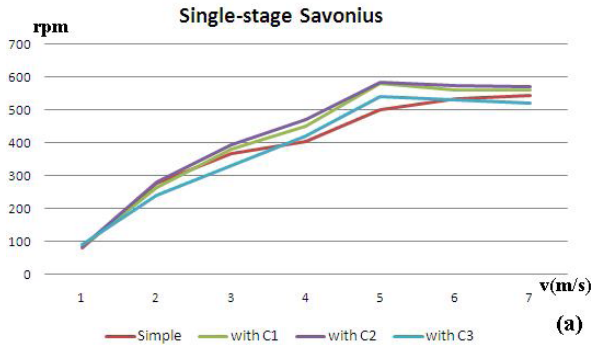

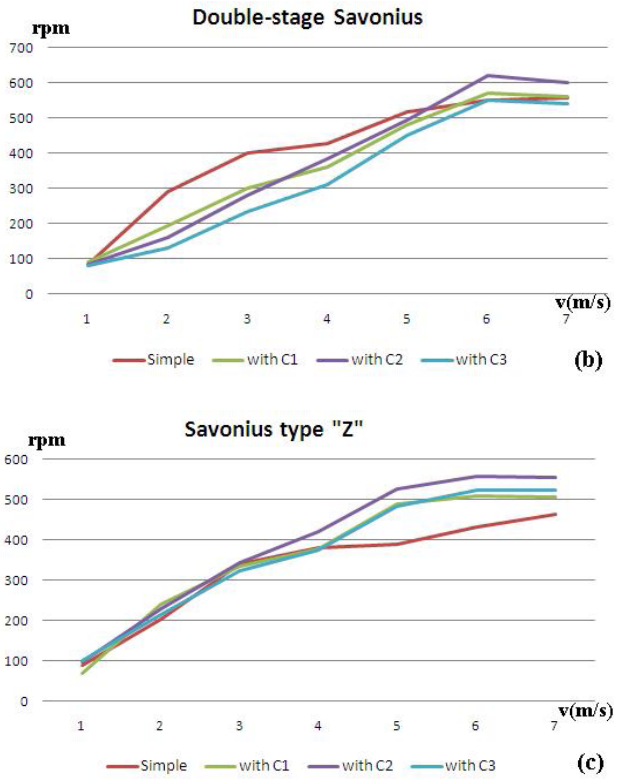

Fig. 13 - The *rpm-v* curves of the vertical axis wind turbines with and without a concentrator

After the graphs which are showing the *rpm-v* curves of the wind turbines with various constructive configurations were made, and by interpreting the results of the experimental tests, it has been observed that the Savonius rotor with two semi-cylindrical blades and two stages is the most efficient between the three vertical axis rotors used in the experiments, starting at the lowest wind speeds and reaching the highest rotational speeds for all the wind speeds for which it was tested, and thus is the most suitable to be used for electricity generation, in the configuration without a wind concentrator. Also, the Savonius type "Z" wind turbines should be taken into consideration for the replacement of Savonius wind turbines with semicylindrical or semi-elliptical blades, because it is a much more simpler and economical solution in terms of construction, even if this rotors can't reach the performances of the above-mentioned rotors.

Both in the case of the wind turbines with two semicylindrical blades and two stages of the rotor, and in the case of Savonius turbines with a type "Z" rotor, providing a wind concentrator leads to an improvement of the rotor speed by 10 to 20%, values that approach or even exceed the values recorded for the Savonius wind rotor with two stages, in both cases the best results being obtained with the "C2" type concentrator, so using wind concentrators is a very useful method for improving the performance of this type of wind turbines. Regarding the case of the Savonius wind turbines with two semicylindrical blades and two stages of the rotor, no significant improvements of the rotor efficiency are brought by the wind concentrator, its rotational speed having even lower values for wind speeds between 0 and 5 m/s. This is caused by the fact that the construction of the Savonius rotors with two stages, where the upper stage is rotated with 90° relative to the lower stage, is based on the very principle of reducing the negative moments acting on the rotor blades, just as in the case of wind concentrators.

It should also be noted that installing wind concentrators on vertical axis wind turbines will cancel the possibility of the turbines to receive wind from any direction, that is why this solution is appropriate only if the air flow has a predominantly unidirectional character, or if some constructive solutions are taken in order to keep the omni-directional nature of this wind turbines, such as the yaw mechanisms used at the horizontal axis wind turbine, with a propeller-type rotor (fig. 14).

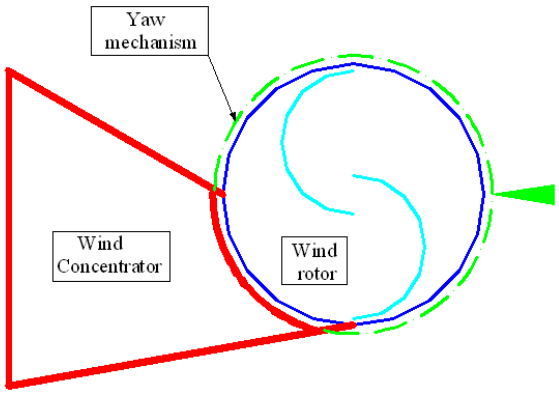

Fig. 14 - Vertical axis wind turbine equipped with a concentrator with a yaw mechanism

5. CONCLUSION

The use of vertical axis wind turbines, which are operating on the principle of aerodynamic drag, can be a very suitable solution for electricity generation in areas where the wind potential is low. However, the relatively low values of the power coefficient of these rotors make them to be very rarely used for equipping wind turbines installations. The improvement of the performance coefficient of these rotors can be achieved by several methods, one of which is the subject of this experimental study, namely equipping the wind rotors with wind concentrators. The most important results obtained after carrying out this experimental study are presented below:

- in the version without a wind concentrator, the rotors with two blades and two stages have the best efficiency;
- by equipping the rotors with wind concentrators, an increase of their efficiency by 10-20% is achieved, but only in the case of single-stage rotors; in the case of double-stage rotors the advantages of the provision of a wind concentrator are insignificant;
- the best results on improving the efficiency of vertical axis rotors were obtained when using concentrators "C2";
- the property of these wind rotors to receive wind from any direction is cancelled when a concentrator is mounted on the rotor, which is why this solution should be adopted only in the case of predominantly unidirectional air

ISSN 2067-5534 © 2012 JSE

currents.

- the use of wind concentrators equipped with yaw mechanisms is appropriate, but this solution should be carefully analyzed in terms of cost-benefit.

Acknowledgement

This paper was supported by the project „Doctoral studies in engineering sciences for developing the knowledge based society – SIDOC" contract no. POSDRU/88/1.5/60078, project co-funded from European Society Fund through Sectorial Operational Program Human Resources 2007 – 2013.

REFERENCES

[1]. Eriksson S., Bernhoff H., Leijon M. – Evaluation of different turbine concepts for wind power, Renewable and Sustainable Energy Reviews 12, 2008, pg. 1419-1434

[2]. Al-Bahadly I. – Building a wind turbine for a rural home, Energy for Sustainable Development 13, 2009, pg. 159-165

[3]. Hau E. – Wind Turbines, Springer, New York, 2006, pg. 81-89

[4]. Deda Altan B., Atilgan M., Ozdamar A. – An experimental study on the improvement of a Savonius rotor performance with curtaining, Experimental Thermal and Fluid Science 32, 2008, pg. 1673-1678

[5]. Deda Altan B., Atilgan M. – An experimental an numerical study on the improvement of the performance of Savonius wind rotor, Energy Conversion and Management, 2008, pg. 3425-3432

[6]. Savonius S.J. – The S-rotor and its applications, Mechanical Engineering 53, 1931, pg. 333-338

[7]. Deda Altan B., Atilgan M. – The use of a curtain design to increase the performance level of a Savonius wind rotors, Renewable Energy 35, 2010, pg. 821-829

[8]. Mussell D. – Build your own wind turbine, The Pembina Institute – Sustainable Energy Solutions, Ontario, 2006

[9]. Hayashi T., Li Y., Hara Y., Suzuki K. – Wind tunnel tests on a three-stage out-phase Savonius rotor, Tottori University, Tottori, 2011

[10]. Kamoji M.A., Kedare S.B., Prabhu S.V. – Experimental investigations on single stage, two stage and three stage conventional Savonius rotor , International Journal of Energy Research, vol 32, 2008, pg. 877-895.

PROMOTION OF THE ORGANIC RANKINE CYCLE BASED COGENERATION: OPPORTUNITIES AND CHALLENGES

VORONCA. M.-M.*, VORONCA S.-L.**, CRUCERU M.***
*Romanian Energy Efficiency Fund, Johann Strauss no. 2A, Bucharest,
**C.N.T.E.E. Transelectrica S.A., Olteni no. 2 - 4, Bucharest
***University "Constantin Brâncuşi" Târgu Jiu, Republicii no. 1, Târgu Jiu
mihai.voronca@free.org.ro

Abstract - Most economic operators are obviously power consumers, but only a few industrial companies report heat consumption for technological purposes. The recent implementation in Romania of modern solutions aiming at a "smarter" use of heat will prove that such companies might become power producers. Challenges still being the need for cost cutting and the competitiveness increase, such kind of 'actors' will be able to face easier the impact of other possible worldwide economic recession events. This paper aims at revealing the opportunities and challenges of promoting cogeneration based on Organic Rankine Cycle. Two relevant cases of investments already implemented by Romanian companies are studied from both the techno*logical** *and economical points of view.*

Keywords: heat waste, heat recovery, residual power, Organic Rankine Cycle, investment, profitability.

1. INTRODUCTION

At the beginning mankind has accidentally discovered fire and then, the biomass to heat. Rapidly, the heat was used not only for heating but also for food preparation purposes. In consequence heat became useful and helped men to develop themselves. The heat has helped man to get more evolved hunting tools, to manufacture goods for living and to start trading them. During all Ages coming after, heat has helped mankind to evolve.

Obtained from coal and centuries after from oil and gas, the heat we use today i.e. for heating, cooling and power generation is expensive and polluting. Traditionally, for heat and power generation purposes the "friendly" water was the working liquid compared to cooling where "environmental aggressive" refrigerant liquids were used. Facing reinforced environmental constraints, several actions aiming at impact mitigation were put in place in the last decades. These were the ways we have learned to limit heat waste and to promote heat recovery. And more importantly, we have started to explore methods of heating, not only power "greening".

2. WATER V.S. ORGANIC FLUID

The technology used for fossil fuel fired power generation in a classic Rankine Cycle (fig. 1) involves a fuel fired steam boiler which produces a certain amount of superheated steam. The rated pressure may vary between 28 to 36 bars and the temperature between 320°C and 360°C.

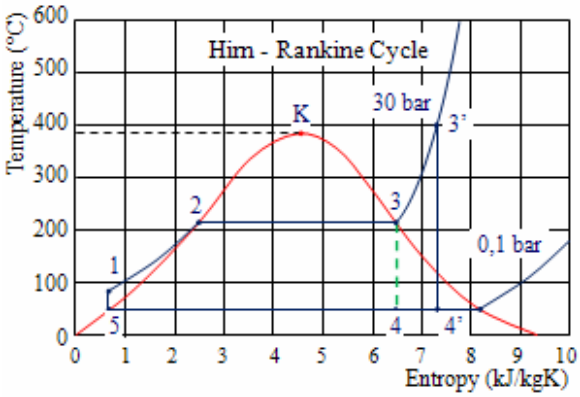

Fig. 1. Hirn - Rankine Cycle:
1-2-3 Boiler Steam Generation; 3-4 Turbine Steam Expansion; 4-5 Condenser Steam Condensation; 5-1 Pressure Increase in Feed Pump (source: http://www.orcycle.be/)

This steam drives the steam turbine which transfers the energy to the generator via gears and coupling. With the single-stage turbine used in small power plants it is possible to obtain power with an electric efficiency of 12-14% from the energy input.

Steam turbines are generally suitable for CHP plants with an electrical output greater than 2MW. The condenser transforms the turbine outlet low pressure steam into liquid which is fed back to the boiler. In combined heat and power schemes (CHP), the condenser's cooling heat is frequently fed into a heating circuit such as district heating.

For superheated steam generation purposes, important amount of heat as well as fuel are needed. The absence of only nowadays adopted environmental constraints has encouraged the extensive use of fossil fuels, relatively accessible in geographical and financial terms.

Increased efforts aiming at heat recovery and "greening" have oriented the scientific works towards

ISSN 2067-5534 © 2012 JSE

the identification of substitute liquids. First "reported victims" were the substances used for refrigeration. Alternatives to Ammonia and Freon as Chlorofluorocarbons and Hydro-chlorofluorocarbons were identified. Today, the prospect of the previously mentioned fluids phasing out is orienting efforts towards the organic fluids use.

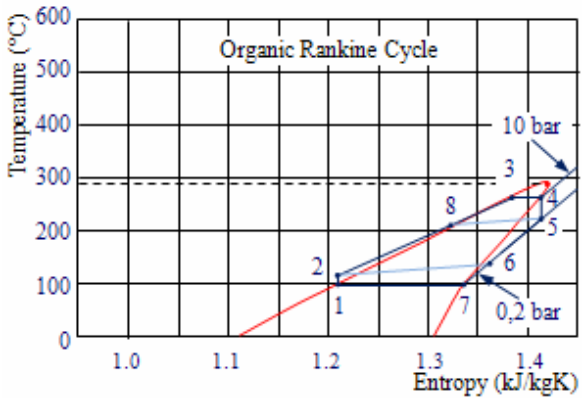

Fig. 2. Organic Rankine Cycle: 2-8-3-4 Evaporator Vapour Generation; 4-5 Turbine Vapour Expansion; 5-6-7-1 Condenser Vapour Condensation; 1-2 Pressure Increase in Feed Pump (source: http://www.orcycle.be/)

When the water is replaced by an organic fluid in a classic Rankine Cycle, this one (fig. 2) is called an Organic Rankine Cycle (ORC). The most modern ORC technology used implies the circulation of the organic fluid in a closed circuit: vaporisation of the high pressure liquid by heat recovered from primary processes or "green" heat exchange within the evaporator, expansion of the vapour within a slow-moving axial turbine based along similar principles to a steam turbine, condensation of low pressure vapour by cooling within the condenser and the increase of liquid pressure with the feed pump. All general thermodynamic laws remain always applicable: the bigger the temperature difference between evaporator and condenser, the higher the cycle efficiency is.

Most of the organic fluids are so called dry fluids. These dry fluids have the advantage that they remain superheated after expansion, so condensation of the fluid in the turbine can be avoided. Some commonly used organic fluids are pentane, propane, toluene, ammonia and some coolants. As these organic fluids have a lower evaporation point than water, the ORC based technology runs properly at a lower temperature of 300°C (in figure 2, the highest temperature of the heat source is about 280°C), and a working pressure of 10.0 bar. Condensation occurs at 100°C (0.2 bars), which makes the cooling heat still usable for heating purposes.

The ORC electric efficiency is around 17% of the total energy input, which is about 3% higher than traditional steam turbines. ORC units are suitable for geothermal and biomass CHP plants with an electric output as small as 200 kW. Single ORC units go up to 2MW in size and multiple units can be installed to increase capacity.

Compared to classic units, the ORC system performs well under partial load because of the low working pressures and temperatures.

The purpose of this paper is to present challenges and opportunities of Organic Rankine Cycle based on cogeneration technologies promotion. The related results and conclusions of a generally recognised methodology based investigation [1] are to be highlighted, too.

2. METHODOLOGY

In Annex III of the Directive 2004/8/EC on the promotion of cogeneration - based solutions on a useful heat demand in the internal energy market [1], the amount of primary energy savings provided by cogeneration production is determined with the formula:

$$PES = \left(1 - \frac{1}{\frac{CHP\ H\eta}{Ref\ H\eta} + \frac{CHP\ E\eta}{Ref\ E\eta}}\right) \times 100\% \ , \quad (1)$$

where:

PES - the primary energy savings;

CHP Hη - the heat efficiency of the cogeneration production, defined as an annual useful heat output divided by the fuel input used to produce the sum of useful heat output and electricity from cogeneration;

REF Hη - the efficiency reference value for separate heat production;

CHP Eη - the electric efficiency of the cogeneration production defined as annual electricity from cogeneration divided by the fuel input used to produce the sum of useful heat output and electricity from cogeneration;

REF Eη - the efficiency reference value for separate electricity production;

The use of this method, the same presented in [2], is motivated by the fact that the" Organic Rankine cycles" is listed in the Annex I of the Directive 2004/8/EC [1]. As indicated in Annex III of the Directive 2004/8/EC [1], such technology could be also classified as high-efficiency cogeneration.

As considered in the precedent paper"Installation of a Cogeneration Unit within a Chemical Company" [2], the purposes of using the previously mentioned method consist in promptly delivering valid data referring to an existing situation analysing the efficiency of the separate production of heat and electricity, while collecting accurate information regarding the efficiency of the Organic Rankine cycle based cogeneration technology. Consequently, in the following chapter authors are proposing a detailed investigation on such ORC technology that facilitates the "power extraction" from waste or recovered heat based on cogeneration premises. Authors propose two theoretical cases which are below considered: geothermal and respectively biomass based cogeneration.

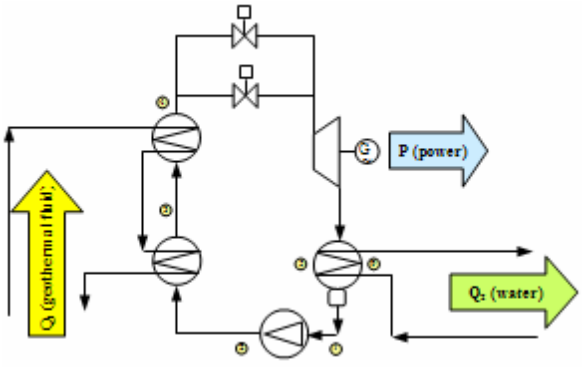

Fig. 3. Geothermal ORC Cogeneration Unit
(source: http://www.electratherm.com/)

The processes depicting the geothermal based thermodynamic cycle of figure 2 implies a high pressure regenerator, an evaporator, a vapour expander coupled to a power generator, a condenser, and a pump (fig. 3). The working liquid is compressed by a feed pump (1→2) and then transferred to the regenerator where the liquid is preheated (2→3) due to second stage geothermal water cooling and then transferred to the evaporator where it is transformed in vapour (3→4). The high pressure organic vapours are expanded into a turbine (4→5). After expansion, the superheated vapours enter the condenser where vapours are transformed into liquid (5→1). Finally, the liquid pressure is then increased with the feed pump (1→2) and circulated back to the regenerator.

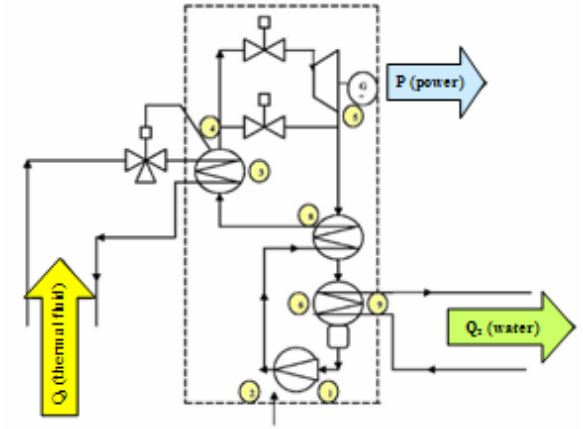

Fig. 4. Biomass fired ORC Cogeneration Unit
(source: 1.2 MW_e High Efficiency Cogeneration Unit, Energy - Serv S.R.L. Bucharest)

The processes depicting the biomass based thermodynamic cycle of figure 2 imply an evaporator, a vapour turbine coupled to a power generator, a condenser, a low pressure regenerator and a pump (fig. 4). The working organic liquid is compressed by a feed pump (1→2) and then transferred to the evaporator where it is transformed in vapour (8→3→4) due to the transfer of heat from high temperature thermal oil to the organic liquid. The thermal oil is initially heated in a biomass fired boiler. The high pressure organic vapours are expanded into a turbine (4→5). As the vapours remain superheated after expansion, a regenerator placed before the condenser is cooling the vapours (5→6) and preheating the liquid before the inlet into evaporator (2→8). From the regenerator outlet the vapours are condensed (6→1) and the liquid pressure is then increased with the feed pump (1→2), sent to the regenerator and circulated back to the evaporator.

3. PROJECT HIGHLIGHTS

3.1. Technical description of a geothermal based ORC cogeneration unit

The considered geothermal based ORC cogeneration unit operates on geothermal water with a temperature of 105ºC (low enthalpy heat source), and transfers the heat to a "R 245 fa" type fluid which moves from liquid to vapour state (process 3→4 in fig. 2). The process occurs within the evaporator as already indicated (fig. 3), with a rated thermal power from 400 kW_{th} to 860 kW_{th} and for a certain amount of geothermal water flow rate available (i.e. 12.6 l/s), the total annual heat amount recovered from the geothermal water could be of about 5,154 $MW_{th}h$/year.

Fig. 5. Twin Screw Expander
(source: http://www.electratherm.com/)

In correlation with the cooling groundwater average temperature of 10ºC (essential for the amplitude of expansion 4→5 of fig. 2) crossing the condenser (fig. 3), the twin screw expander also known as a Lysholm type motor (fig. 5), coupled to a synchronous power generator with the rated electric power from 30 kW_e to 65 kW_e, leads to a total annual gross amount of generated power of 382 MW_eh/year (i.e. the equivalent of a total annual net amount of 303 MW_eh/year).

Following various manufacturers' technical specifications, the rated power of the considered cogeneration unit may vary in-between 30 and 65 kW at a rated voltage of 380 V and frequency of 50 Hz, the operation being possible for environmental temperatures from -29ºC to 49ºC. The power factor is 97% and distortions due to harmonics are of 2% for voltage and of 10% for intensity. The noise level is 92 dB at 3 m distance. Lysholm type motors operate at low speed without gear box or oil pump and have a 3:1 turn down ratio.

For an adequate groundwater flow rate (i.e. the equivalent of 5.7 l/s), a total annual amount of about 4,747 $MW_{th}h$/year (in addition to the initial energy content of the ground water) is transferred from the

ISSN 2067-5534 © 2012 JSE

condenser with a rated thermal power from 370 kW_{th} to 795 kW_{th} of the considered ORC cogeneration unit and sold to the district heating system for sanitary water preparation purposes.

The thermodynamic net efficiency of power generation for geothermal based ORC cogeneration unit is 7%, value which will be associated to the variable CHP $^{G}E\eta$.

3.2. Technical description of a biomass based ORC cogeneration unit

The considered biomass based ORC cogeneration unit operates on wooden waste from a wood processing factory, along with two other biomass fired boilers for hot water, and respectively warm water production.

The biomass fired boiler integrated to the ORC cogeneration unit has the rated capacity of 8 MW_{th} and transfers the generated heat to a thermal fluid at a rated temperature of 320˚C. Facing moderate heat fluxes due to the low caloric value of wooden waste (i.e. 9.000 kJ/kg), the thermal fluid can easier take over heat than the water, the related heat transfer efficiencies being as much as 5% to 8% higher for hot oil systems than conventional steam ones.

Leaving the biomass fired boiler, the thermal fluid enters the evaporator of the ORC cogeneration unit where the transformation (3→4 in fig. 2) of the organic fluid (i.e. silicon oil) occurs from liquid to vapour.

The vapour expansion (4→5 in fig. 2) powers a blades type turbine (fig. 4) with good efficiency (up to 90%), low mechanical stress due to low peripheral speed, low RPM allowing the direct drive of the synchronous generator without reduction gear, no erosion of the turbine blades due to the absence of the moisture in the vapour nozzles and very long operational life of the machine due to the characteristics of the working fluid that, unlike steam, is non eroding and non corroding for valve seats tubing and turbine blades.

The turbo generator has a gross rated electric power of 1,317 kW_e or a net rated electric power of 1.2 MW_e.

To increase the overall efficiency of the ORC cogeneration unit, the regenerator with a rated capacity of 4 MW_{th} placed before the condenser decreases the superheated vapour enthalpy (5→6 in fig. 2) for preheating purposes and the condenser with a rated capacity of 5.4 MW_{th}, transforms the vapours in liquid (6→1 in fig. 2).

For the considered biomass fired ORC cogeneration unit on annual basis operation, the total annual generated "useful" heat amount for warm water purposes is of about 35,418 $MW_{th}h$, and an additional "residual" annual generated power amount of 6,450 MW_eh.

The thermodynamic net efficiency of power generation for the biomass fired ORC cogeneration unit is 12%, value which will be associated to the variable CHP $^{B}E\eta$.

3.3. Estimated Primary Energy Savings

Authors are assuming that the projects are implemented by industrial companies which are eligible customers, in line with the definitions from Directive 2003/54/EC [3]. For energy savings calculation reasons, authors have kept the assumption that the electricity market is still dominated by fossil fuel-based electricity producers [2]. Consequently, the efficiency reference value of 31.85% [4] for separate electricity production in Romanian thermal power plants is to be associated to the variable REF Eη from the formula (1).

For the variable CHP Eη from the formula (1), the values CHP $^{G}E\eta$ and CHP $^{B}E\eta$ are to be in each case assigned, in order to determine the estimated primary energy savings for geothermal based and biomass based cogeneration units.

The value associated to the variable REF Hη from the formula (1) is 92%. Authors are deeming that separate heat generation is to be considered as efficient as possible, in order to limit the favourable effect of using renewable energy sources in the analysed cases for power generation.

Annex II of the Directive 2004/8/EC [1] mentions that the overall efficiency for micro-cogeneration units should be calculated based on certified values. Authors have assumed the overall efficiency values provided by manufacturers (i.e. Electratherm USA, Turboden Italy). The considered overall efficiency of the geothermal based ORC cogeneration unit is 98.39% and for biomass based ORC cogeneration unit is 82.72%, respectively. For the already specified CHP $^{G}E\eta$ and CHP $^{B}E\eta$, the thermodynamic efficiencies of condensers integrated to the considered ORC cogeneration units assigned as the values CHP $^{G}H\eta$ and CHP $^{B}H\eta$ of variable CHP Hη in formula (1) are 91.39% and 70.72%.

Based on the methodology from Annex III of the Directive 2004/8/EC [1], the estimated primary energy savings ^{G}PES of the geothermal based ORC cogeneration unit are:

$$^{G}PES = \left(1 - \frac{1}{\frac{CHP\ ^{G}H\eta}{Ref\ H\eta} + \frac{CHP\ ^{G}E\eta}{Ref\ E\eta}}\right) \times 100\% = \left(1 - \frac{1}{\frac{91.39}{92.00} + \frac{7.00}{31.85}}\right) \times 100\% = 17.57\%. \quad (2)$$

Similarly, the estimated primary energy savings ^{B}PES of biomass based ORC cogeneration unit are:

$$^{B}PES = \left(1 - \frac{1}{\frac{CHP\ ^{B}H\eta}{Ref\ H\eta} + \frac{CHP\ ^{B}E\eta}{Ref\ E\eta}}\right) \times 100\% = \left(1 - \frac{1}{\frac{70.72}{92.00} + \frac{12.00}{31.85}}\right) \times 100\% = 12.70\%. \quad (3)$$

Both determined ^{G}PES and ^{B}PES values qualify the ORC cogeneration units as highly efficient, as Annex III stipulates that the "cogeneration production from cogeneration units shall provide primary energy savings calculated according to point (b) of at least 10% compared with the references for separate production of heat and electricity".

For primary energy savings calculation purposes, it should be assumed that both annual amounts of heat and electricity from cogeneration are to be considered as separate types of generation, where, on one hand, the heat is produced within modern heat plant with 92% efficiency (a disadvantageous assumption for the intended comparison), and on the other hand power is generated in thermal power plants with 31.85% efficiency [4].

In the case of geothermal based ORC cogeneration unit, the annual amount of heat $^{G}H_{CHP}$ is 1.319 MJ/year. For a thermodynamic efficiency CHP ^{G}Hη of 91.39%, the resulting annual primary energy consumption $^{G}PEC_{CHP}$ is:

$$^{G}\mathrm{PEC}_{CHP} = \frac{^{G}\mathrm{H}_{CHP}}{\mathrm{CHP}\ ^{G}\mathrm{H}\mu} = \frac{1.319\,\mathrm{MJ/year}}{91.39\,\%}$$
$$^{G}\mathrm{PEC}_{CHP} = 1.443\ \frac{\mathrm{MJ_{PE}}}{\mathrm{year}} \quad (4)$$

For the separate heat and power generation, considering that the total annual amount of heat $^{G}H_{SEPARATE}$ is 1.319 MJ/year and the total annual amount of electricity $^{G}E_{SEPARATE}$ is 0.084 MJ/year for REF Hη of 92% and REF Eη of 31.85%, %, the resulting annual primary energy consumption $^{G}PEC_{SEPARATE}$ is:

$$^{G}\mathrm{PEC}_{SEPARATE} = \frac{^{G}\mathrm{H}_{SEPARATE}}{\mathrm{REF\ H}\eta} + \frac{^{G}\mathrm{E}_{SEPARATE}}{\mathrm{REF\ E}\eta};$$
$$^{G}\mathrm{PEC}_{SEPARATE} = \frac{1.319\,\mathrm{MJ/year}}{92\%} + \frac{0.084\,\mathrm{MJ/year}}{31.85\%}; \quad (5)$$
$$^{G}\mathrm{PEC}_{SEPARATE} = 1.698\,\frac{\mathrm{MJ_{PE}}}{\mathrm{year}}.$$

In conclusion, the resulting annual primary energy savings for the geothermal based ORC cogeneration unit $^{G}PEC_{SAVINGS}$ is

$$^{G}\mathrm{PEC}_{SAVINGS} = {}^{G}\mathrm{PEC}_{SEPARATE} - {}^{G}\mathrm{PEC}_{CHP};$$
$$^{G}\mathrm{PEC}_{SAVINGS} = 1.698\,\frac{\mathrm{MJ_{PE}}}{\mathrm{year}} - 1.443\,\frac{\mathrm{MJ_{PE}}}{\mathrm{year}}; \quad (6)$$
$$^{G}\mathrm{PEC}_{SAVINGS} = 0.255\,\frac{\mathrm{MJ_{PE}}}{\mathrm{year}}.$$

In the case of biomass based ORC cogeneration unit, the annual amount of heat $^{B}H_{CHP}$ is 9.838 MJ/year. For a thermodynamic efficiency CHP ^{B}Hη of 70.72%, the resulting annual primary energy consumption $^{B}PEC_{CHP}$ is:

$$^{B}\mathrm{PEC}_{CHP} = \frac{^{B}\mathrm{H}_{CHP}}{\mathrm{CHP}\ ^{B}\mathrm{H}\mu} = \frac{9.838\,\mathrm{MJ/year}}{70.72\,\%}$$
$$^{B}\mathrm{PEC}_{CHP} = 13.912\ \frac{\mathrm{MJ_{PE}}}{\mathrm{year}} \quad (7)$$

For the separate heat and power generation, considering that the total annual amount of heat $^{B}H_{SEPARATE}$ is 9.838 MJ/year and the total annual amount of electricity $^{B}E_{SEPARATE}$ is 1.792 MJ/year for REF Hη of 92% and REF Eη of 31.85%, the resulting annual primary energy consumption $^{B}PEC_{SEPARATE}$ is:

$$^{B}\mathrm{PEC}_{SEPARATE} = \frac{^{B}\mathrm{H}_{SEPARATE}}{\mathrm{REF\ H}\eta} + \frac{^{B}\mathrm{E}_{SEPARATE}}{\mathrm{REF\ E}\eta};$$
$$^{B}\mathrm{PEC}_{SEPARATE} = \frac{9.838\,\mathrm{MJ/year}}{92\%} + \frac{1.792\,\mathrm{MJ/year}}{31.85\%}; \quad (8)$$
$$^{B}\mathrm{PEC}_{SEPARATE} = 16.319\,\frac{\mathrm{MJ_{PE}}}{\mathrm{year}}.$$

In conclusion, the resulting annual primary energy savings for the geothermal based ORC cogeneration unit $^{B}PEC_{SAVINGS}$ is

$$^{B}\mathrm{PEC}_{SAVINGS} = {}^{B}\mathrm{PEC}_{SEPARATE} - {}^{B}\mathrm{PEC}_{CHP};$$
$$^{B}\mathrm{PEC}_{SAVINGS} = 16.319\,\frac{\mathrm{MJ_{PE}}}{\mathrm{year}} - 13.912\,\frac{\mathrm{MJ_{PE}}}{\mathrm{year}}; \quad (9)$$
$$^{B}\mathrm{PEC}_{SAVINGS} = 2.407\,\frac{\mathrm{MJ_{PE}}}{\mathrm{year}}.$$

Considering both the geothermal based and biomass based ORC cogeneration units, the annual amounts of energy saved are significantly greater that those determined with the relations (6) and (9) as long as renewable energy sources are used for power and heat generation against fossil fuels. In conclusion, the total annual amount of energy saved by using geothermal energy is 1.698 MJ_{PE}/year and the total annual amount of energy saved by using biomass is 16.319 MJ_{PE}/year.

3.4. Adequate Financial Prospects

In the case of the geothermal based ORC cogeneration unit, the power extraction from geothermal heat is financially adequate due to avoided costs related to fuel and power purchasing expenditures [2] and to earnings from heat supply. The aggregation of limited financial costs (i.e. royalty of 4% p.a.) for using the underground geothermal water, with free of charge generated power to cover the pumping demand (i.e. power supply price of 107 □/MW_eh, VAT excluded) and earnings from heat sold to the district heating system (i.e. heat supply price of 13 □/MW_{th}h, VAT excluded), could represent annual financial benefits amounting to 91,291 □/year. Investment favourable circumstances are created by the opportunity to access such "cheap heat", authors naming here the geothermal energy, and the possibility to increase the heat supply in the district heating system.

In the case of the biomass based ORC cogeneration unit, the power extraction from waste heat (wooden waste) is financially adequate exclusively due to avoided costs related to fuel and power purchasing expenditures [2]. The annual financial benefits (i.e. power supply price of 68 □/MW_eh, VAT excluded) could be evaluated at an amount of 439,917 □/year. Access to "no cost" or "low cost" wooden waste as well as important amounts of heat for drying purposes and power needed in technological processes are opportunities creating a favourable investment environment.

ISSN 2067-5534 © 2012 JSE

3.5. Favourable Environmental Impact

The use of such ORC technologies for cogeneration purposes is environmentally friendly as long as the heat is generated by using renewable energy sources. As indicated in paragraph 3.3, for a total annual heat amount extracted for geothermal energy is 1.698 MJ_{PE}/year representing the equivalent of 525 toe/year. Based on the records published by the International Energy Agency in 2010 [5], specifying that one toe_{TPES} in Romania would emit 2.28 tonnes of CO_2, it results that the avoided emissions of CO_2 are 1,198 tonnes CO_2/year.

Similarly, the equivalent of the total annual amount of 16.319 MJ_{PE}/year energy saved by using the biomass is 5,052 toe/year. Based on the same records published by the International Energy Agency in 2010 [5], it results that the avoided emissions of CO_2 are11,517 tonnes CO_2/year.

Both cases could justify the authors' opinion that ORC technology based cogeneration is greening the environment.

3.6. Total Investment

The total investment for the geothermal based cogeneration unit (www.electratherm.com) is expected to amount to □193,182 (Table 1). The investment is supposed to rise the annual financial benefits amounting to 91,291 □/year, representing the equivalent of 47% from the total investment.

Table 1

Geothermal Cogeneration Project	□
Geothermal based ORC cogeneration unit (evaporator, expander, condenser, pump, preheater etc.)	151,515
Other equipment, raw materials etc.	18,939
Design, Engineering, Erection Works, Commissioning	22,727
Total	**193,182**

Costs in Table 1 do include custom duties (as the manufacturer is from Reno, Nevada, United States of America), storage taxes, transportation fees and authorisation taxes and do not include VAT.

Following the estimations of the Feasibility Study depicting the chosen technical solution, the total investment for the biomass based cogeneration unit is expected to come to □5,227,273 (Table 2). The investment is supposed to rise annual financial benefits amounting to 439,917□/year, representing the equivalent of 8% from the total investment size.

Table 2

Biomass Cogeneration Project	□
Biomass based ORC cogeneration unit (thermal oil boiler, evaporator, expander, condenser, pump, regenerator etc.)	4,772,727
Other equipment, raw materials etc.	189,394
Design, Engineering, Erection Works, Commissioning	265,152
Total	**5,227,273**

Costs in Table 2 do not include custom duties (as the manufacturer is an Italian company), storage taxes and VAT, but include transportation fees and authorisation taxes.

4. RESULTS AND DISCUSSIONS

4.1. Performance Indicators Values

To determine the investment performance indicators [6] authors have adopted the notations from [2], respectively a - the discount rate, h - the year of expenditure or earning, d - the duration of erection works, D - the lifetime of investment V_h - the annual revenue in year h, C_h - the annual expenditure in year h, and I_h - the annual investment in year h.

Based on the discounted cash flow CF_h determined with the relation (10):

$$CF_h = [V_h - (I_h + C_h)]\frac{1}{(1+a)^h},\ h = \overline{1, D+d} \quad , (10)$$

the net present value NPV was obtained with the relation (11):

$$NPV = \sum_{h=1}^{d+D}\frac{V_h}{(1+a)^h} - \sum_{h=1}^{d+D}\frac{I_h + C_h}{(1+a)^h} > 0 \quad , (11)$$

the internal rate of return IRR being analytically calculated with the relation (12):

$$IRR = a_{min} + (a_{max} - a_{min})\frac{NPV_+}{NPV_+ + |NPV_-|} \quad . (12)$$

Relations (13) are used for the gross payback time GPT and the discounted payback time DPT:

$$\sum_{h=1}^{GPT}[V_h - (I_h + C_h)] = 0\ ,\sum_{h=1}^{DPT}\frac{V_h - (I_h + C_h)}{(1+a)^h} = 0\ . \quad (13)$$

For the case of geothermal based ORC cogeneration unit, the values associated to the investment performance indicators were obtained with a discount rate of a = 12%, for a duration of erection works d = 1 year, a lifetime of investment D = 20 years, with annual net revenues V_h = □91,291, and annual expenditures C_h = 0, for an investment in the year d of I_h = □193,182 (for any other year h from the interval d, D + d, I_h being null). The values are presented in Table 3.

Table 3

Geothermal based ORC Cogeneration Project					
Investment Performance Indicators					
a	12	%	**C_h**	0	□
V_h	91,291	□	**I_h**	193,182	□
GPT	2.1	years	**NPV**	488,711	□
DPT	2.6	years	**IRR**	47	%

The values associated to the investment performance indicators for the biomass based ORC cogeneration unit were determined in similar conditions, exception making the annual net revenues V_h = □439,917 and the investment in year d I_h = □5,227,273. Against an initial value of the discount rate of 12% leading to inappropriate values of investment performance indicators, authors have considered a discount rate of 5% as recommended in financial analyses aiming at accessing the financial resources from Structural Instruments. The values for this presumption are presented in Table 4.

Table 4

Biomass based ORC Cogeneration Project					
Investment Performance Indicators					
a	5	%	**C_h**	0	□
V_h	439,917	□	**I_h**	5,227,273	□
GPT	11.9	years	**NPV**	255,065	□
DPT	18.5	years	**IRR**	6	%

4.4. Financing: decisions to take

Information presented in tables 3 and 4 has been obtained by authors based on cash flow projections in both cases of ORC based cogeneration and without taking into consideration a possible participation to the Tradable Green Certificates Scheme in Romania, financially rewarding investments leading to the power generation based on capitalisation of renewable energy sources. A very predictable rise of the electricity price in 2013 as effect of national power liberalisation has not been taken into account, either.

Both cases of ORC based cogeneration investments are valuable as long as energy savings and CO_2 emission mitigations are obtained. Additionally, the "power extraction" from recovered or waste heat partially transforming initial consumers in power producers represents another challenging advantage.

In the case of the geothermal based ORC cogeneration technologies, the investment is commercially attractive and is to be very rapidly implemented as long as the values associated to the investment performance indicators (in table 3) are good looking even for decision makers of the banking sector. A Romanian company is expected to implement such investment in the very next future.

For the implementation of investments aiming at promoting biomass based ORC cogeneration, the values from table 4 do not encourage a commercial approach but they present adequacy for an action aiming at accessing financial resources from Structural Instruments, which were designed especially for such investments. After a longer than initially considered period for such financial engineering setting up, the first Romanian biomass based ORC cogeneration unit is presently under implementation and is to be commissioned in June 2012 at the latest.

After their commissioning before mid-2012, both investments will generate more than the initially estimated benefits, demonstrating that the ORC based cogeneration technologies are financially viable.

5. CONCLUSIONS

An inventory of end-users reporting basically heat consumption for technological purposes will probably reveal that not so many industrial sectors are involved. But even so, companies generating waste heat or having good prospects for heat recovery do exist and might be targeted to apply for ORC based cogeneration. As this paper shows, the recent implementation in Romania of modern solutions aiming at such "smarter" use of heat will prove that such end-users might become power producers. Two relevant sectors were considered: wooden furniture industry and geothermal based heat generation for district heating purposes. Authors have noted that information about the implementation of such ORC based technologies in petrochemical industry is available too.

As it was presented, in line with low values associated to the thermodynamic efficiency of Organic Rankine Cycle, the related based cogeneration asks for a complete use of condensers' cooling heat for technological purposes. This is mainly the reason for which the power "leaving" the Cycle is called "residual", in line with the provisions of the EU relevant pieces of legislation appealing to high efficient cogeneration.

Alternatively, "forcing" the increase of generated power in an ORC based cogeneration unit is possible, if required so. But the operation is less efficient as long as the evacuated heat in excess cannot be used. Consequently, the heat "resource" (wasted or recovered) is inefficiently exploited.

ORC technologies are now mature and results irrefutable. For certain cases, less attractive financial prospects will come to an appropriate end; premises of an already announced 2013 electricity price increase and the operation of Tradable Green Certificates Scheme are solid.

ORC based cogeneration requirements are (i) the "heat resource" being available, accessible and affordable and (ii) steady heat use demand.

The implementation of such applications encourage authors to consider that cogeneration in Romania by using ORC based technologies represents the new investment trend in energy end user behaviour change, with a favourable cost cutting, security of supply improvement and competitiveness increase.

REFERENCES

[1]. *** Directive 2004/8/EC of the European Parliament and the Council on 11 February 2004 on the promotion of cogeneration based on a useful heat demand in the internal energy market and amending Directive 92/42/EEC, Official Journal of the European Union L52, 2004, pp. 50 - 60.

[2]. M.-M., Voronca, S.-L. Voronca, M. Cruceru, 'Could the Sustainable Technology Help Overcoming Crisis? Case Study: Installation of a Cogeneration Unit within a Chemical Company', Journal of Sustainable Energy, Volume II - nr. 1, ISSN: 2067-5534, 2011.

[3]. *** Directive 2003/54/EC of the European Parliament and of the Council of 26 June 2003 concerning common rules for the internal market in electricity and repealing Directive 96/92/EC, Official Journal of the European Union L176, 15.07.2003, 2003, pp. 37 - 53.

[4]. *** Order of the Minister of Environment and Water Management No. 85 from 26 January 2007 approving the Methodology for the elaboration of the National Allocation Plan, Ministry of Environment and Water Management, Official Monitor of Romania, Part I, Year XIX - No.101, 09.II.2007, pp. 8 - 36.

[5]. *** Key World Energy Statistics 2010, OECD/IEA, International Energy Agency, 9, rue de la Federation, 75739 Paris Cedex 15, www.iea.org, 2010, pp. 54 - 55.

[6]. M.-M. Voronca (coordinator), T. Constantinescu, M. Cruceru, A.M. Fodi, A. Marin and S.L. Voronca, FINANCING ENERGY EFFICIENCY INVESTMENTS, AGIR Publishers, Bucharest, ISBN 973 - 720 - 200 - 0, 2008.

 ISSN 2067-5534

METHOD FOR DETERMINING PARAMETERS OF THE HIDROGENERATORS VOLTAGE REGULATORS

HERISANU A.*, CICIRONE C.**, DUMITRESCU S.,** ZLATANOVICI D.**
*HIDROELECTRICA SA-SH Curtea de Arges, ** ICEMENERH Bucuresti
danz@icemenerg.ro

Abstract - The paper presents an original method in live determination of the main parameters of the automatic voltage regulator of hydro generators. The proposed method can be used for any kind of AVR and excitation system. The proposed method consists in simulating voltage variations on the reaction channel of AVR and recording its response in its size while the generator is still connected to the grid. The technique of measuring is based on using virtual instrumentation. The sampling rate for recording quantities is 0.2 ms. In the end it is presented an exemplification of measurement result to a 5.75 MW hydro generator with DC excitation generator and a 19.51 MW hydro generator with rotating diodes excitation and digital AVR.

Keywords: voltage regulator, excitation, parameters, virtual instrumentation.

1. INTRODUCTION

Excitation system and automatic voltage control is made up of adjustable high D.C. power source and control circuits, protection, supervision and control (known as Automatic Voltage Regulator - AVR). This system ensures the rotor current (excitation current) suppling and adjustement of an operating generator and the prefixed value maintaining of the terminal voltage. AVR is an automatic adjustement system with negative feedback from the generator terminal voltage and with variable tension setting to external command.

In case of a sudden reduction/drop of the generator terminal voltage, AVR will occur by the rapid growth of the excitation voltage, action called excitation forcing for returning to initial value.

AVR's main parameters which ensure interaction between generator and grid that is connected are: AVR's statism (S_{SU}), excitation forcing threshold (K_f), excitation system nominal response of the excitation voltage (t_{RUex}), excitation system nominal response (R_n), AVR's accuracy (□), AVR's behavior in automatic operate of a reserve electricity power on AVR's suppling voltage and override tension values at full load throw (override, override time and the total response time).

2. METHOD FOR DETERMINING THE AVR PARAMETERS

The AVR manufacturers determine these parameters by software simulation of AVR's setting voltage perturbations and recording their effects. But the software of the AVR is not available for exploitation. In these circumstances it has been developed a method to determine these parameters [1,2] and an appropriate measurement system based on hard simulation of disturbances on the voltage response and recording their effects.

For some of the parameters it is used the simulation method of perturbation on the AVR input response voltage. The disturbances are made with 3-phase assembly having equal resistance shunting contactor, serially connected on the three wires that bring response voltage to AVR input from measurement transformers (voltage reducer) from the generator terminals . (Fig. 1). The initial state contactor is closed. By opening the contactor, the resistance are placed in circuit and voltage drop occurs on the AVR input. Therefore, AVR will command increasing excitation voltage to bring the voltage initial value to the AVR input, the action having the effect of increasing the terminal voltage about perturbation value.

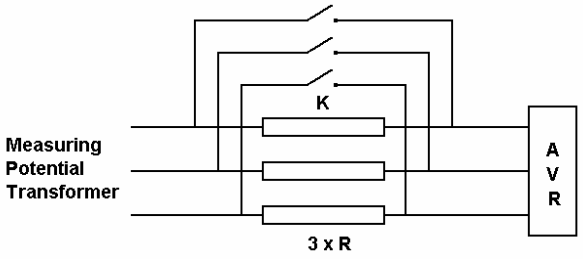

Fig.1 - Scheme of montage for disturbance simulation

The value of the disturbance created depends on the resistance R and on the AVR current drawn. For digital AVR the drawn current by AVR is of the order 0.02 ÷ 0.05 A, so that creating 10 ÷ 30% disturbances, the resistance should be in the 1000 ÷ 6000 Ω and 0,5 ÷ 2 W For analog AVR the drawn current is of the order 1.5 to 2 A, so that creating 10 ÷ 30% disturbances resistors of 2-50 Ω and 20 to 40 W are necessary. The simulation of the disturbances is made with the generator connected to the grid, operating at rated load.

Figure 2 shows the scheme of measurement used to determine the above parameters, placed in the wiring

diagram for HG excitation system with rotating diode excitation (a) and DC generator (b).

The measurement system was developed based on using virtual instrumentation. System includes transducers, the system of creating step disturbance, data acquisition system and dedicated software package. The system allows simultaneous recording of generator parameters, with a sampling rate of 0.2 ms.

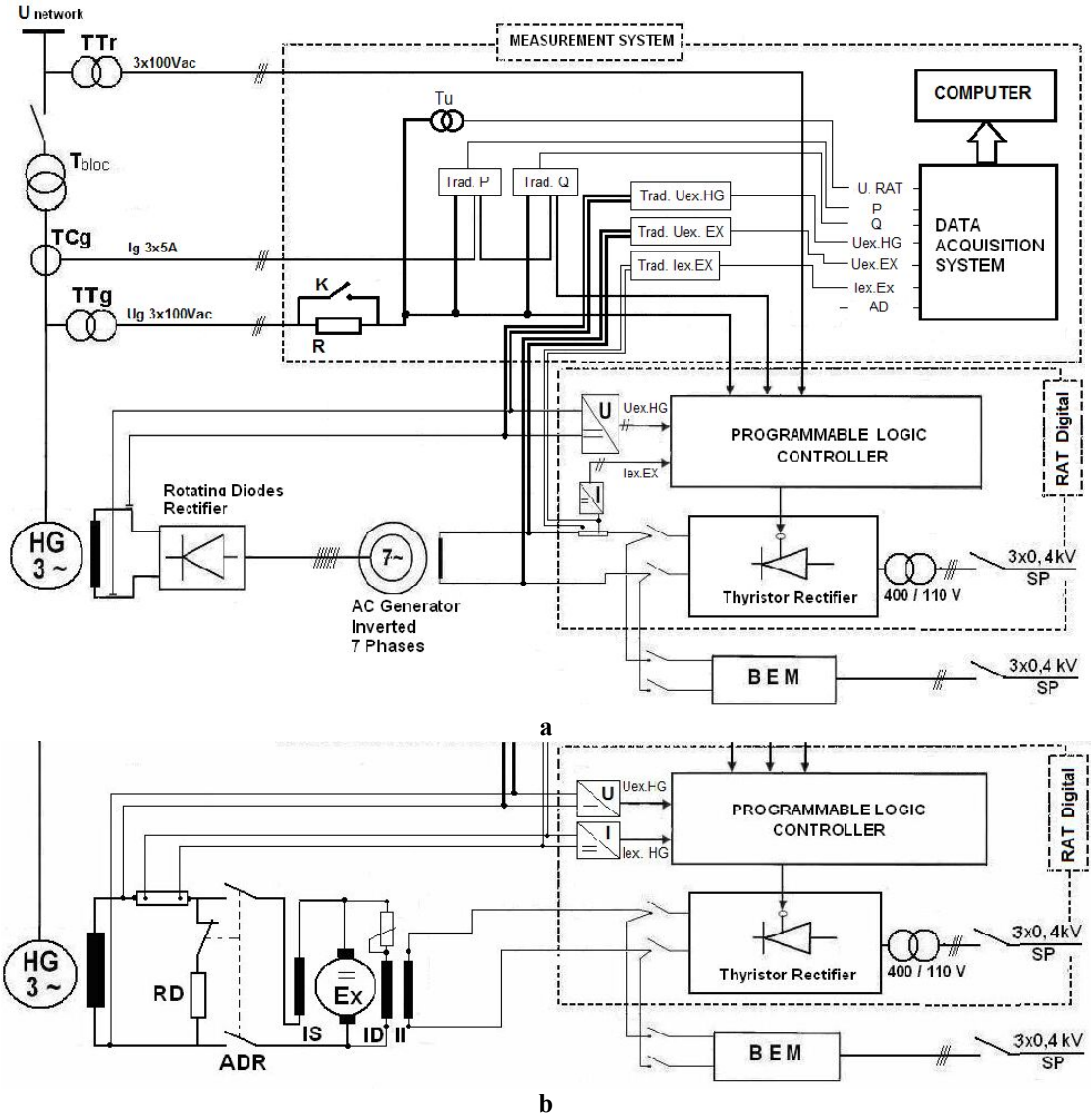

Fig.2 - Measurement scheme for excitation with rotating diodes (a) and DC rotating machine (b)

The measurement system was developed based on using virtual instrumentation. System includes transducers, the system of creating step disturbance, data acquisition system and dedicated software package. The system allows simultaneous recording of generator parameters, with a sampling rate of 0.2 ms.

Measurement scheme is the same whatever the type of excitation is: AC reversed rotary machine and rotating diodes or DC machine, excepting the purchase of the generator excitation current. For excitation with rotating diodes and AC reversed rotary machine there is no acces to the generator excitation current and therefore are acquired the excitation current and voltage of the exciter.

Apart from trying to simulate the operation perturbation at nominal load, the following tests are made: idle running, automatic operate of a reserve electricity power on the AVR suppling bar and rated load throw [3,4,5].

The statism is determined by applying a step disturbance of approximately -5% in AVR input response

voltage, generator operating with rated load (for example Fig.3). From records the values are determinated before and after a disturbance (stabilized values) for the terminal voltage and reactive power. AVR statism value is calculated with:

$$S_{SU} = 100 \frac{\Delta U_g}{U_{gn}} \frac{Q_{gn}}{\Delta Q_g} \quad (\%) \qquad (1)$$

$$\Delta U_g = U_{gf} - U_{g\,i}$$
$$\Delta Q_g = Q_{gf} - Q_{g\,i}$$

where:

ΔU_g - terminal voltage variation due to disturbance;
ΔQ_g - reactive power variation due to disturbance;
U_{gi}, Q_{gi} - baseline terminal voltage and reactive power;

ISSN 2067-5534 © 2012 JSE

U_{gf}, Q_{gf} - final values of terminal voltage and reactive power;
U_{gn},Q_{gn} - nominal values of terminal voltage and reactive power;

Threshold forcing excitation, the response time of the excitation voltage and excitation system nominal response is determined by applying a step disturbance of -20 ÷ - 30% to AVR voltage response and registration generator excitation voltage and terminal voltage (for example Fig.4)

Threshold voltage forcing excitation U_{exp} is the maximum value of the generator excitation voltage, at forcing, after a disturbance.

The response time in excitation voltage $t_{R\ Uex}$ is the time elapsed since disturbance application moment, read on AVR curve $U_{g\ RAT} = f(t)$, and the moment on $U_{ex} = f(t)$ when the generator excitation voltage reaches:

$$U_{R\ ex} = U_{exn} + 0{,}95\ (U_{ex.p} - U_{ex.n}) \quad (2)$$

where:
$U_{ex.p}$ - threshold voltage of excitation forcing,
$U_{ex.n}$ - excitation rated voltage.

If is impossible to reach the rated voltage excitation, the calculation takes into account the initial value of excitation voltage.

To determine the excitation system rated response on the same diagram it is delimited the range from 0.5 s when the excitation voltage begins to rise as a result of the step disturbance. It is determined by graphical integration the surface AMNPA between the portion of the curve U_{ex} bounded by the interval 0.5 s and horizontal interval corresponding to the rated voltage excitation U_{exn}. Triangle APQ is constructed so that its surface is equal to the area AMNPA. QP segment is determined by the relationship:

$$QP = \frac{2\ S_{AMNPA}\ (V\ s)}{AP\ (s)}\ (V) \quad (3)$$

The response of the excitation system nominal response is calculated with:

$$R_n = \frac{QP\ (V)}{U_{ex\ n}\ (V)} \frac{1}{0{,}5\ (s)} \quad (4)$$

Determination of the AVR accuracy is made with generator in the no load excited regime at rated voltage (for example Fig.6). There are recorded every 5 seconds 181 RMS values of terminal voltage for 15 minutes (starting at t = 0). Recording values of voltage across the generator, calculate the average value $U_{g\ med}$ of the 181 values recorded:

$$U_{g\ av} = \frac{\sum U_{g\ i}}{N}\ (V) \quad (5)$$

Absolute error from the mean values:

$$\Delta U_{gi} = \left| 100 \frac{U_{gi} - U_{g\ av}}{U_{g\ av}} \right|\ (\%) \quad (6)$$

where:
$U_{g\ i}$ - voltage effective value between phases measured during moment 'i';
$U_{g\ av}$ - average value of all the 181 measured values;
N - number of measured values of voltage

AVR accuracy is the maximum deviation $\Delta U_{g\ i}$

$$\varepsilon = MAX\ (\Delta U_{g\ i}) \quad (7)$$

Determination of the override parameters are made in rated load throw test, which corresponds to the application of a disturbance with an amplitude of about (+) 18 ÷ (+) 25%. The test is done by opening the switch on from the high voltage transformer block, as an unexpected event, caused by a grid protection. When disconnecting the load, the generator remains in idle mode and at the first moments (at least 1-2 times) the excitation current has the generator rated value (much more than the idle runnig excitation current). Therefore, the terminal voltage (and hence voltage seen by AVR) is a step leap which can reach a value of about 1.18 to 1.25 of U_{gn} (maximum value is a function of reactances and time constants of the generator). AVR intervention occurs and how quickly it occurs to restore the terminal voltage to a steady value should be admissible for this band around the nominal value (± 5% of U_{gn}). Terminal voltage and generator excitation voltage are recorded (for example Fig.7).

Terminal voltage override (SR) is the increasing of the terminal voltage value from rated value, after the rated load throw and it is determined by the relationship:

$$SR = \frac{U_{g\ max} - U_{gn}}{U_{gn}}\ (\%) \quad (8)$$

where:
$U_{g\ max}$ - the maximum terminal voltage after rated load throw ;
$U_{g\ n}$ - terminal rated voltage;

Override time of $1{,}1U_{gn}$ (t_{SR}) is the length of time that the terminal voltage has a value greater than $1{,}1\ U_{gn}$, after rated load throw and it is read from the chart curve $U_g = f(t)$

Total response time or duration transient (Δt_{as}) is the interval between the start of the terminal voltage increase and when it finally comes back in a band of ± 5% as a result of AVR action, after rated load and it is read from $U_g = f(t)$.

The determination of AoR behavior in automatic operate of a reserve electricity power on the 0.4 kV bar is made by disconnecting the main power switch of the AVR an of the exciter excitation transformer. After the automatic operate of a reserve electricity power break the switch of suplemental reserve is automatically closed. During automatic operate of a reserve electricity power

break generator operating without excitation. After the appearance of AOR supply voltage and excitement exciter, he restored the excitation parameters, the terminal voltage and reactive power, practically to the same values as those from the beginning. The test is made during the generator is operating at minimum technical power. Terminal voltage, generator excitation voltage, exciter voltage excitation from manual disconnection time to return to the original parameters (for example Fig.10) are registred. Initial parameters and ending parameters are compared after the break. The test is considered to be successful if the generator remains stable, without oscillations and if the excitation parameters, the terminal voltage and reactive power get back to the same values as those from the beginning.

Acceptance criteria of AVR parameters [6,7,8] are presented in Table 2.

3. TWO HYDROGENERATORS WITH DIGITAL AVR APPLICATION

Tests were conducted at two hydro generators from two different plants: HG1 of 5.75 MW with DC excitation generator and HG2 of 19.5 MW with reversed AC generator and rotating diodes excitation (Table 1). Both have digital AVR with indirect regulation.

Table 1 - Tested generators parameters

Parameters	Simbol	UM	HG 1	HG 2
Generator rating	P_{gn}	MW	5,75	19,5
Rated reactive power	Q_{gn}	MVAr	2.78	9.8
Rated power factor	$\cos \varphi_n$		0,9	0,9
Rated terminal voltage	U_{gn}	kV	6,3	10,5
Rated stator current	I_{gn}	kA	587	1250
Excitation type			DC generator	Rotating diods
Rated load field voltage	$U_{ex.n}$	V_{cc}	150	104
Rated field current	$I_{ex.n}$	A_{cc}	387	710
AC exciter voltage	$U_{ex.Ex.n}$	V_{ca}		36,5
DC exciter voltage	$U_{ex.Ex.n}$	V_{cc}	390	42
Exciter field current	$I_{ex.Ex.n}$	A_{cc}	230	29,4

At HG1 trials were conducted in two stages. Results from the first stage showed that a number of parameters: voltage threshold of forcing, response time, rated response and override value are not within the acceptance criteria laid down in standards. Accordingly AVR supplier was requested to modify gain coefficients and time constants transfer function of the AVR for improvement of these performances. After completing the settings, it was performed a new round of tests. Table 2 presents results of the two stages of testing.

Fig. 3 shows the registration test to determine statism. Test results for the two stages are similar and therefore this parameter is presented only in stage II test results. The generator operated in charge at P_g = 5 MW and 0.73 MVAr constant. It was performed by simulation, a step disturbance on the AVR entry of - 5.3%. There were recorded the generator terminal voltage U_g, the AVR input voltage, U_{RAT} and reactive power Q_g. From the records it was extracted initial and final values of voltage and reactive power: U_{gi} = 0.977 u.r., U_{gf} = 1.001 u.r., Q_{gi} =0.73 MVAr., Q_{gf} =2.41 MVAr, which by using relation 1 is determined the statism S_u = 4.0 %. The value corespond to the requirements acceptance criteria.

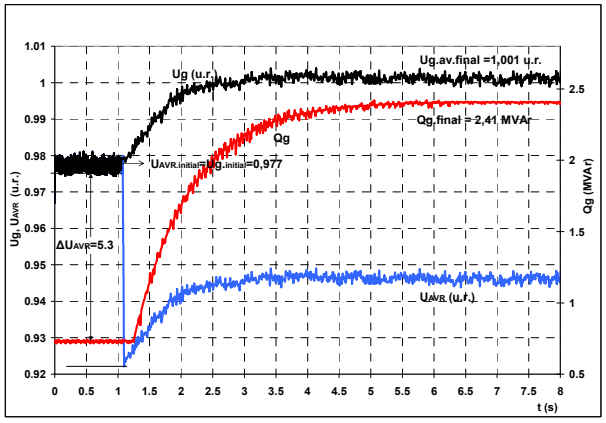

Fig. 3 - Registration test to determine statism, HG1

Fig. 4 presents the test recording for determining the forcing threshold, response time and rated response at the test stage I. The generator operated with the following parameters: P_g = 5.5MW, Q_g = 1.8 MVAr, $U_{g.i}$ = 5985 kV (0.95 u.r) and $U_{ex.i}$ = 130 V_{DC} (very close to the rated regime of HG). It was applied a step perturbation ΔU_{AVR} = - 23 %. Threshold value obtained was U_{exp} = 272 V respectively 1,34 u.r. and exciter excitation voltage was $U_{ex.Ex.}$ = 138 V_{cc}. The procedure described in paragraph 2 and the relations 2, 3 and 4 were determined successively: U_{Rex}= 1.32 u.r. resulting response time t_{RUex} = 0.48 s, S_{AMNPA} = 0.09 u.r/s, QP = 0.36 u.r. and rated response u.r. R_n =0.72 u.r./s. The conclusion was that the AVR does not realize criteria for acceptance threshold voltage of forcing (minimum 1.8), for response time (max. 0.4 s) and nominal response (minimum of 1.5 u.r. / s).

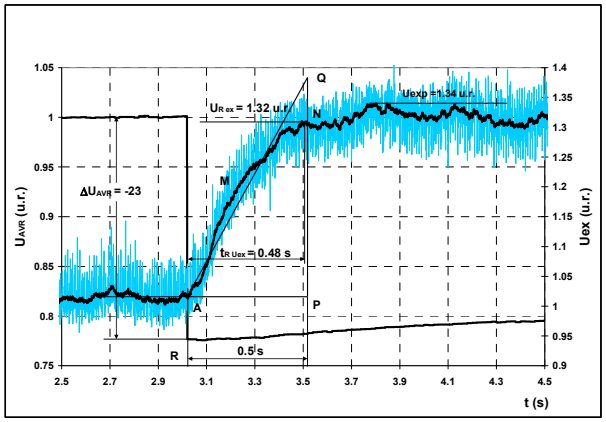

Fig.4 - The test for determining the forcing threshold, response time and rated response, stage I, HG1

After changing the AVR's settings it was performed phase II trials and the following values were obtained: K_f =1,95 $U_{R\ ex}$= 1.9 u.r., t_{RUex} = 0.325 s, S_{AMNPA} = 0.345

ISSN 2067-5534 © 2012 JSE

u.r. s , QP = 1.38 u.r. şi R_n =2.76 u.r./s, (Fig.5) which correspond to the acceptance criteria.

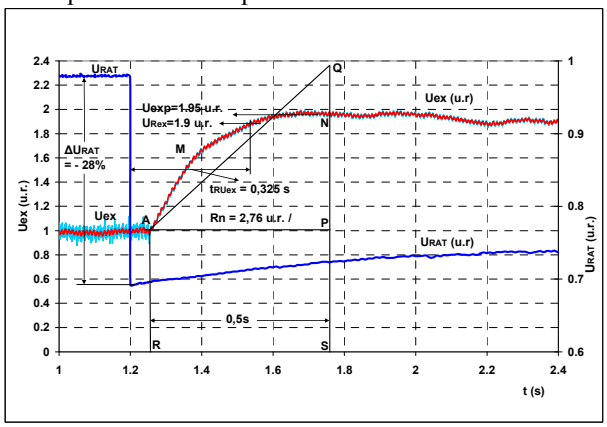

Fig.5 - The test for determining the forcing threshold, response time and rated response, stage II, HG1

Figure 6 presents the test recording to determine the accuracy. Test results for the two stages are similar and therefore this parameter is presented only in stage II test results .The generator operated in the no load exited regime at rated voltage 6.3 kV. Was recorded voltage at the generator terminals U_g for 15 min = 900 s, with a cadence of a 5 point and obtaining 181 values. With relations 5,6,7 calculate $U_{g\ average}$ =6.0 kV and ε = 0,39 %

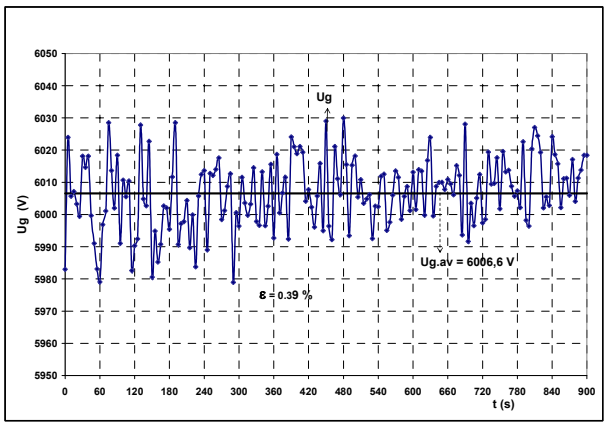

Fig.6 - Registration test to determine accuracy , HG1

Figure 7 presents the rated load throw test to determine the override values. This was tested by disconnecting the line switch on the 20 kV in secondary transformer block.

Initial load values were P_g = 5.55 MW and Q_g = 1.2 MVAr and at stage II P_g = 5.77 MW, Q_g = 1.00 MVAr. In the first phase there were obtained nonconforming/inconsistent values with the requirements: SR = 0.125 u.r., override time of 1.1 U_{gn}, t_{SR} = 1.2 s and total response time Δt_{as} = 3 s. After changing the settings there were obtained SR=0.101 u.r., t_{SR} = 0, Δt_{as} = 1.36 s, and values were consistent/ conforming with the acceptance criteria (Tab.2)

Fig. 8 shows the registration test to determine statism at the HG 2. The generator operated in charge at P_g = 15 MW and 0.21 MVAr constant. It was performed by simulation, a step disturbance on the AVR entry of - 5.45 %. From the records it was extracted initial and final values of voltage and reactive power: U_{gi} = 0.9832 u.r., U_{gf} = 1.0025 u.r., Q_{gi} =0.21 MVAr., Q_{gf} =4.21 MVAr, which by using relation 1 is determined the statism S_u = 4.73 %.

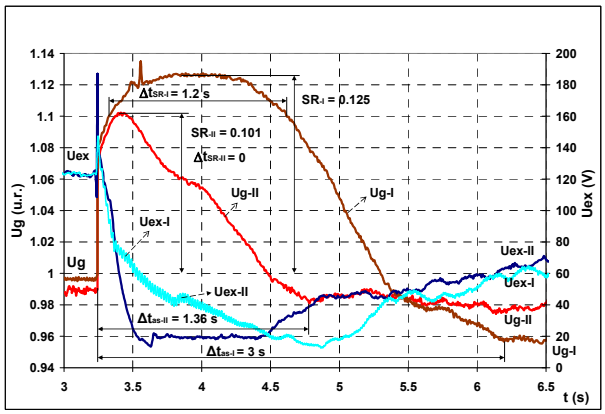

Fig.7 - Rated load throw test to determine override values, HG1

At HG 2 all tests were performed to determine the AVR's parameters. All parameters were within the acceptance criteria requirements. In load throw with line disconnect switch, the automatic system disconnected the AVR and thus ordered the HG de-energize and could not determine the total response time, the generator didn't come back to its rated voltage. Measurement results are presented in Table 2.

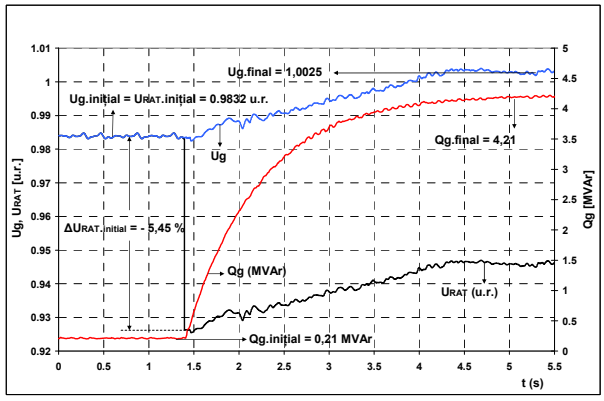

Fig. 8 - Registration test to determine statism, HG2

Fig. 9 presents the test recording for determining the forcing threshold, response time and rated response at the HG 2. The generator operated with the following parameters: P_g = 20 MW, Q_g = 6.5 MVAr, $U_{g.i}$ = 10.49 kV (0.99 u.r) and $U_{ex.i}$ = 101 V_{DC} (very close to the rated regime of HG). It was applied a step perturbation ΔU_{AVR} = - 32 %. Threshold value obtained was U_{exp} = 175 V respectively 1,74 u.r. and exciter excitation voltage was $U_{ex.Ex.}$ = 138 V_{cc} (respectively 3.3 $U_{ex.Exn}$). The procedure described in paragraph 2 and the relations 2, 3 and 4 determined successively: U_{Rex}= 0.772 u.r., t_{RUex} = 0.24 s, S_{AMNPA} = 0.265 u.r/s, QP = 1.06 u.r. and rated response u.r. R_n =2.12 u.r./s.

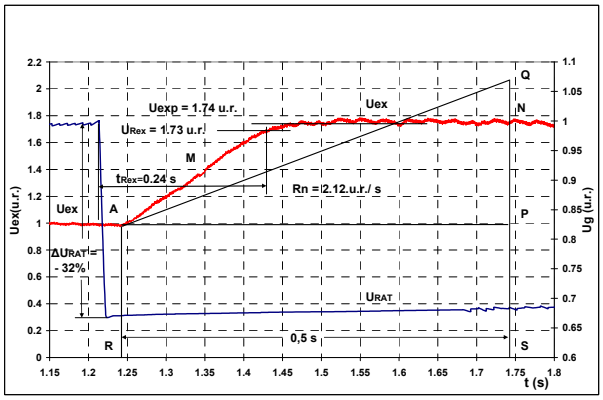

Fig.9 - The test for determining the forcing threshold, response time and rated response, HG2

Figure 10 presents the test recording to verify the behavior on high voltage supply to the automatic operate of a reserve (AOR) electricity power for HG 2.

The test was performed by disconnecting manually the main power switch of the exciter excitation transformer, which supply also the AVR causing the action of the automation AOR to thr bar on 0.4 kV. The generator was loaded at P_{gi} =3.47 MW and Q_{gi} = 4.05 MVAr. After disconnecting the primary power supply switch, the Automatic Transfer Switch connected up to approx. 9 seconds (pause AOR), during which HG worked without excitation and reactive power almost zero. After AVR's emergence power, it restored the excitation parameters, the terminal voltage and reactive power, practically the same values as those from the beginning: P_{gf} = 3.48 MW, şi Q_{gf} = 4.075 MVAr. The AVR behaved correctly on the automatic operate of a reserve electricity power break. (pause AOR)

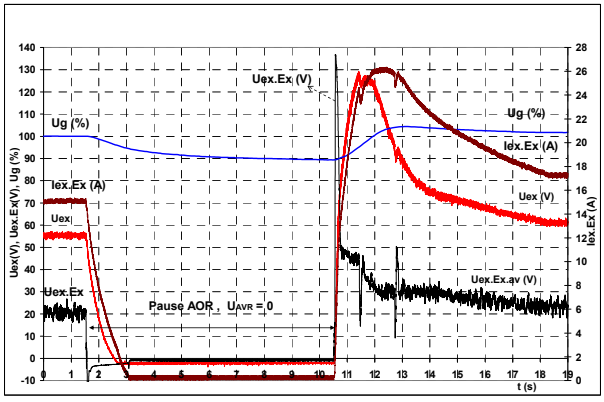

Fig.10 - AOR break behavior for HG 2

Table 2 presents summary results of measurements at two hydro generators and acceptance criteria. For HG1 presents results from the two stages, before and after changing the AVR's settings

Table 2 - Test results

Parameter	UM	Demand*	HG1 st I	HG1 st II	HG 2
AVR Statism	%	(1-12)	4.56	4,00	4,73
Voltage forcing threshold	u.r.	≥1.6 (≤ 5 MW)	1.34	1.95	1.75
		≥1.8 (≥ 5 MW)			
Response time in excitation voltage	s	≤ 0,4**	0.48	0,325	0,24
Excitation system rated response	u.r./s	≥ 1,5	0.264	2,96	2,12
AVR accuracy	%	≤ 1	0.74	0,39	0.67
AVR behavior to pause AOR			OK	OK	OK
Generator tension override	u.r.	≤ 0,1	0.13	0,1	0,1
Override time of $1,1U_{gn}$	s	≤1	1.2	0***	0***
Total response time	s	≤ 3	3	1,36	-

*According SR 9385-1:2008, cap. 6.4,
** For indirect regulation system,
*** The voltage didn't pass over $1,1U_{gn}$

4. CONCLUSIONS

Test methods, by live attempts with the generator connected to the grid and presented in this paper have revealed the real performance of the AVR and determine the classification or not to the acceptance criteria requirements. It has to be mainly mentioned the hard simulation method of disturbance on the input side of the AVR, which is an original method of the authors' work. The hardware and software equipment, also original, allowed detailed record of transitory events and a high degree of precision machining.

Applications presented have confirmed the efficiency of testing and allowed parameters were found not fit the requirements and acceptance criteria, and thus able to intervene and correct settings so that the performance can be improved. The improvement was confirmed by a new phase of testing. Currently AVR ensure correct interaction, free of any problem, between generator and grid.

REFERENCES

[1] Zlatanovici D., Budulan P., Cicirone C., Framework procedure for checking the conditions of connection to the electricity transmission network of procedures and consumers of electricity, Revista Energetica, 2002 , vol.50,nr.12, p.527, ISSN 1453-2360

[2] Cicirone C., Zlatanovici R., Dumitrescu S., Zlatanovici D., Computerized methods for testing of the hydrogenerators automatic voltage regulator, Rev. Tehnologiile Energiei , Nr.1, 2008, p.16, ISSN 1842-7189

[3] IEEE Std.421.1-1986 IEEE Standard Definitions for Excitation Systems for Synchronous Machines

[4] IEC 60034-16-1: 2011- Rotating electricalmachines Part 16-1: Excitation systems for synchronous machines - Definitions

[5] SR 9385-1:2008 Synchronous Hydro Generators. Part 1: General Technical Conditions

[6] IEEE Std.421.2-1990 IEEE Guide for Identification, Testing, and Evaluation of the Dynamic Performance of Excitation Control Systems.

[7] IEC/TS 60034-16-3: 1996 - Rotating electrical machines - Part 16: Excitation systems for synchronous machines - Section 3: Dynamic performance

[8] SR 9385-2:2008 - Synchronous Hydro Generators. Part 2: Rules and methods for quality verification

ISSN 2067-5534 © 2012 JSE

IDENTIFICATION OF ELECTROMAGNETIC DISTURBANCES IN MODERN POWER SYSTEMS

MIRON A., CHINDRIŞ M.D., CZIKER A.C.
Technical University of Cluj - Napoca, Memorandumului no.28, Cluj - Napoca
anca.miron@eps.utcluj.ro

Abstract – the paper presents a method for temporary disturbances identification and analysis. In the infield standards the analysis of the voltage dips and swells is made using the same method that is the calculus of the r.m.s voltage on a cycle updated every half of cycle. This method brings the disadvantages of more calculus then needed. Thus, the authors propose a new methodology for the identification and analysis of the mentioned short duration disturbances. The originality of the method consists in the distinction between the identification and the analysis stages. In this way less time is needed to find if any disturbance occurred and extra calculus is eliminated.

Keywords: voltage dip, voltage swell, time domain analysis, modern power systems

1. INTRODUCTION

The modern power systems have a dynamic operating state that most of the time is harmonic polluted and unbalance. In this electromagnetic environment appear temporary disturbances like voltage dips and voltage swells that accentuate the real state negative effects.

Voltage dips and swells are the consequences of transient events, thus they have a transitory character and impress to the power system a temporary operating state.

The voltage dips sources are represented by faults localized in the production, transport, distribution and electrical energy use installations and they affect all consumers connected to the supply power network at that moment. These faults can be the consequences of natural phenomenon (atmospheric discharge, storm, snow, frost etc.) or of other nature (advanced wear, bad quality of equipment materials, high level of pollution, wrong maneuvers etc.).

The main causes localized in the supplier's side are faults due to the breakdown of equipments isolations, switching or atmospheric overvoltages etc. Voltage dips can also appear because of voltage losses produced in a network before protections disconnect a defected element.

A user can himself produce voltage dips in its own installations even if there is no disturbance from the supply network. These voltage dips are produced due to the following causes: faults in the internal network, working of installations that have a high current at start or handling of installations with fluctuating load.

Voltage dips determine negative effects especially on electronic equipments that are very sensitive to the magnitude variations of the supply voltage, thus in some situations a simple voltage dip can cause the stopping of devices that have electronic commands.

Voltage swells are of interest especially in the field of selection and coordination of conductors' isolation. As a result, the main objective is to reduce the deteriorations determined by dielectric stresses and to raise the working safety of electric equipments.

Voltage swells are caused typically by three phenomenons [1]:

- Atmospheric (lighting): appear generally due to atmospheric electric discharge in installations and are characterized as being single-pole (amplitudes of thousands of kV), strongly damped and very short duration (μs). Their shape depends on the type of installation earthing, particularly of the electric parameters of this installation;
- Switching: they are alternative voltage swells that appear generally because of a switching operation or a fault, and they are characterized as being strongly damped (magnitude is 1.5 – 3 times the magnitude of line-to-line voltage) and short duration (between μs to ½ cycle - 10 ms). These voltage swells can be with steep front (in case of circuit breakers) or slow front (in the case of capacitors or electric machines working in open-circuit);
- Temporary: they are caused by switching activities (i.e. disconnection an important load), faults (phase-to-ground faults) and also by non-linear phenomenon (harmonics and ferro-resonance). These voltage swells have the shape of poorly damped oscillations with relatively large duration.

Besides the voltage swells determined by atmospheric causes or maneuvers in the transport and distribution networks, there can appear also voltage swells injected by users. They can be induced by ignition of discharge lamps, arc furnace operation or welding equipment, operating equipment with static switching, high power engine start etc.

Voltage swells from power networks, that have a random character, are not dangerous to the people, but they can affect the sensitive equipments, which even if are not damaged, suffer an early ageing.

Considering the aspects described in the former paragraphs, it can be understood the necessity of voltage dips and swells identification and analysis in a quick and

efficient manner, in order to limit their effects as soon as possible after the occurrence of the event.

The paper continues with a section that contains the description of the standard methodology for voltage dip and swell analysis. On the other hand, the methods proposed in the specialty literature are also briefly described. The next five sections present the methodology used for the identification and analysis of voltage dips and swells, followed by some examples, which underline the utility of the proposed method. The paper ends with a section of conclusions.

2. BACKGROUND

The disturbances identification is the process that finalizes with the finding of the electric signals' characteristic parameters, which correspond to the influence of the electromagnetic disturbances on the functioning of the power systems.

A voltage dip is defined to be the decrease with ΔU_i (Fig. 1 and 2) of the r.m.s. value of voltage in any power network's node, for a time interval t_i, in which the voltage is always lower than the nominal value U_n. Voltage dips can affect only a phase, two phases or all phases at the same time [2].

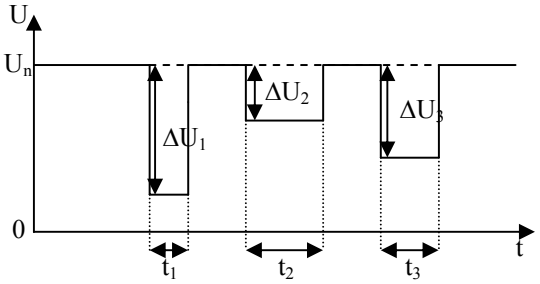

Fig. 1 - Examples of voltage dips. R.m.s. voltages

A voltage dip is characterized with the help of three quantities: amplitude, duration and occurrence frequency. The amplitude is defined as the difference between the r.m.s. value of the nominal voltage and the minimum r.m.s. value of the voltage during the voltage dip. The amplitude, ΔU_i, can take values between 0.1 and 0.95 from the nominal supply voltage, U_n. The duration of a voltage dip represents the time interval t_i (Fig. 1, $i = 1...3$) and can have values between 0.01 and 60 s. In Fig. 2 is illustrated a voltage dip, considering the harmonic pollution, and using instantaneous values.

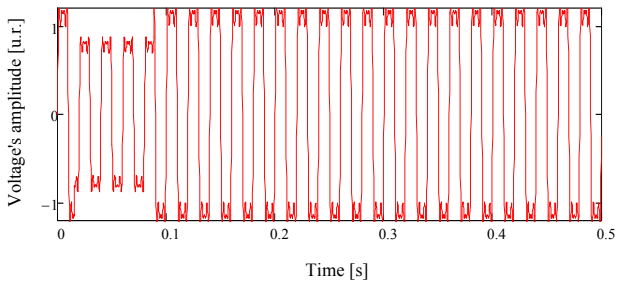

Fig. 2 - Voltage dip. Instantaneous values

In 10% from the observed events, voltage dips don't have a shape that can be properly characterized using only the amplitude and the duration. From the practice point of view, a general characterization by using the two quality indices: amplitude and maximum duration on the three phases of the three phase power system can be accepted [3, 4, 5, 6].

In power systems appear situations of voltage swells (Fig. 3) when the voltage value suffers a sudden increase of very short duration (from several tens of μs to one ms) and very high amplitude (several times the nominal value) followed by recovery of the voltage's value to the initial level [7].

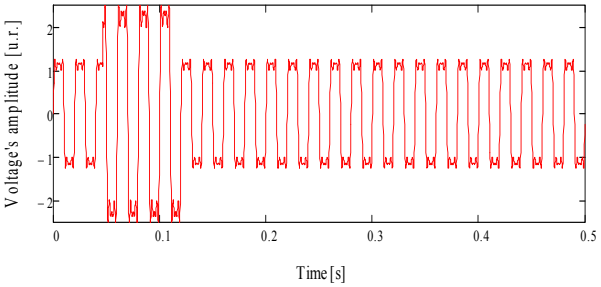

Fig. 3 - Voltage swell. Instantaneous values

As in the case of voltage dips, the voltage swells characteristics depend on the causing source as follows: atmospheric phenomena determine voltage swells with amplitude as much as thousands of kV, short duration and steep front; switching processes cause voltage swells strongly cushioned, amplitude 1.5 to 3 times the nominal voltage and short duration; a load switching determine long duration and amplitude oscillation close to the amplitude of the nominal voltage. The main negative effect of voltage swells is the ageing of electric equipments isolations.

Under present infield standards [8], the measured value for voltage dips and swells (further on in order to simplify the exposure will use the term disturbance when referring to voltage swells and dips) is the r.m.s. value for a cycle, denoted in [8] with $U_{rms(1/2)}$, on each phase of an three phase power system. This value is used to determine the characteristics, but also to identify the disturbance's occurrence.

The disturbance is detected when the measured value $U_{rms(1/2)}$ falls below (exceeds) a threshold value to the supply voltage, U_{din}, which was declared before the occurrence of the disturbance or to the U_{sr}, the r.m.s. voltage measured some time before the detection started.

In single-phase systems, a disturbance begins when the voltage $U_{rms(1/2)}$ goes out of range (0.9 and 1.1 of the reference voltage), and ends when the measured voltage is between the limits plus (minus) the hysteresis voltage (in general, it is 2% of the supply voltage).

In multi-phase systems a disturbance begins when the voltage $U_{rms(1/2)}$ on at least one phase goes out the threshold interval and ends when the voltage on all phases is between the defined limits. In [8] is specified that the opening thresholds voltage and the hysteresis voltage are chosen by the user as needed.

In previous paragraphs the reference voltage is the voltage that the disturbances are related with. The user

ISSN 2067-5534 © 2012 JSE

can choose this voltage as having a fixed value, namely the supply voltage, or a value range. According to [8], this voltage is calculated using a first order filter with a time constant of 1 minute. The filter is characterized by the following mathematical relationship:

$$U_{sr}(n) = 0{,}9967 \cdot U_{sr}(n-1) + 0{,}0033 \cdot U_{(10)rms}; \qquad (1)$$

where $U_{sr}(n)$ is the reference voltage used in the current analysis window, $U_{sr}(n-1)$ – the previous value of the reference voltage and $U_{(10)rms}$ – the most recent value measured as r.m.s. voltage on an interval of 10 cycles.

At the start of disturbance detection, voltage reference value is set, and then updated every 10 periods.

In the infield literature [9 – 18] several analytical methods (wavelet transform, S transform etc.) and artificial intelligence techniques (artificial neural networks, expert systems) are proposed for the voltage dips and voltage swells identification. In [9 – 15, 16] the authors apply the wavelet transform with the aim of solving different aspects concerning the transients' issue that appear in the distribution networks. Thus in [9, 10] the discrete wavelet transform with Daubechies mother wavelet is used for the identification of voltage sags, voltage swells, outages and transients. The multi-resolution analysis is used to create models for the circuit elements so as to use an equivalent scheme for the calculus of the circuit during transients operating states in [14]. Morlet wavelet is applied in [15] in order to perform the multi-resolution analysis for the detection of transients contained by the electric signals. In [17] the S transform is the base of a pattern recognition technique for the detection, classification and quantification of power quality disturbance waveforms. An expert system dedicated for the classification and analysis of power system events (voltage dips or voltage swells) in presented in [18].

As it was former presented, the standard identification and analysis of the disturbances is made by determining the r.m.s value of voltage even if the disturbances appeared or not. Thus extra calculus is performed and more memory is needed. On the other hand the use of the wavelet transform implies many calculations in order to detect properly the exact moment the disturbances occured. These disadvantages were eliminated in the proposed algorithm that is described in the next sections.

3. ALGORITHM ANALYSIS

The proposed algorithm dedicated for identification and analysis of temporary disturbances is based on time domain analysis, and supposes two steps. Firstly the signal is processed in order to find out if any sudden changes occurred in the string values of the digital electric signal. The result dictates if the 2nd step must or not be performed. If so, the analysis is continued and the signals' parameters that characterize the disturbances are determined: start time, end time and signal's amplitude during the event. According to these quantities disturbance's duration and amplitude are gotten. The first characteristic is calculated by making the difference between the end and start moments, while the amplitude is the difference between the reference value and minimum r.m.s. voltage in the case of voltage dips and the difference between the maximum r.m.s. value and the reference value during voltage swells. Fig. 4 illustrates the principle of the proposed algorithm.

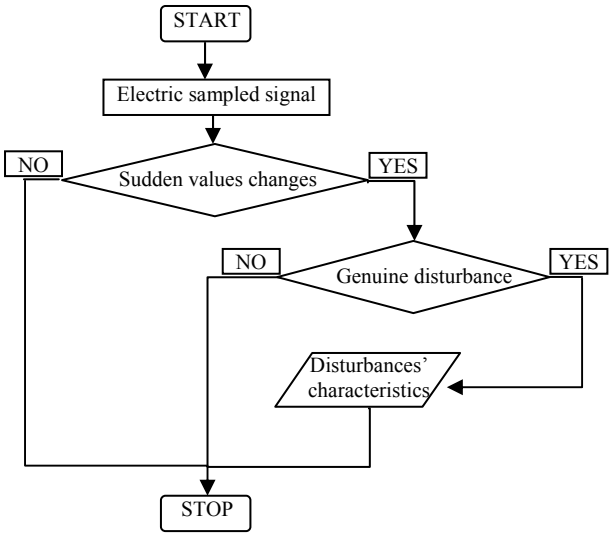

Fig.4 - The principle diagram of the proposed algorithm

The 1st algorithm's step is realized using the „edge detection", and applying the convolution between the analyzed signal and Morlet function.

4. TIME DOMAIN IDENTIFICATION

The disturbances are characterized by the appearance of a sudden change (increase in the case of voltage swells and drop in the case of voltage dips) of the voltage r.m.s. value and consequently of the instantaneous values. In this case the usage of time domain analysis is the most understanding approach. Thus the edge detection method is used, and the mathematical relationships are:

$$P(k) = \left| \sum_{n=0}^{M-1} u(n) \cdot f_{tr}(k,n) \right| \qquad (2)$$

$$f_{tr}(k,n) = f\left(\frac{n-k}{2} \right) \qquad (3)$$

where $P(k)$ is the string values that contains information about the sudden changes appearance, $u(n)$ – the string values of the sampled electric signal, $f(n)$ – the used function (named the "identification function"), $f_{tr}(n)$ is a translation of the identification function, M represents the number of the electric signal samples and $k = 0 \ldots M-1$.

In order to find the proper identification function, several functions that are used in the case of wavelet transform: Morlet, Shannon, Mexican Hat and 2nd Gauss derivative, were studied. These functions were chosen because their properties make them proper for the identification of transients. The functions' mathematical description is presented in table 1 [19, 20, 21, 22, 23].

The graphical representations of the identification functions are illustrated in the next imagines.

Table 1 - Identification functions

Identification functions	Mathematical relationship Time variation
Morlet	$f(t) = c(\sigma)\cdot \pi^{\frac{-1}{4}} \cdot e^{\frac{-1}{2}t^2} \cdot \left(e^{i\sigma\cdot t} - k(\sigma)\right)$ $c(\sigma) = \left(1 + e^{-\sigma^2} - 2e^{-\frac{3}{4}\sigma^2}\right)^{-\frac{1}{2}}$ $k(\sigma) = e^{-\frac{1}{2}\sigma^2}, \quad \sigma = 6$
Shannon	$f(t) = \frac{\sin\left(\frac{\pi\cdot t}{2}\right)}{\frac{\pi\cdot t}{2}} \cdot \cos\left(\frac{3\cdot\pi\cdot t}{2}\right)$
Mexican Hat	$f(t) = \frac{2}{\sqrt{3\sigma}\cdot\pi^{\frac{1}{4}}} \cdot \left(1 - \frac{t^2}{\sigma^2}\right) \cdot e^{\frac{-t^2}{2\sigma^2}}, \sigma = 0.4$
2nd Gauss derivative	$f(t) = \left(1 - t^2\right) \cdot e^{\frac{-t^2}{2}}$

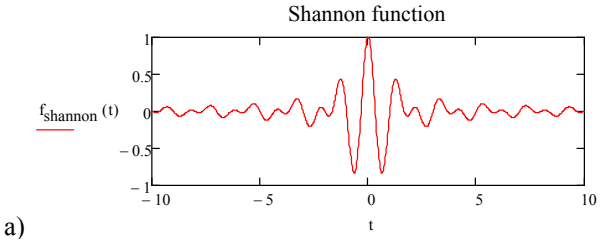

a)

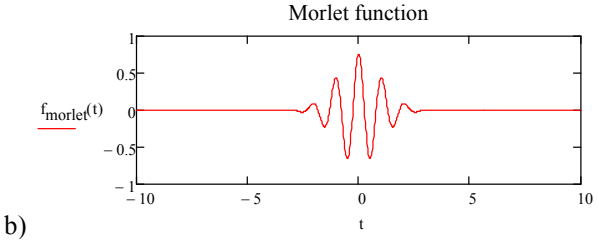

b)

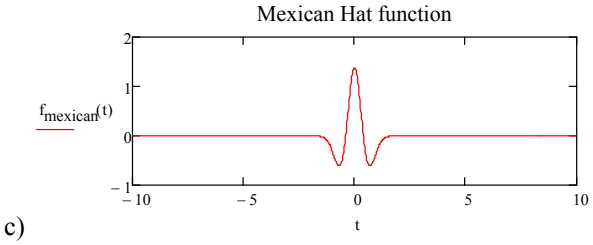

c)

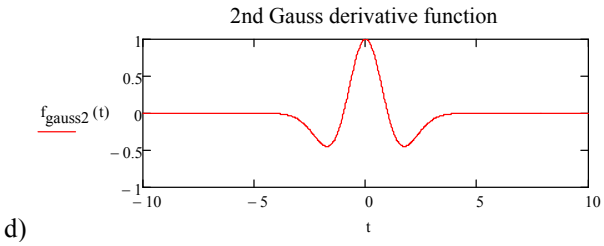

d)

Fig. 5 - Identification functions time variation

With the intention to compare the identification functions and to underline the choosing of Morlet function, the digital signal from Fig. 2 was analyzed and the results are presented in the graphics from Fig. 6.

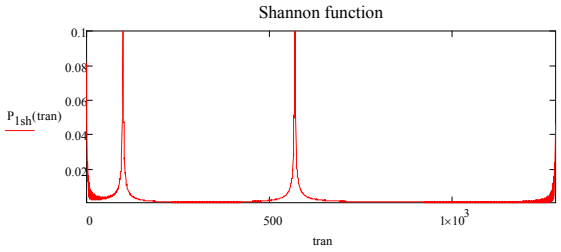

a)

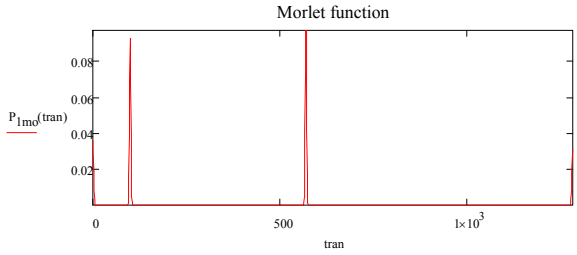

b)

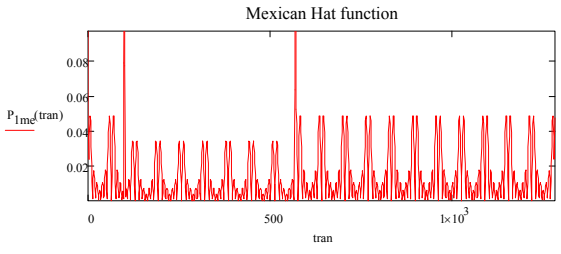

c)

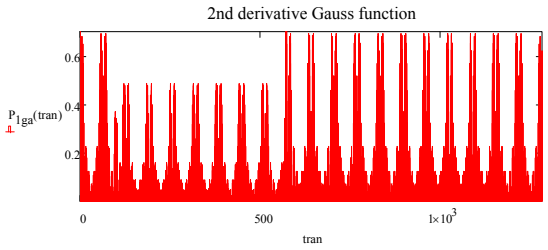

d)

Fig. 6 - Analysis of digital signal containing a voltage dip

The graphics show that in the cases of Shannon and Morlet functions the results indicate properly the moments when the signal's values suffer a sudden change; while in the case of the other functions the obtained data is quite difficult to process as to determine the exact moments.

By analyzing the resulted data from several signals analysis, the selected identification function was the Morlet function. This function is a complex one, but it can be used to process real signals, on which the convolution operation projects them to modulus-phase form. The phase plot is particularly suited for the detection of singularities. In the identification the real part of the function was used, and the parameter σ was set to 6. This value was obtained after several calculations with other σ values.

ISSN 2067-5534 © 2012 JSE

5. ANALYSIS

At the 1st step, after determining if a sudden change occurred in the signal structure, to find out the disturbance type (voltage dip, voltage swell or a simple insignificant change), the r.m.s. voltage is determined on a cycle that surrounds the transition point. The obtained value is compared with the reference value, which is chosen at the beginning of the analysis, and depends on the voltage r.m.s. value before the event start. As the real operating state of the power network is considered, namely the presence of harmonics disturbances and the unbalanced steady state.

The 2nd step supposes the analysis that is made on the digital signal as to determine the specific parameters of the voltage dip or swell. The analysis is performed on 10 time cycles (about 20 ms). This method is similar to the one proposed in [8], the difference is that the r.m.s. value is actualized every quarter of cycle ($U_{rms(1/4)}$), thus a more appropriate shape is obtained.

The start time is considered when the disturbance graphic intersects the level corresponding to the 90 % or 110 % and ends when the graphic grows more than 90.2% or drops below the threshold of 109.2 % (is taken account the hysteresis voltage). Fig. 8, 9, 10 and 11 illustrate the described procedure that is the moment when the graphic crosses the limits levels. All moments are found depending on the zero moment (the 1st signal sample) of the digital signal.

The identification and analysis were implemented as a virtual instrument (VI) using the graphical G programming language. First several VIs for the single-phase analysis were developed and then these ones were used to build a complex VI that makes the identification and analysis for three-phase electric signals.

The algorithm was verified on several digital waveforms containing voltage dips and voltage swells virtually created. Thus the disturbances characteristics could be easy controlled and compared with the obtained results.

6. EXAMPLES

Several complex waveforms were studied as to verify the algorithm, but in the paper only four representative examples are illustrated: a typical voltage dip, a typical voltage swell, a very short duration voltage swell and a variation of the voltage r.m.s. values that is not a disturbance. The temporary disturbances were included in the structure of non-sinusoidal unbalanced three-phase signals. In order to simplify the examples presentation, only the single-phase analysis is described. Consequently, the support waveform is a single-phase non-sinusoidal electric signal. In Fig. 7 is presented the base waveform containing the typical voltage dip. Table 2 contains the disturbances instantaneous characteristics included in the examples.

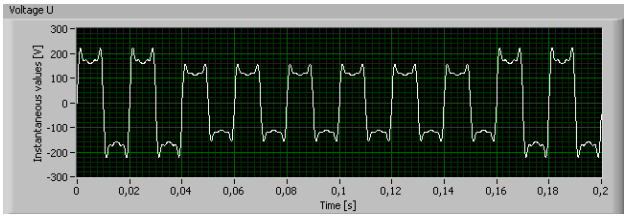

Fig. 7 - Non-sinusoidal electric signal containing a voltage dip

Table 2 - The instantaneous characteristics of the temporary disturbances

Instantaneous characteristics / Example	t_0 [s]	d [s]	A [%]
1	0.04	0.12	70
2	0.04	0.12	170
3	0.14	0.002	1500
4	0.1	0.08	95

t_0 [s] – start moment
d [s] – time duration
A [%] – minimum amplitude % (comparing the reference value) of the digital signal during the temporary disturbance

Fig. 8 contains the variation in time of the r.m.s. values for the first example. It also includes the explanation of the way the start and end moments are determined. It can be observed that the disturbance is a usual voltage dip.

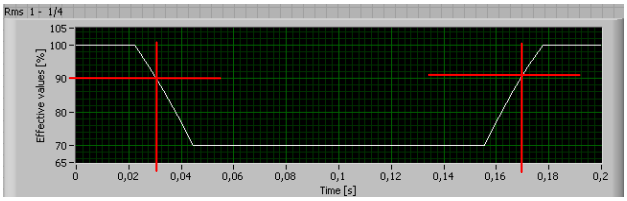

Fig. 8 - Variation in time of the r.m.s. values for the 1st example

Fig.s 9 and 10 illustrate the r.m.s. values of the waveform in the case of a typical and a very short duration voltage swell, respectively. The way the voltage swells' characteristics are determined can be seen in the corresponding figures.

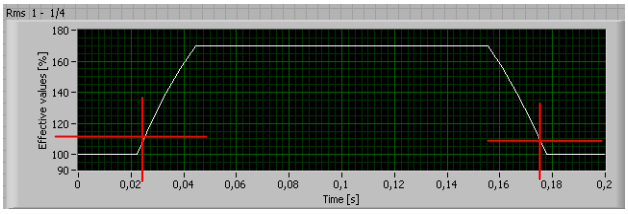

Fig. 9 - Variation in time of the r.m.s. values for the 2nd example

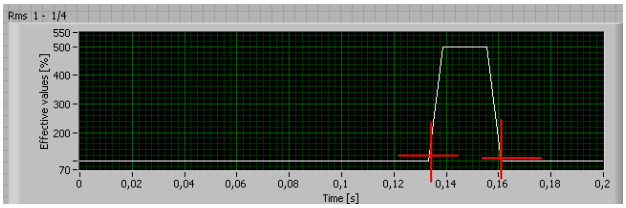

Fig. 10 - Variation in time of the r.m.s. values for the 3rd example

The 4th example, whose variation in time of signal is illustrated in Fig. 11, underlines the thresholds that define the disturbances definition intervals and the fact that the algorithm and the developed virtual instruments work properly.

Table 3 contains a comparison between the results obtained using the standard method (that was also implemented as a virtual instrument) and the proposed one. The results show that both methods determine properly the disturbances amplitude. Differences appear in the disturbances durations case, because of the way the r.m.s. values are updated, namely in the standard method case the r.m.s. value is updated every half of cycle, while in the case of the proposed method every quarter of cycle. This fact also brings an advantage for the proposed method that is a closer to reality disturbance shape.

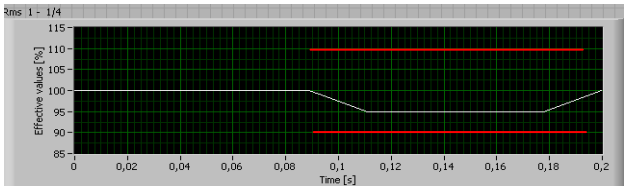

Fig. 11 - Voltage r.m.s. values time variation. Example 4

Table 3 - Comparison between the obtained results and the standard method

Standard method			Proposed method		
t_0 [s]	d [s]	A [%]	t_0 [s]	d [s]	A [%]
Example 1					
0.03	0.13	70	0.03	0.125	70
Example 2					
0.03	0.13	170	0.025	0.135	170
Example 3					
0.13	0.02	498	0.125	0.02	500
Example 4					
-	-	-	-	-	-

t_0 [s] – start moment
d [s] – time duration
A [%] – minimum amplitude % (comparing the reference value) of the digital signal during the temporary disturbance

7. CONCLUSION

The papers presents a method for voltage dips and voltage swells identification in single and three-phases power networks. Consequently, further on the situation of the temporary disturbances identification is explained by describing the aspects from infield standards and the characteristics of real electric signals which contain voltage dips and voltage swells.

The method offers the same precision as the wavelet transform, but it has the advantage of using less calculations. On the other hand, comparing it with the method proposed in standards the proposed method is quicker (less calculation is performed).

The presented examples show that both the standard and the proposed method gives accurate results concerning the amplitude of the disturbances, but more exact is the proposed method when determining the start and end moment, that is the duration and the disturbances' shape.

The proposed method offers more advantages comparing the standard method:

- Less calculus – disturbance is first identified and then the characteristics are determine;
- The exact moment of disturbance start and end are precisely determined;
- The disturbance shape is more close to the reality.

Future research can be made in order to include more disturbances in the algorithm and to decrease the time needed for calculus (develop more advanced virtual instruments).

Acknowledgements

This paper was supported by the project "Develop and support multidisciplinary postdoctoral programs in primordial technical areas of national strategy and research – development - innovation" 4D-POSTDOC, contract nr. POSDRU/89/1.5/S/52603, project co-funded from European Social Fund through Sectorial Operational Program Human Resources 2007-2013.

REFERENCES

[1]. Csuros L, *Power systems protection. Volume 2: Systems and methods. Chapter 11 – Voltage swell protection*, Published by The Institution of Electrical Engineers, London, Great Britain, 1996

[2]. Bollen M.H.J., *Characterization of voltage sags experienced by three phase adjustable-speed drives*, IEEE Transactions on Power Delivery, vol.12, no.12, pp.1666-1671, October 1997

[3]. Baggini A., and others, *Handbook of power quality*, John Wiley & Sons, Ltd, 2008, Great Britain

[4]. Zhang L.D., Bollen M.H.J., *A method for characterizing unbalanced voltage dips (sags) with symmetrical components*, IEEE Power Engineering Letters, pp. 50-52, July 1998

[5]. Bollen M.H.J, Hager M., Roxenius C., *Voltage dips in distribution systems: load effects, measurements and theory*, CIRED, 17th International Conference on Electrical Distribution, Barcelona, 12 – 15 May 2003, session 2, paper no 47

[6]. Heine P., *Voltage sags in power distribution networks*, PhD Thesis, Department of Electrical and Communication Engineering, Helsinki University of Technology, Espoo, Finlanda, 2005

[7]. Vahidi B, and others, *Modeling of lightning transient voltage swell by using different models of grounding system*, www.aedie.org/9CHLIE-paper-send/227-VAHIDI.pdf

[8]. 61000-4-30 Ed. 2: Electromagnetic compatibility (EMC) - Part 4-30: *Testing and measurement techniques - Power quality measurement methods*

[9]. Nath S, Dey A., Chikhani A.Y., *Detection of power quality disturbances using wavelet transform*, World Academy of Science, Engineering and Technology 49, 2009, pp. 869 – 873

[10]. Chen S., Zhu H.Y., *Wavelet transform for processing power quality disturbances*, EURASIP Journal on Advanced in Signal Processing, Vol. 2007, article ID 47695

 ISSN 2067-5534 © 2012 JSE

[11]. Tse N.C.F., *Practical application of wavelet to power quality analysis*, Power Engineering Society General Meeting, 24-28 June 2007**,** ISBN: 1-4244-1298-6, pag. 1-6

[12]. Hamid E.Y., Mardiana R., Kawasaki Z. – I., *Wavelet – based compression of power disturbances using the minimum description length criterion*, Power Engineering Society Summer Meeting, 15 – 19 July 2001**,** Vol.3, ISBN: 0-7803-7173-9, pag. 1772 – 1777

[13]. Littler T.B., Morrow D.J., *Wavelets for the analysis and compression of power system disturbances*, IEEE Transactions on Power Delivery, Vol.14, No.2, April 1999, pp. 358 - 364

[14]. Zheng T., Makram E.B., Girgis A.A., *Power system transient and harmonic studies using wavelet transform*, IEEE Transactions on Power Delivery, Vol.14, No.4, October 1999, pp. 1461 - 1468

[15]. Huang S.-J., Hsieh C.-T., Huang C.L., *Application of Morlet wavelets to supervise power system disturbances*, IEEE Transactions on Power Delivery, Vol.14, No.1, January 1999, pp. 235 - 243

[16]. Gaouda A.M., Salama M.M.A., Sultan M.R., Chikhani A.Y., *Power quality detection and classification using wavelet-multiresolution signal decomposition*, IEEE Transactions on Power Delivery, Vol.14, No.4, October 1999, pp. 1469 - 1473

[17]. Chikhani A.Y., Dash P.K., Basu K.P., *Time-frequency based pattern recognition technique for detection and classification of power quality disturbances*, TENCON 2004, 2004 IEEE Region 10 Conference, vol. 3, pp. 260 – 263

[18]. Styvaktakis E., Bollen M.H.J., Gu I.Y.H., *Expert system for classification and analysis of power systems events*, IEEE Transactions on Power Delivery, vol. 17, no. 2, April 2002, pp. 423 - 428

[19]. Bollen M.H.J., Gu I.Y.H., *Signal processing of power quality disturbances*, IEEE Press, A John's & Sons, Inc., Publication, U.S.A., 2006

[20]. Poularikas W.K., e.t., *Digital signal processing*, The Electrical Engineering Book, Ed. Richard C. Dorf, CRC Press LLC, 2000

[21]. DSG Pollock, *A Handbook of Time series analysis, signal processing, and dynamics, Signal processing and its applications*, Academic press, 1999, London, United Kindom

[22]. R.L.Allen and D.W. Mills, *Signal analysis, Time, frequency, scale and structure*, IEEE Press and Wiley interscience, John Wiley and The sons publication, 2004

[23]. Box, G.E.P., and G.M. Jenkins, (1970), *Time Series Analysis, Forecasting and Control*, Holden-Day, San Francisco

DIFFERENT METHODS TO FUNCTIONALIZATION OF MULTIWALLED CARBON NANOTUBES FOR HYBRID NANOARCHITECTURES

PRODANA M., IONITA D., BOJIN D., DEMETRESCU I.
University "Politehnica" of Bucharest, Splaiul Independentei, No 313, Bucharest-060042, Romania,
md_ionita@yahoo.com

Abstract - Multiwalled carbon nanotubes (MWCNTs) were functionalized with various functional groups in order to obtain new hybrid materials with better properties used for manny applications. Four methods of functionalization were used in this paper to obtain functionalized multiwalled carbon nanotubes: MWCNT-COOH, MWCNT-COOAg, MWCNT-COOCu and MWCNT-NH_2. The morphology of these materials was analized with transmission electron microscopy (TEM) and the chemical bonds were put in evidence using infrared spectroscopy (FTIR) analisys.

Keywords: carbon nanotubes, functionalization, dispersion, TEM, FTIR.

1. INTRODUCTION

Since their discovery in 1991 by Iijima [1], carbon nanotubes (CNTs) have attracted great interest in most areas of science and engineering due to their unique physical and chemical properties, which enable them to be applied for a wide range of applications [2–5].

A common technique to improve dispersion and realize such a great capability of CNTs is through chemical functionalization, which enables chemical covalent or non-covalent bonding between the CNTs and material of interest. The covalent side-wall modifications of nanotubes have been well described in several review papers [6, 7].

Taking into account that nanotubes are heterogeneous materials and their dimensions, functionalization surface charge, and agglomeration have impact on reactivity we have to understand how we can improve the dispersion of these materials. The functional groups which can be attached to the CNTs surface range from small molecules to macromolecules can be used in different applications, especially in the nanocomposites field. Applications in compound materials, electronic devices, nanosensors or gas storage material and solar cells are intensively explored. All these potential applications require an extended functionalization of the nanotubes to make them processable and to tune their properties.

The present study proposes a modality of increasing the degree of dispersion in different solvents using four modalities of functionalization.

The nanotubes functionalization is performed according a chemical procedure introducing -COOH groups, -COOAg, -COOCu and $–CONH_2$.

Regarding silver nanoparticles there are several elaboration methods including biogenic production [8, 9]. Our method involves 100 mL of aqueous solution of silver nitrate with a concentration of 0.25 M, and 85 mL 0.25 M trisodium citrate. While stirring vigorously, 0.6 mL of 10 mM $NaBH_4$ was added to the solution. Following this the silver nanoparticles were deposited onto carbon nanotubes.

Multiwalled carbon nanotubes of curled shape have about 20-40 nm in diameter and 0.1-10 μm length are provided by Sigma Aldrich with a purity of 90%.

It has been shown in the literature that functionalized CNTs has several applications in different fields, which makes this area of research very attractive indeed for many researchers. The present study presents a detailed methodology for functionalizing MWCNTs with different functional groups of value for a variety of different purposes.

2. METHODOLOGY FOR FUNCTIONALIZING MWCNTs

2.1. Functionalization of MWCNTs

Multiwalled carbon nanotubes were covalently functionalized by the oxidation procedure. As shown literature [10], this oxidation treatment disrupts the π bonding symmetry of sp^2 hybridize carbon atoms and produces a high density of functional groups along the entire length of CNTs, such as carboxyl, carbonyl, and phenolic groups.

MWCNTs (3.0 g) were dispersed in 98% concentrated sulphuric acid under ultrasonication at 50°C for 6 h to produce oxidized carbon nanotubes (MWCNT-COOH) [11]. The samples were washed with ultrapure water and dried at 50 °C for 12 h.

The final products were nanotube fragments whose ends and sidewalls were decorated with various oxygen-containing groups (mainly carboxyl groups) (Fig. 1). Moreover, the percentage of carboxylic functional groups on the oxidized MWCNTs surface does not exceed 4% in the best cases which corresponds to the percentage of MWCNTs structural defects [12].

 ISSN 2067-5534

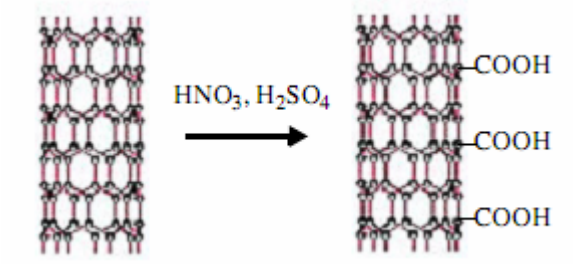

Fig. 1 - Chemical modification of carbon nanotubes (CNTs) through thermal oxidation

With these groups present, carbon nanotubes show a very good dispersibility in aqueous solvents, where they remain stable for months.
The larger surface area of MWNTs can be used as templates to prepare nanoparticulate hybrid systems consisting of Ag and Cu nanoparticles.

2.2. Preparation of MWCNT-COOAg

One gram of MWCNT-COOH was dispersed in 100 mL of distilled water through ultrasonication.
To this solution, 100 mL of 0.2 M Ag nitrate solution was added with constant stirring at 60°C to generate Ag ions grafted carbon nanotubes (MWCNT-COOAg). After the completion of reaction, solid products were collected by centrifuging and dried under vacuum at 50°C. Ag ions grafted onto carbon nanotubes were reduced at 200° C to generate Ag nanoparticles on the carbon nanotube surface.
The complete scheme for the modifcation of the nanotube surface and the attachment process of the gold nanoparticle on the nanotube surfaces is shown in Fig. 2.

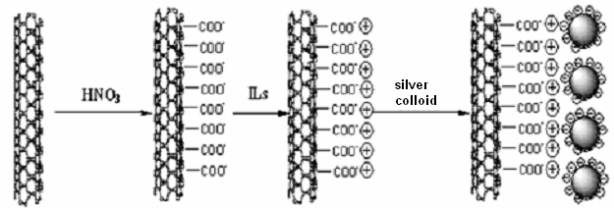

Fig. 2 - Schematic process for anchoring silver nanoparticles to nanotubes

2.3. Preparation of MWCNT-COOCu

One gram of MWCNT-COOH was dispersed in 100 mL of distilled water through ultrasonication.
To this solution, 100 mL of 0.2 M $CuCl_2$ solution was added with constant stirring at 80°C to generate Cu ions grafted carbon nanotubes (MWCNT-COOCu).
After the completion of reaction, solid products were collected by centrifuging and dried under vacuum at 50°C. It is expected that during drying process, Cu ions developed on the carbon nanotube surface get reduced to Cu nanoparticles and adhered on the surface by Van der Waals force of interaction.

The schematic representation of the obtaining processes of MWCNT-COOCu is show in Fig. 3.

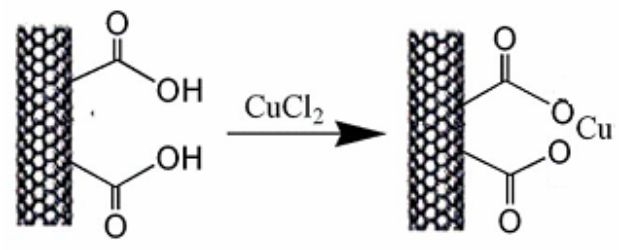

Fig. 3 - Schematic process for anchoring cooper nanoparticles to nanotubes

2.4. Synthesis of MWCNT-NH_2

Dried MWCNT-COOH (0.1 mg) was reacted with excess $SOCl_2$ (25 mL) at room temperature for 30 minutes. The residual $SOCl_2$ was removed by washing with tetrahydrofuran THF and filtered with ultrapure water.
The MWCNTs were dried for 20 minutes at the room temperature.
The new functionalized nanotubes MWCNT-$SOCl_2$ (10 mg) are added in etilendiamine in excess for 10 hours at the room temperature. The mixture was washed with THF and filtered. The nanotubes were dried at 80°C for 10 hours.

2.5. Synthesis of nanoarhitectures based on MWCNTs and hydroxyapatite (HA)

Another type of nanoarchitecture with nanoparticles was biomimetic coating with HA (hydroxyapatite) on MWCNTs surface. Such coating was elaborated via immersion in a solution of 0.042M $Ca(NO_3)_2x4H_2O$ and 0.025M $NH_4H_2PO_4$ at a pH of 4.8.
Functionalized MWCNTs material was dispersed in a dispersive material and ultrasonically prepared for 10 min.
It was studied the synthesis of HA from a Ca/P solution and to obtain the growth of the crystals were used carbon nanotubes. The temperature was kept at 37°C, the temperature of human body. This factor leads to the formation of cubical HA.
The morphology was tested with transmission electron microscopy.

3. RESULTS

3.1. TEM Analysis

Nanosized particles are investigated using Transmission Electron Microscopy analysis (TEM) with an EM-410 Philips, 60kV microscope. Acid treatment removes the impurities as amorphous carbon particles and also introduces the –COOH groups on the surface of MWCNTs.
The formation of Ag and Cu nanoparticles (nAg and nCu) on the MWCNTs surface is confirmed by TEM.

TEM analysis shows in Figs. 4 MWCNTs having 20-40 nm in diameter MWCNTs functionalized with Ag ions and MWCNTs functionalized with Cu ions grafted onto carbon nanotubes that were reduced at 200° C.
Regarding distribution of silver and cooper nanoparticles ImageJ soft were used. Particle sizes of Cu solutions were determined and the average diameter is between 10.8-39.9 nm meanwhile particle size of Ag solutions were determined and the average diameter is between 11.8-17.9 nm as is shows in Figs. 5.

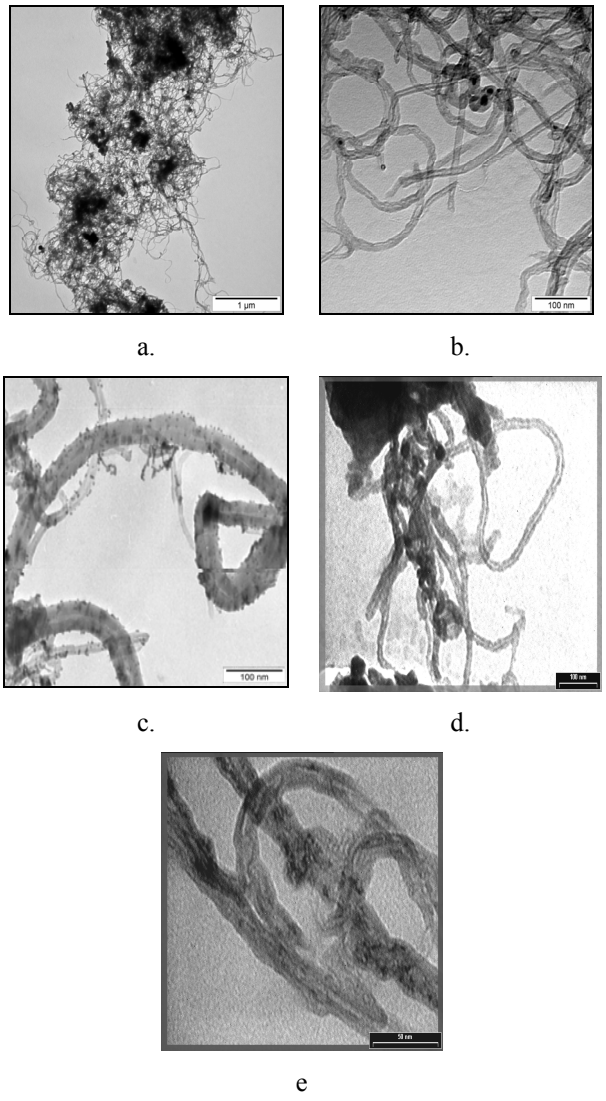

Fig. 4 - TEM images for a. MWCNTs; b. MWCNT-COOH and c. MWCNT-COOAg d. MWCNT-COOCu and e. MWCNT-NH_2

It can be seen that the silver and cooper particles preferentially adhere to the surfaces of MWCNTs rather than to other regions without MWCNTs.
Dark spots correspond to Ag and Cu nanoparticles and the tubes correspond to MWCNTs. The side walls of MWCNTs are evenly decorated with Ag or Cu nanoparticles. The densities of attached nanocrystals are high. Observed nanoparticles appear to have a narrow size distribution, and no free particles are observed in the background of the TEM images, which confirms all formed Ag or Cu nanoparticles are durably attached to the nanotubes. These nanoparticle-decorated nanotube heterostructures could be used in catalytic, electronic, optical, medical and magnetic applications.

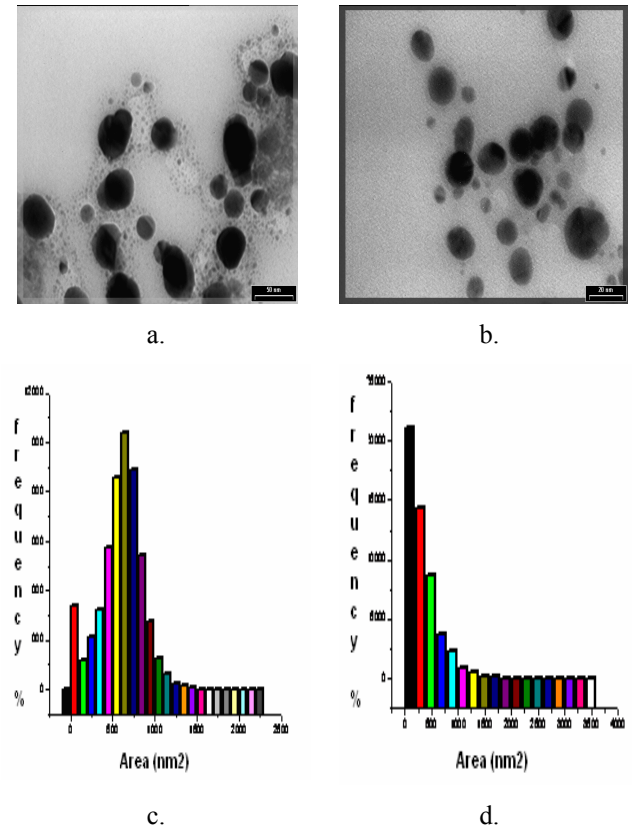

Fig. 5 - TEM images for a. nCu; b. nAg and c. size distribution histogram for nCu d. size distribution histogram for nAg

Meanwhile, the –COOH and $–NH_2$ functionalization doesn't change the morphology of multiwalled carbon nanotubes but improve the degree of dispersion.
Figs. 6 shows the TEM micrographies for the hybrid samples, functionalized with Ag and Cu nanoparticles, immersed in a solution with 0.042 M $Ca(NO_3)_2x4H_2O$ and 0.025 M $NH_4H_2PO_4$.
TEM images shows that the crystallites of 100 nm in width and 500 nm in length were grown radially originating from a common center to the intersection of two MWCNTs and perpendicularly to the longitudinal direction of MWCNTs. HA layers first starts to grow in zone with more agglomerations of MWCNTs as it is shows in Fig. 6.
The MWCNTs maintained their typical tubular structure in the HA matrix, as shown in Fig. 6a, and would therefore be expected to act as an excellent reinforcement in the HA matrix.
Potential and realized applications of the resulting functionalised MWCNTs/HA composite coatings are bioactive coatings.
Using immersion method of obtaining the hybrid material based on MWCNTs and HA, we observe the

ISSN 2067-5534 © 2012 JSE

different morphologies depending of the functionalized groups of the MWCNTs. (Figs.6)

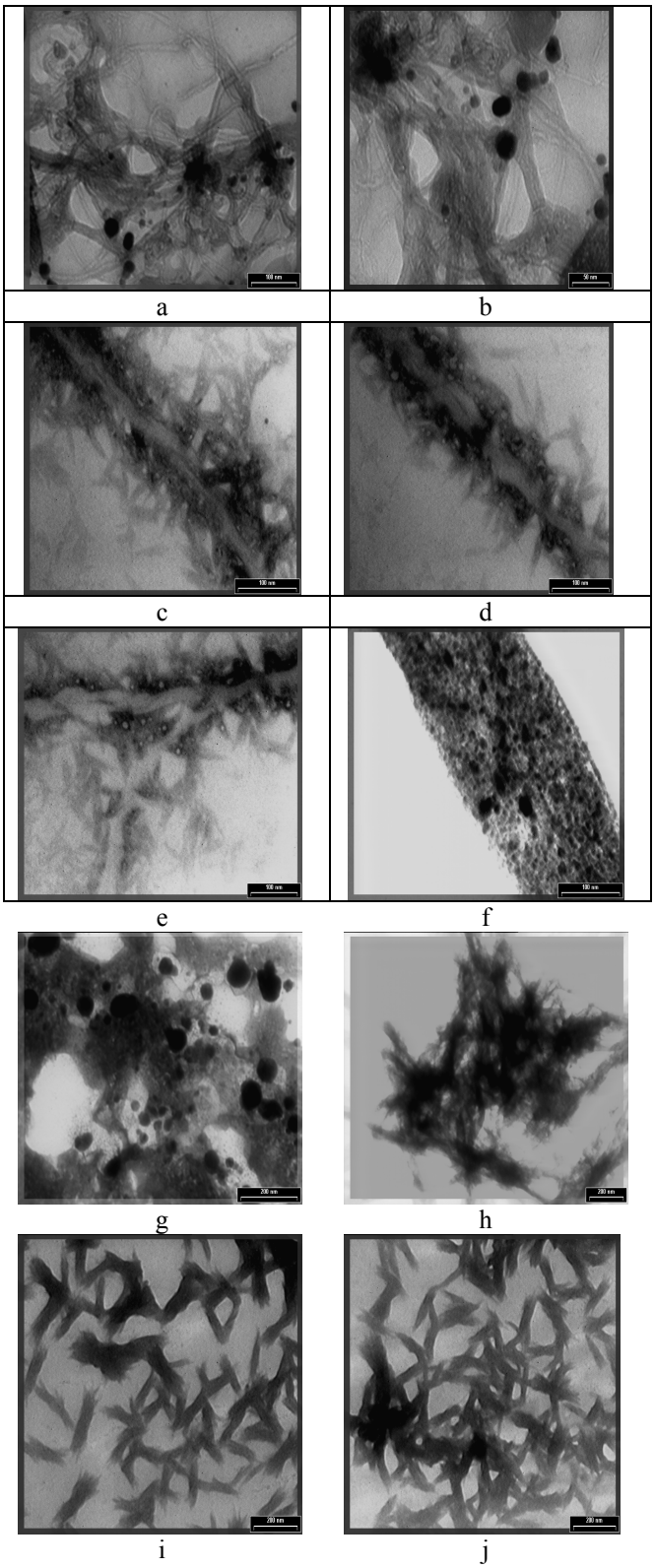

Fig. 6 - TEM images for a,b,c,d,e) MWCNT-COOAg/HA and f,g,h,i,j) MWCNT-COOCu/HA

The EDS spectra, showing the constituent elements of the HA coatings with MWCNTs, are presented in Fig. 7. The presence of the MWCNTs was confirmed by the peaks for carbon in the EDS spectrum of the MWCNTs/HA composite coating.

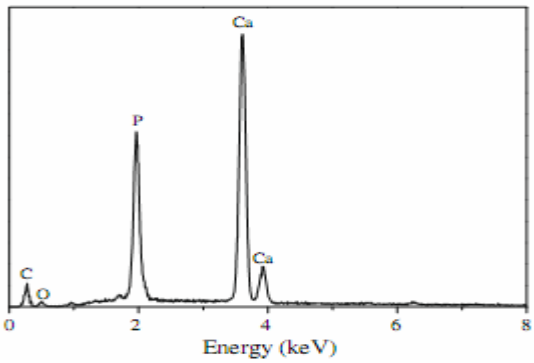

Fig. 7 - EDS spectrum of hybrid material MWCNTs/HA

3.2. FTIR analysys

The –COOH and $–NH_2$ functionalization is put in evidence by FTIR measurements.

FTIR has been used to map the chemical distribution of carbon nanotubes MWCNTs, acid treated MWCNT-COOH and MWCNT-NH_2. Infrared Microscopy Spectral data were recorded by an ATR Perkin- Elmer equipment. FTIR spectra from the MWCNTs show a broad peak at 3436 cm^{-1}, which refers to the O-H stretch of the hydroxyl groupwhich can be ascribed to the oscillation of carboxyl groups. Carboxyl groups on the surfaces of as-received MWCNTs could be due to the partial oxidation of the surfaces of MWCNTs during purification by the manufacturer. This feature moves to 1726 cm^{-1} and is associated with the stretch mode of carboxylic groups as observed in the IR spectrum of the acid-treated MWCNTs (Fig. 8a) indicating that carboxylic groups are formed due to the oxidation of some carbon atoms on the surfaces of the MWCNTs by sulphuric acid. The IR spectra of oxidized MWCNTs shows four major peaks, located at 3750, 3450, 2370, and 1562 cm^{-1}. The peak at 3750 cm^{-1} is attributed to free hydroxyl groups. The peak at 3436 cm^{-1} can be assigned to the O-H stretch from carboxyl groups (O=C−OH and C−OH), while the peak at 2364 cm^{-1} can be associated with the O−H stretch from strongly hydrogen-bonded −COOH. The peak at 1565 cm^{-1} is related to the carboxylate anion stretch mode. The peak at 1631 cm^{-1} can be associated with the stretching of the carbon nanotube backbone. The peaks at around 2877 and 2933 cm^{-1} correspond to the H−C stretch modes of H−C=O in the carboxyl group.

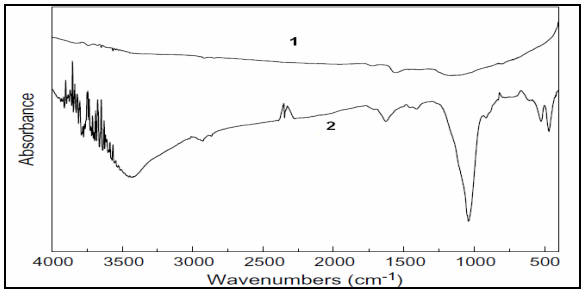

a.

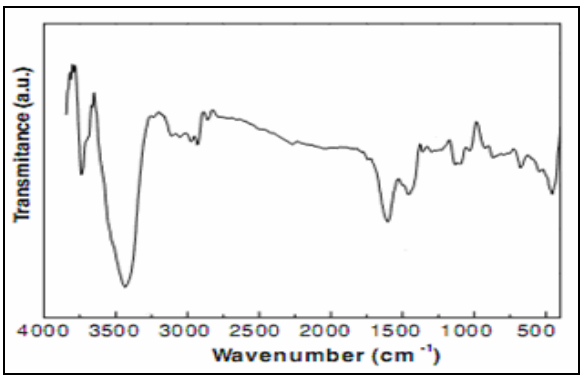

b.

Fig. 8 - FTIR spectra of: a) 1. MWCNTs, 2. MWCNT-COOH; b) MWCNT-NH_2

For MWCNT-NH_2 (Fig. 8b) the bands at 2918 and 2850 cm^{-1} represent asymmetrical and symmetrical stretching of CH_2 groups. The C–N stretching vibration and the scissoring in-plane N–H distortion of free primary amine group are observed at 1040 cm^{-1} and 1628 cm^{-1}, respectively. The broad band at 3410 cm^{-1} is attributed to the NH_2 stretching.

4. CONCLUSIONS

The functionalized MWCNTs obtained using different functional groups were analyzed using Fourier Transform Infrared (FTIR) spectroscopy.

The immersion in Ca/P solution was used with good results for obtaining HA coatings on carbon nanotubes surface. We obtained the HA on the MWCNTs surface with different size and morphology puts in evidence by TEM. Functionalized MWCNTs and HA formed some systems appear like a booklet with unique morphology that can be used in a different applications.

Acknowledgments: Authors recognise financial support from the European Social Fund through POSDRU/89/1.5/S/54785 project: "Postdoctoral Program for Advanced Research in the field of nanomaterials".

REFERENCES

[1]. Iijima, S. – Helical microtubules of graphitic carbon, Nature, vol. 354, 1991, pg. 56-58

[2]. Baughman, R.H., Zakhidov, A.A., de Heer, W.A. – Carbon Nanotubes , Science, vol. 297, 2002, pg. 787–792

[3]. Gooding, J.J. – Nanostructuring electrodes with carbon nanotubes, Electrochim. Acta, vol. 50, 2005, pg. 3049–3060.

[4]. Lin, Y., Taylor, S., Li, H., Fernando, K.A.S., Qu, L., Wang, W., Gu, L., Zhou, B., Sun, Y.P. – J. Advances toward bioapplications of carbon nanotubes, Mater. Chem.. vol. 14, 2004, pg. 527–541

[5]. Bianco, A., Kostarelos, K., Partidos, C.D., Prato, M. – Biomedical applications of functionalised carbon nanotubes, Chem. Commun., vol. 5, 2005, pg. 571–577

[6]. Banerjee, S., Hemraj-Benny, T., Wong, S.S. – Covalent Surface Chemistry of Single-. Walled Carbon Nanotubes, Adv. Mater., vol. 17 , 2005, pg. 17–29

[7]. Tasis, D., Tagmatarchis, N., Bianco, A., Prato, M. – Chemistry of carbon nanotubes, Chem. Rev., vol. 106, 2006, pg. 1105–1136

[8]. Lkhgvajav, N., Yasa, I., Celik, E., Koizhaganova, M., Sari, O. – Antimicrobial activity of colloidal silver nanoparticles prepared by sol-gel method, Digest J. Nanomat. Biostruct., vol. 6, 2011, pg. 149-154

[9]. Popescu, M., Velea, A., Lörinczi, A. – Biogenic production of nanoparticles, Digest J. Nanomat. Biostruct., vol. 5, 2010, pg. 1035 – 1040

[10]. Yu, R., Chen, L., Liu, Q., Lin, J., Tan, K.L., Ng, S.C., Chan, H.S.O., Xu, G.Q., Hor, T.S.A. – Platinum deposition on carbon nanotubes via chemical modification, Chem. Mater., vol. 10, 1998, pg. 718- 722

[11]. Prodana, M., Ionita, D., Ungureanu, C., Bojin, D., Demetrescu, I. – Enhancing antibacterial effect of multiwalled carbon nanotubes using silver nanoparticles, Dig. J Nanomater. Bios., vol.6, 2011, pg. 549-556

[12]. Balasubramanian K., Burghard, M. – Chemically Functionalized Carbon Nanotubes, Small, vol. 1, 2005, pg. 180–192

ISSN 2067-5534 © 2012 JSE

TEMPERATURE MEASUREMENTS TO OHTL FROM TPG

RODEAN I., MORAR D.
NPGC "Transelectrica"-SA, no.2-4 Olteni, Bucharest,
ioan.rodean@transelectrica.ro, daniel.morar@transelectrica.ro

Abstract - This paper presents methods for operational analysis of OHTL elements. The OHTL, which were taken in consideration, are very old. The active conductor, the clamps and the fittings are with defects. The technical difficulties for operate the power grid and their resolutions are presented in the paper. The analysis methods taken in consideration are based on the operational reliability, the technical parameters of equipments and their variations in operation periods, the importance of the equipments parameters, the statistic and the reliability, and the specific parameters. In this paper is presented a specific example for this application, on an OHTL from an important zone. The system used for study is RITHERM RIBE type. The results of the analysis were applied on some OHTL of NPGC "Transelectrica"-SA, which is the National Power Grid Operator, and are presented in this paper.

Keywords: OHTL, Operation, RITHERM, Temperature.

1. INTRODUCTION

We studied the operational behaviour of OHTL from the Power Grid.

The equipments are old and are near limits of their life cycle. Their parameters need to be verified to conclude that they correspond, compared with the requirements from the Power Grid about the parameters: safety, economics and quality.

The tasks of European Power Networks are to develop their structure and to operate on their safety limits. In the case of failure of some OHTL, the study achieved of the Energetic Companies from Europe shows that on remaining OHTL, the loads grows till 180%.

To operate with OHTL to their safety limits needs to be known the exact conditions of the active conductor and the fittings and, of course, the value of their parameters.

The methods chosen to measure the OHTL parameters are present in this paper.

We used the equipment from RIBE Germany [1].

2. REQUIREMENTS FOR MONITORING SYSTEMS COMPATIBILITY

In the substations are connections of the information for monitoring and control equipments from substations and the OHL. The information flow in a substation consists of technical data acquired, especially on-line, from the equipments with monitoring systems, SCADA and other systems. The monitoring systems are operated by the existing computer networks in which they may or may not be separated from other systems.

The data existing in these systems are used by a large number of users, which are very different.

In the substation we found systems with a single function or systems with several functions. Thus, SCADA has many functions, but the main one being the command function and the second are the surveillance functions of the equipment, especially at the transformers units and the circuit breakers.

From operational experience gained it's shown that systems which meet several functions have given the lowest safety for TPG and highest risk of failure. On the other hand, they provide a more complete picture of the supervisory equipment. Also, too many information makes the operation difficult and decreases the accuracy of actions and the response.

Therefore maintaining a high level of safety information, in terms of actions taken by operators, can be achieved by creating, for each category of users, the different access levels, and various loads by software.

Also for the safety of operational systems is recommended to function in different networks, protected from each other. It is recommended that, for correct operation and real-time, SCADA to contain only the command-control functions and the overall technical parameters of the grid and general signs of operation of equipment. The proper technical parameters for the functioning of equipments should belong to the monitoring system. In the same idea and other systems would be advisable to include only their specific functions. The specific technical parameters for the functioning of equipments, managed by those systems should belong to the monitoring system. Those monitoring systems must contain a network of high speed data transmission and network management with a large number of terminals [2].

So, all systems will be separate, for safety reasons, and will have the multiple functions. But there are users who need information from multiple systems and with different degrees of access from one system to another.

Those are some of the reasons for achieve a management plan appropriate for these goals.

A solution could be the using of the software for each type of system (preferably with the same software), with separate screens for each level of authorization/access, and use a central server, which can be accessed by each operator. The central server will play the role of manager.

3. DESCRIPTION OF EQUIPMENTS

In the transport of the electric energy are many factors influencing: the safety condition of the Power Grid, the quality of the electric energy, the economic factors and their normal operation. Those factors also have influence on the life time of the equipments (their wear).

The RITHERM system offers the optimum monitoring of the OHTL conductor temperature. The RITHERM system measures the OHTL parameters on-line.

The RITHERM system can makes the measurements of following parameters of the OHTL:

-The temperature of the active conductor

-The load on OHTL

The system also has sensors for:

-The temperature of air (ambiance)

-The wind speed

The system calculates the limits of parameters and corrects the erroneous measurements of parameters (load, temperature). The factors taken in consideration by the system are: the ambient temperature, the wind speed, the load on OHTL and the conditions of operation of the active conductor and the fittings.

This system uses the SAW technology, with radar wave for measurement. Comparing the other similar systems, the RITHERM system no needs to feed from external sources. The RITHERM system parameters are continuously measured with an SAW sensor, which are no need to be powered, being mounted on the active conductor. The RITHERM system reads the parameters from the sensor/central unit, then transmit the information to the server and finally at the users. For this task the RITHERM system is used an independent source [1].

The communication between receiver and central unit is achieved by optical support and the communication between central unit and user's server are routed by GPRS systems [1].

The software, which was installed on user's PC at his headquarter, offers the values of the OHTL parameters on-line on PC screen. The software offers the on-line viewing of the parameters in graphics mode.

The GPRS transmission by the RITHERM system is optimum, reducing the open time of the system to minimum [1].

The energy source of the RITHERM system is based on the solar energy system.

4. OPERATION METHOD FOR THE EQUIPMENT

The RITHERM system is functional on an OHTL from Romanian Power Grid System: OHTL Fântânele-Gheorgheni 220kV, from Sibiu Transmission Subsidiary. The RITHERM system is in function, for measure the temperature of the active conductor.

The OHTL Fântânele-Gheorgheni 220kV is in function from 1960. Their components are original. So, both the conductor and the fittings are very old.

That temperature measurement of the OHTL's active conductor is necessary to monitor behaviour of this OHTL in operational time.

The OHTL's active conductor is the ACSR 400/93 mm^2 type. The electric resistances of the splices are very high, because of their components, which are aging.

The values of the temperature recorded from the OHTL Fântânele-Gheorgheni 220kV with the RITHERM system shows that the temperature of fittings and splices are higher than the active conductor and this fact need to be changed in the future.

The values of the temperature of the fittings were verified using the infrared systems. The apparatus used for infrared measurement is the Fluke type.

The values of the OHTL's parameters obtained from the RITHERM system were analyzed and the results were compared with the theoretical calculus. The limits for the difference between the theoretical calculus and the practical results were established at an error coefficient of 2.3%.

For analyze the data, provided by the system, the authors have chosen the method based on the probabilistic models [2]. Was used the specific data from this OHTL for promote acquisition of new equipments for supervisory the others OHTL considered.

However, the system chosen proved to be reliable.

The conclusions of this study on the OHTL are:

-The OHTL needs to be rehabilitated (especially the fittings)

-The measurements achieved with the RITHERM system was successfully

The measurements of OHTL's fittings in the infrared are shown in the Fig. 1.:

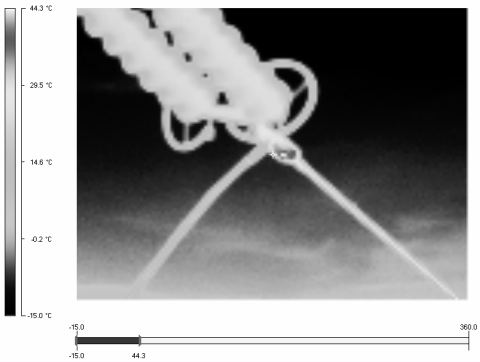

Fig. 1 - The infrared graphic of the OHTL's fittings

The values of the temperature recorded by the RITHERM system are presented in the Fig. 2.:

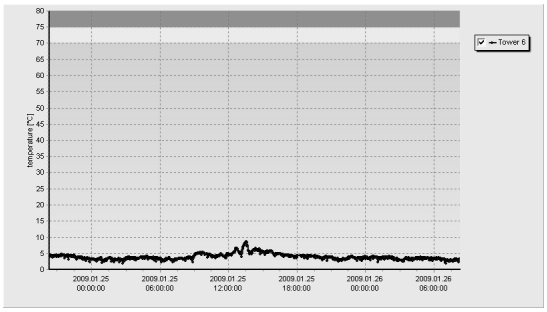

Fig. 2 - The temperature of the active conductor

ISSN 2067-5534

The values of the ambient temperature recorded by the RITHERM system are presented in the Fig. 3.:

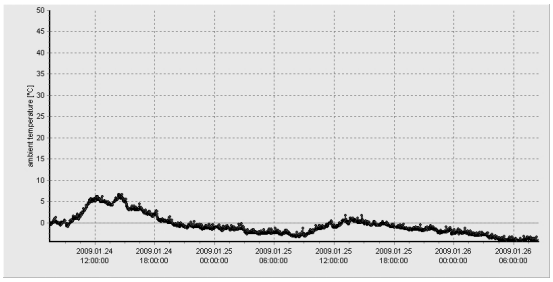

Fig. 3 - The temperature of air

The OHTL was evaluated about its reliability and the reliability of each component, taking into account the number of failures of the equipment. The result of this evaluation is shown in table 1.

Table 1 - Representative data obtained by RITHERM.

no.	date	conductor temperature [^{0}C]	ambient temperature [^{0}C]	load [MW]
1	12.12.2008 11:14	5,8	1,7	8
2	12.12.2008 11:15	5,4	2,1	8
3	12.12.2008 11:17	5,3	1,7	8
4	12.12.2008 11:18	5,6	1,7	8
5	09.12.2010 19:43	6,0	3,3	22
6	09.12.2010 19:44	6,1	3,2	21,5
7	09.12.2010 19:45	6,0	3,2	21,5
8	29.12.2010 22:07	3,4	-6,6	14,4
9	29.12.2010 22:10	3,6	-6,5	14,4
10	29.12.2010 22:14	3,6	-6,7	14,4
11	29.12.2010 22:15	3,7	-6,6	16,3
12	29.12.2010 22:20	3,7	-6,9	16,3
13	29.12.2010 22:25	4,0	-6,5	16,3
14	30.12.2010 09:18	0,3	-12,3	11,5
15	30.12.2010 09:19	0,2	-12,3	11,5
16	30.12.2010 09:20	0,1	-12,2	11,5
17	30.12.2010 09:23	-1,2	-12,4	11,5
18	04.01.2011 05:28	0,9	-4,4	37,3
19	04.01.2011 05:29	0,8	-4,6	37,3
20	04.01.2011 05:30	0,7	-4,6	44,4
21	04.01.2011 05:31	0,7	-4,7	44,4
22	05.01.2011 07:14	7,1	-10,1	21,9
23	05.01.2011 07:15	7,0	-10,1	24,3
24	03.03.2011 09:14	9,2	1,8	10,8
25	03.03.2011 09:15	9,2	1,8	11,1
26	03.03.2011 09:16	9,5	1,7	11,1
27	06.06.2011 23:43	17,9	16,9	6,5
28	06.06.2011 23:44	17,9	17,0	6,5
29	06.06.2011 23:45	18,1	16,9	5,7
30	06.06.2011 23:46	18,0	17,1	5,7
31	05.06.2011 16:57	40,4	26,3	16,7
32	05.06.2011 16:58	40,7	26,3	16,7
33	05.06.2011 16:59	41,222	26,263	11,2
34	08.08.2011 21:59	26,0	22,7	1,2
35	08.08.2011 22:00	25,5	22,9	2
36	21.08.2011 15:41	40,5	25,9	4,4
37	24.08.2011 14:46	50,74349213	31,58158112	6,8

From this data were resulted the following conclusions:

- The periods were recorded with power losses in the LEA
- The periods in which the LEA had the corona losses
- The periods when on LEA was recorded the values of power below the natural power
- Periods when on LEA was recorded the values of power over the natural power or overload
- Changes in climatic parameters in the area during these years
- Components of the LEA that had some flaws
- Events in the LEA that resulted in damage to components
- Solutions for adjusting the TPG parameters to reduce power losses

5. CONCLUSION

As far as the reliability offered by the OHTL, the work was focused mainly on the great achievements, achieved quite recently and putted into operation. Other systems were also analyzed, but because there were not obtained the satisfactory results, none comment was

given here.

We will extend the surveillance on OHTL with new monitoring systems, which will have other functions, such as: the loads supervision, climatic parameters for determination of power losses (active power losses, corona losses, and other reactive power losses), swings, sags and gaps of the conductors.

REFERENCES

[1]. Lemke Diagnostics GmbH – RITHERM. User manual LD-SAW-OHTL, Schwabach, Germany, 2008

[2]. Morar D. – Metode performante de exploatare a staţiilor şi reţelelor de înaltă tensiune, Ph.D. thesis, The "Politehnica" University from Bucharest - PUB, Power Generation & Use Chair Dept., Faculty of Power Engineering, Bucharest, 2011

ISSN 2067-5534 © 2012 JSE

ENSURING ENERGY SECURITY IN FUTURE: A STUDY ON DIFFERENT STRATEGIC PLANS AND RELATED ENVIRONMENTAL IMPACTS

DEWAN MOWDUDUR RAHMAN*, NAVID BIN SAKHAWAT**, RIASAD AMIN*, FAISAL AHMED ***
*Department of EECE, Military Institute of Science and Technology, Dhaka, Bangladesh.
**Department of EEE, BRAC University, Dhaka, Bangladesh.
***Department of CIT, Islamic University of Technology, Gazipur, Bangladesh
mowdudur@gmail.com

Abstract – Energy is a pre-requisite for the civilization. However, usage of energy is not free of toll. Rising temperature by 0.44˚C during the last thirty years and 13% rise in atmospheric CO_2 concentration surely indicating us to make a quick transition from this harmful usage of energy to a safer one. If global warming, melting of polar ice, rise in sea level and consequent flooding of coastal areas continues like present manner, then millions of lives would be in danger and hundreds of thousands would be turned into climate refugee. It is not impossible to secure human race from danger in the long run. However, it involves with long-term planning, innovative idea generation and common people awareness. In this paper authors discussed about the pattern of problem aroused from conventional energy usage, the future threat from this and its ultimate solution. We present three possible scenarios of using different sources to meet energy requirements with respective credibility and possible impacts in order to find out the best-fitted solution for future energy security and ensure sustainable development.

Keywords: Energy security, environmental impacts, fossil fuel, nuclear energy, renewable energy.

1. INTRODUCTION

World is now passing an energy constraint time. As an easily accessible source, we have been dependent on fossil fuel so far. Meanwhile, fossil fuel use continues to impose massive environmental and economic costs. Now, time has come to choose between paying to continue the status quo and investing in a new energy future. World population is assumed to expand from an estimated 6.7 billion in 2008 to 8.5 billion in 2035 and electricity demand grows by around 80% by 2035, requiring 5900 GW of total capacity addition [1]. Therefore, this upcoming huge demand is not possible to meet by our fossil fuel reserve. Nuclear energy can be a solution in this context, however, is not also a risk-free solution. So far little is known about the damages associated with nuclear energy plant accidents. Moreover, the brutal effects of these kinds of incidents pass from one generation to another through radioactivity and can cause an everlasting suffering for human race. Therefore, we need to consider renewable energy as a viable alternative for energy security. Although it is more capital incentive than fossil fuel, we have to take some desperate measures in order to convert this into our main energy source. In addition, to make it possible we have to device a strategic plan with a combination of various types of energy in order to achieve energy security in future rather than exclusively depending on fossil fuel or nuclear energy.

2. CLIMATE CHANGE EFFECTS

Climate change is one of the most pressing environmental concerns of the 21st century. Developing countries are the most vulnerable to these risks [2] because of their generally low adaptive capacities [3]. No country alone can take interconnected challenges posed by climate change involving controversial political decision, daunting technological change, and far reaching global consequences. Emission of CO_2 is one of the main causes of global warming, melting of polar ice, rise in sea level, and consequent flooding of coastal areas. CO_2 is the main green house gas (GHG) emitted from various sources and power sector is solely responsible for 30% emission of CO_2 throughout the world [4]. Furthermore, the CO_2 emissions from power generation are projected to increase 46% by 2030 [5]. Man made CO_2 emission is closely linked to the combustion of coal, oil and gas. Moreover during past thirty years only coal consumption has increased by 48% [6]. According to International Energy Agency (IEA), projected CO_2 emission by 2020 will be 9927 Million tons. According to [7], in the 100 years span from 1880 to 1980, average global temperature has increased by 0.47˚C. However, from then in only 30 years span, temperature increased by 0.44˚C. If greenhouse gas (GHG) emissions continue to increase at the present rate, it is predicted that the average global temperature will increase by about 1˚C by the year 2025 and by 3˚C at the end of the century and the sea level will increase by 15 to 95 cm [8]. This will definitely engulf the coastal areas and low-lying countries and will make thousands of climate refugees. Key challenges to

tackling climate change in the world will be: Ensuring energy security; Ensuring food security and comprehensive disaster management; Addressing water scarcity and health; Dealing with forced migration and overall environmental degradation.

3. ENERGY SOURCES

The energy sources can be split into three categories: fossil fuels, renewable sources and nuclear sources. The fossil fuels are coal, petroleum, and natural gas. The renewable energy sources are solar, wind, hydroelectric, biomass and geothermal energy. The nuclear-powered sources are fission and fusion.

3.1 Fossil Fuels

These constitute the main forms of energy used worldwide. These are formed over a period of millions of years by the decomposition of animals and plants. These are not renewable sources as it would take too long to form these again in a natural process. These generally consist of carbon, sulphur and hydrogen and therefore, upon combustion form carbon dioxide, sulphur dioxide and water vapor (H_2O). Whilst the latter is relatively harmless the previous two are responsible for global warming and acid rain. Oil, coal and gas are the main forms of fossil fuel.

3.2 Nuclear Energy

Nuclear energy originates from the splitting of uranium atoms in a process called fission. Fission releases energy that can be used to make steam, which is used in a turbine to generate electricity. Uranium is a non-renewable resource that cannot be replenished on a human time-scale. Uranium is extracted from open-pit and underground mines. On average, uranium ore contains only 0.1% uranium. Most nuclear reactors require one specific form of uranium, uranium-235 (U-235). This form represents only 0.7% of natural uranium. To increase the concentration of U-235, the uranium extracted from ore goes through an enrichment process, resulting in a small quantity of usable 'enriched' uranium and huge volumes of waste. Today, the 439 commercial nuclear reactors in operation generate around 15% of the world's electricity [9].

3.3 Renewable Energy

Renewable energy is sustainable as it is obtained from sources that are inexhaustible (unlike fossil fuels). Renewable energy sources include wind, solar, biomass, geothermal and hydro, all of which occur naturally on our planet. Renewable energy, generally speaking, is clean energy and non-polluting. It is a sustainable energy source which can be relied on for the long-term. Renewable energy is cost-effective and efficient. On a global scale, 19% of electricity comes from renewable in 2008 [1].

4. PROBLEMS WITH FOSSIL FUELS

Fossil fuels have been a widely used source of energy every since the industrial revolution just before the dawn of the 20th century. Fossil fuels are relatively easy to use to generate energy because they only require a simple direct combustion. However, a problem with fossil fuels is their environmental impacts. Not only does their excavation from the ground significantly alter the environment, however, burning fossil fuels such as oil, coal, and gas results in the production of carbon dioxide and other greenhouse gases, which cause global warming. This is a stark truth, but the scientific facts point to significant warming, indicated by sea levels rising, hotter temperatures and freakish storm weather patterns, like tsunamis and hurricanes, becoming more and more regular. The most important thing is that, fossil fuels are not plentiful and despite obfuscation by several countries, fossil fuels especially oil production is now at the peak worldwide. As each oilfield has been being mined and depleted indicates us, we are running out of fossil fuel supplies.

Table 1 - Global crude oil reserves by region [10]

Country	bbl Mn	Percentage
Middle East	754,000	59.9
Africa	125,200	10
South and Central America	123,200	9.8
Euracia (excluding Central Asia)	101,000	7.6
North America	70,900	5.6
Asia-Pacific	42,000	3.4
Central Asia	40,000	3.2

Table 2 - Global natural gas reserve by country [11]

Country	Proved Natural Gas reserve (million cubic meters)
Russia	47,570,000
Iran	29,610,000
Qatar	25,370,000
Saudi Arabia	7,807,000
United States	7,716,000
Turkmenistan	7,504,000
United Arab Emirates	6,453,000
Nizeria	5,292,000
Venezuela	5,065,000
Aljeria	4,502,000
Iraq	3,170,000
Australia	3,115,000
Chaina	3,030,000
Rest of the World	**35,216,543**

ISSN 2067-5534 © 2012 JSE

5. PROBLEMS WITH NUCLEAR ENERGY

Nuclear power is often described as "the most expensive way to boil water". Despite its proponents now claiming it to be cost-effective, cost estimates for proposed projects have consistently proved inaccurate. Nuclear reactors present too large a liability for insurance companies to accept. One major accident, costing hundreds of billions of Euros (the total Chernobyl cost is estimated at □358 billion) would bankrupt them. Governments, and ultimately their taxpayers, are forced to shoulder this financial liability. The cost of clean-up after a nuclear power plant closes and the safe management of nuclear waste for many generations is also largely carried by the states instead of the companies themselves. In addition to substantial capital costs for construction of power plants, nuclear energy includes significant external costs like applying safeguards to sensitive activities, such as fuel making, securing nuclear facilities against terrorist attacks, decommissioning reactors, storing highly radioactive waste and paying for insurance to cover the costs of an accident. The declining nuclear industry is attempting to latch on to the climate crisis and concerns about energy security, by promoting itself as a "low carbon" solution. The Energy Scenario produced by the International Energy Agency shows that, even if existing world nuclear power capacity could be quadrupled by 2050, its share of world energy consumption would still be below 10%. This would reduce carbon dioxide emissions by less than 4% [12]. Other radioactive products formed in nuclear reactors can be used to produce dirty bombs. A nuclear power plant produces 10-15 tons of Spent Fuel a year on average. One ton of spent nuclear fuel typically contains about 10 kilograms of plutonium – enough for a crude nuclear bomb. Therefore we can say that, a typical nuclear power plant produces sufficient plutonium every year for 10-15 crude nuclear bombs.

Table 3 - Proved uranium reserves by country, 2008 [13]

Country	Amount (tonnes per year)	Global percentage (%)
Australia	1,243,000	23
Kazakhstan	817,000	15
Russia	546,000	10
South Africa	435,000	8
Canada	423,000	8
US	342,000	6
Brazil	278,000	5
Namibia	275,000	5
Niger	274,000	5
Ukraine	200,000	4
Jordan	112,000	2
Uzbekistan	111,000	2
India	73,000	1
China	68,000	1
Mongolia	62,000	1

6. STRATEGIES FOR FUTURE ENERGY SECURITY

Energy crisis is becoming more and more threatening day by day. Fossil fuel can possibly meet the present energy demand, however, it is not abundant at all and we can not continue depending on this forever.

Table 4 - Cost of electricity estimated by Massachusetts Institute of Technology (MIT) and University of Chicago report

Electricity Generation Type	MIT report (2003)	University of Chicago report (2004)
	Cost (cents per kWh)	
Coal	4.2	3.3 to 4.1
Natural Gas (Combined Cycle Gas Technology)	3.8 to 5.6	3.5 to 4.5
Nuclear	6.7	6.2

Most importantly, if we completely rely on this then the world would not be habitable because of pollution from fossil fuel and we would all die before running out of fossil fuel reserve. Nuclear energy can be considered as a solution because of the seemingly pollution free nature of nuclear plants. However, the construction cost, period of time required for construction and fatal accidental risks have to be considered before setting up a strategic plan to exploit nuclear energy as a viable option. Moreover, in this case, renewable energy can be considered as a viable option for future energy security. It is completely pollution free and abundant in nature. However, it is not possible to shift the pattern of energy source usage in a short period of time. It will definitely require time to change our traditionalistic view and be pro-active for a better and safe future in order to find out a sustainable solution for energy security. We have to go for a fossil-nuclear-renewable energy combination first then have to divert completely to a safe source of energy with adopting capability enhancement. The following sub-sections present 3 possible ways of facing our future energy demand with respective consequences:

6.1. Fossil fuel only

It is the worst case scenario. In this variant, we consider the scenario where fossil fuel is the only energy source. If we completely rely on fossil fuel then by the time being this usage will increase definitely as energy demand always increases day by day.

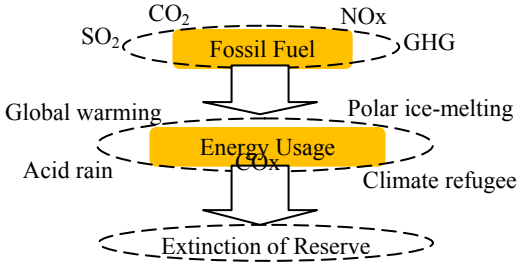

Fig. 1 - Illustration of the effects and end result of using fossil fuel only.

Due to depending more on fossil fuels, more pollution will take place and the reserve will run out very quickly. Global warming will reach its peak and environment will turned out rough. At the end, we will have nothing left to use as fossil fuel is not abundant at all.

6.2. Combination of fossil fuel and nuclear energy

In this scenario, we consider two sources for meeting the energy demand: one is fossil fuel and the other is nuclear energy. It would not be a wise decision to make this choice. In this case, we are allowed to meet our energy demand by fossil fuel and nuclear energy. By the time being, we will decrease our fossil fuel usage and increase nuclear energy usage. At one point of time, we will be running out of fossil fuel reserve. Then we have to rely on nuclear energy only for our total energy demand. However, it would not be free of toll. It has radiation and waste disposal problems, proliferation risk and fatal accidental fear. Most importantly, fuel of nuclear energy is not abundant. On average, uranium ore contains only 0.1% uranium. So one day it will be ended up also and then we would have nothing left to use.

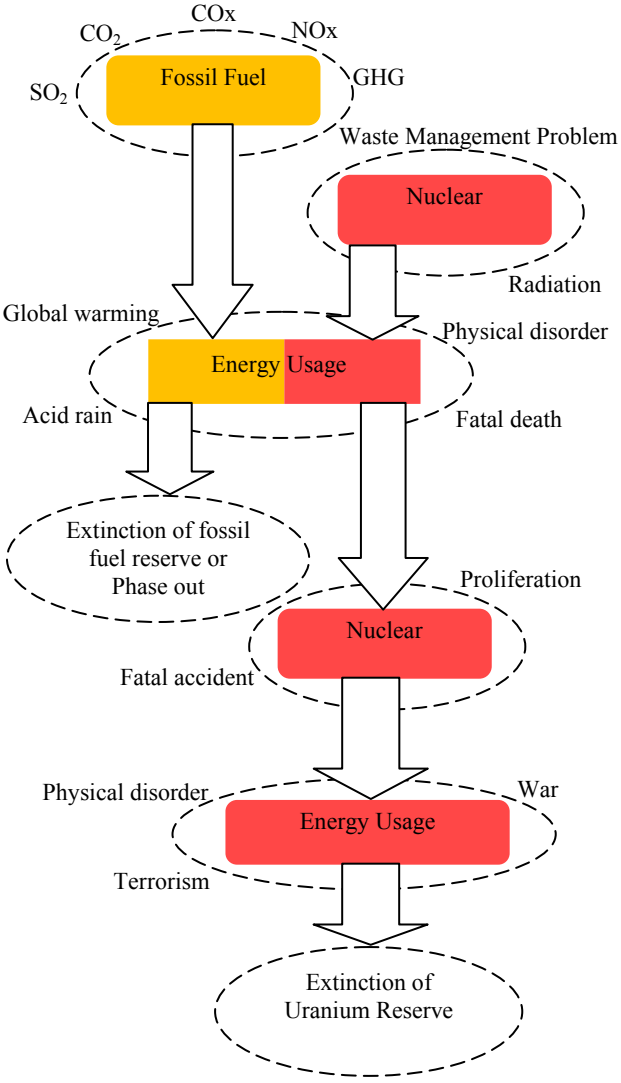

Fig. 2 - Illustration of the effects and end result of using a combination of fossil fuel and nuclear energy.

6.3. Combination of fossil fuel, nuclear energy, and renewable energy sources

This is the scenario where a combination of fossil fuel, nuclear energy, and renewable energy sources will be exploited, and definitely is the most suitable option to get rid of the present energy crisis and ensure a sustainable development for future. We have to start with these three types of fuel but gradually have to shift our consumption pattern from fossil fuel to nuclear energy and then to renewable energy completely. However, it is not possible to meet our entire energy demand from renewable sources over night.

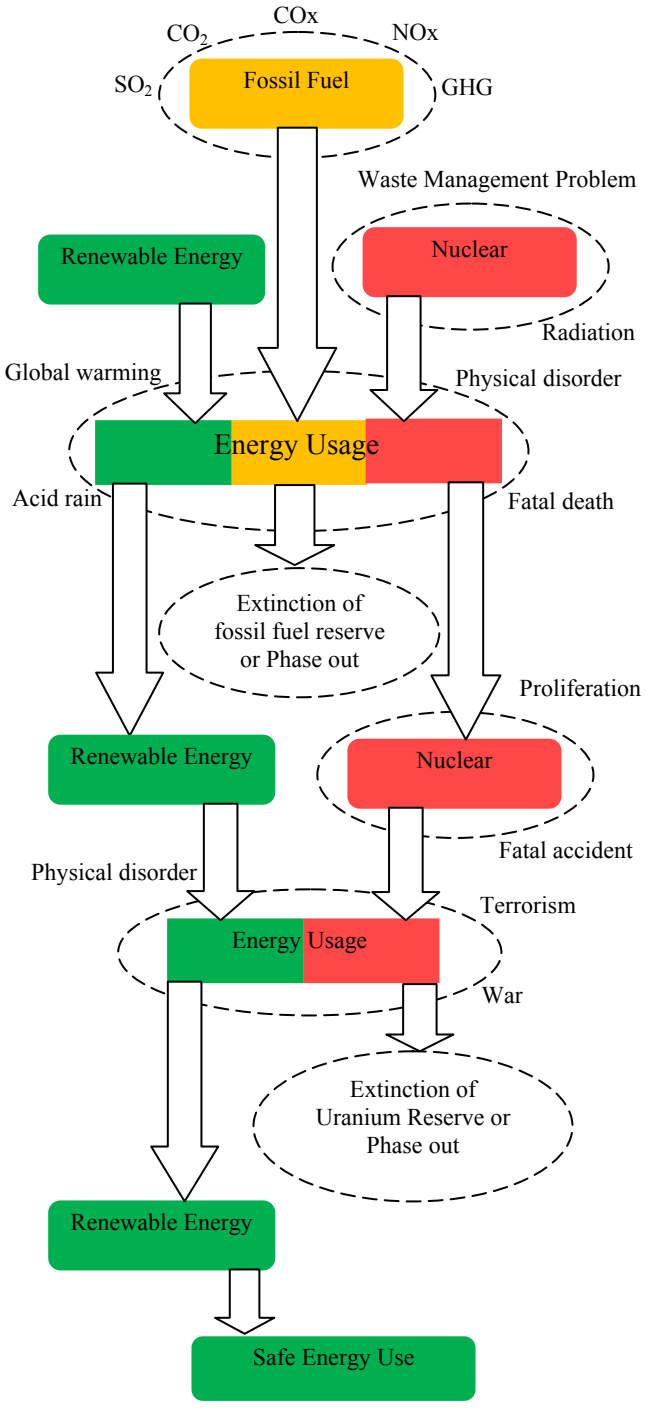

Fig. 3. Illustration of the effects and end result of using a combination of fossil fuel, nuclear energy, and renewable sources.

ISSN 2067-5534 © 2012 JSE

It is a continuous process involved with research and development, idea generation, and common people awareness. Initially, we have to face some problems caused by fossil fuel pollution and nuclear energy risks. However, we have to accept those as transitional effects and thus, gradually we will achieve the capability of harnessing all of our energy requirements from renewable energy sources.

7. CONCLUSION

Modern age is passing an energy deficient time and the coming days, people will definitely be hungry for energy. Today, more than 1.4 billion people worldwide lack access to electricity: 585 million people in sub-Saharan Africa (including over 76 million in Nigeria and some 69 million in Ethiopia) and most of the rest in developing Asia (including 400 million in India and 96 million in Bangladesh) [1]. This scenario urges us to take drastic actions in order to ensure energy security for future as well as for sustainable development. This issue needs to be addressed considering a compact energy policy includes: security of supply, environmental impact, world competitiveness and social concerns. Subsidy artificially lowers energy prices, which encourages wasteful energy consumption, exacerbate energy price volatility by blurring market signals, incentivize fuel adulteration and smuggling, and undermine the competitiveness of renewable sources. Therefore, we have to eradicate subsidies to fossil fuel, stop further exaggeration regarding nuclear energy and think about renewable energy with a broader mind.

ACKNOWLEDGMENT

Authors acknowledge the immense help received from the scholars whose articles are cited and included in references of this manuscript.

REFERENCES

[1] International Energy Agency, World energy Outlook 2010. Available: http://www.iea.org
[2] Boer, Y.D. - Adaption: A critical part of future action on climate change. Statement at the Congress: Adaption of Society to Climate Change, UNFCCC, 2009
[3] Intergovernmental Panel on Climate Change (IPCC), 2007. Climate change 2007: impacts, adaption and vulnerability, Contribution of Working Group II to the Fourth Assessment Report of IPCC. Cambridge, UK.
[4] Jilani, T., Gomi, K., and Matsuoka, Y.- Integration of sustainable and low carbon society towards 2025 in Bangladesh, In International Conference on Climate Change Effects and Energy Development in Bangladesh, Germany, 2011.
[5] Mondal, M.A.H., Denich, M.- Assessment of renewable energy resources potential for electricity generation in Bangladesh, Renewable and Sustainable Energy Reviews, vol.14, pg. 2401-2413, 2010
[6] Earth Policy Institute from BP, 2009. Statistical Review of World Energy, London.
[7] Earth Policy Institute, National Aeronautics and Space Administration (NASA), Goddard Institute for Space Studies (GISS), Global Land-Ocean Temperature Index in 0.01 degrees Celsius (online). Available: http://data.giss.nasa.gov/gistemp/tabledata/GLB.Ts+dSST.txt
[8] Intergovernmental Panel on Climate Change (IPCC), Climate Change 2007: Synthesis Report Summary for Policymakers, The 8th Session of Working Group II of the IPCC, Brussels , pg. 2-3.
[9] IAEA Power Reactor Information System, October 2008 (Online). Available:http://www.iaea.org/programmes/a2/
[10] BP Statistical Review of World Energy, 2009.
[11] Central Intelligence Agency (CIA), The World Factbook. Available: http://www.cia.gov, accessed on 14th December, 2011
[12] Energy Technology Perspectives, IEA/OECD, June 2008
[13] Martín, M.Á.P., 2010. Geo-Economics in Central Asia and the 'Great Game' of Natural Resources: Water, Oil, Gas, Uranium and Transportation Corridors (WP), Real Instituto Elcano (online). Available: http://www.realinstitutoelcano.org, accessed on 14th December, 2011.

ENERGY CONSUMPTION EVOLUTION IN CONSTRUCTIONS DOMAIN FROM ROMANIA

DINU R.C.*, POPESCU N.*, MIRCEA I.*, DINU E.M.**
*University of Craiova, Faculty of Electrical Engineering, Decebal no.105, Craiova
**S.C. ELECTROPUTERE S.A., Calea Bucureşti, no. 80, Craiova
rcdinu@elth.ucv.ro, npopescu@elth.ucv.ro

Abstract: As in a building, it is unthinkable to conduct the main activities, in the absence of energy sources (electrical energy, thermal energy, gas, hot water, fuels, etc.), any consumption reduction-through a more efficient use of energy is reflected positively in the building budget. The less power we consume, the less money we shall pay for it. This think is valid only in the circumstances in that the energy consumption from building are metered, therefore only if we play what we consume. Because the energy is used in a building, in the shape of thermal energy for heating and household hot water preparation, electrical energy (electricity) for lighting and for electromechanical installations supply, the buildings require a certain quantity of energy, indifferent of destination. In this paper, the authors analyse especially the evolution of the energy consumption afferent to civil buildings, that of all goods, have the longest duration of use and participate with a percentage of 30...40% to the primary energy requirement.

Keywords*:* civil buildings, energy consumption, energy sources, metering, evolution.

1. INTRODUCTION

The *energy* is used in a building in the shape of thermal energy for heating and household hot water preparation, electrical energy for lighting and for electromechanical installation supply. The Romania's position in the geographical zone with temperate-continental civilization climate with excessive tints, as well as the current civilization level make about 40% from the primary energy consumed to the country level to be used in the shape of thermal energy for the heating of the public spaces and individual housing and for the consumption hot water production [1]. This percentage justifies the permanent interest given to the heating problem in the Romanian society.

On the line of durable development in constructions, performance levels record a continuous evolution. Thus, irrespective of the heating system type, the average duration of the heating period and the conventional outdoor air temperatures, it was pursued the obtaining of the comfort parameters in the residential, administrative and industrial buildings with specific primary energy consumptions as low, that lead finally to a small percentage of environmental pollution and heating costs bearable for the population.

Where thermal energy is delivered from a specialized production installation, by means of a thermal agent pumped into transport and distribution infrastructure to more consumers, we are dealing with a centralized system of supply with thermal energy (HSSC).

2. BUILDINGS CLASSIFICATION AND HOUSING FUND EVOLUTION [1]

Civil buildings, in that the man is the main user, can be divided into two big categories:

A. residential buildings, hostels, hotels:

a.1. individual buildings (single family homes, coupled, row houses);

a.2. multi-storey buildings with more apartments, buildings of type block of flats;

B. public or tertiary buildings (buildings with other destinations than dwelling houses) such as: hospitals, clinics, nurseries, buildings for educational, social and cultural buildings (theatres, cinemas, museums), public institutions (shops, commercial spaces, firms, offices, banks) and others industrial buildings.

Buildings with other destination than housing may be classified by:

b.1. mode of occupancy into buildings (with continuous occupancy or discontinuous occupancy);

b.2. class of thermal inertia (buildings with big, average or small inertia).

Irrespective of buildings destination, these must satisfy a series of quality requirements, that are basically: resistance and stability, safety in exploitation, safety to fire, hygiene, people's health, restoration and protection of environment, thermal insulation, waterproof insulation, energy savings and protection against noise.

The main constructive systems practiced for existing buildings were the following [3]:

1. Integral prefabricated buildings, with height regime preponderant of 5 levels, but also 9 levels, built between 1960-1990 (about 1.2 million buildings are approximately 37% of all apartments);

2. Buildings with mixed structure, being with frames and reinforced concrete structural walls, exterior walls BCA brick masonry or with prefabricated panels of facede, with height regim of 5 and 9 levels height of 5 and 9 levels;

ISSN 2067-5534 © 2012 JSE

3. Buildings with reinforced concrete walls, made using sliding formworks and strength structure of monolithic reinforced concrete frames, having shops on the ground floor (built in a small number);
4. Buildings with brick masonry structure, with height regime of 2 ... 4 levels;
5. Buildings with walls of wood, adobe (a mixture of straw and earth) or framework.

According to the Statistical Yearbook on January 1, 2000, our country's population was 22.455.000 inhabitants, Romania being situated on an average position in viewpoint of density (94 inhabitants/km^2). Population distribution by age groups indicates the constant process of demographic aging and, implicit, a decrease in occupancy of dwellings from 2.83 persons/dwelling in 2000 to 2.77 persons/dwelling in 201 (table 1) [1].

Table 1 - Evolution of the population and of the dwelling fund

Item	Year	Population forecast [inhabitants]	Occupancy degree forecasted, [persons/housing]	Number of dwellings
1	1995	22.681.000	2,92	7.782
2	2000	22.455.000	2,83	7.923
3	2005	22.800.000	2,80	8.120
4	2010	23.200.000	2,77	8.375

Regarding the dwellings fund evolution in the country, as well as their level of endowment with equipement (table 2 and table 3), it observes a dwellings number increase.

Table 2 - Dwellings d evolution

Item	Year	Number of dwellings		Habitable space	
		[pieces]	[%]	[10^3·m^2]	[%]
1.	Prior to 1980	6.999.000	88,3	236.566	86,9
2.	1981...1985	7.645.000	96,5	233.413	85,8
3.	1985...1990	8.006.000	101,0	146.847	90,7
4.	1991	7.659.000	96,6	258.518	95,0
5.	2000	7.923.000	100	272.039	100

Table 3 - Degree of edowment with electrical and thermal installations, for the residential buildings

Item	Degree of endowment		Medium	
			Urban, [%]	Rural, [%]
1.	Dwellings equipped with central heating systems, characterised theoretically by mears of high energy efficiency		87,00	1,70
2.	Dwellings that are connected to a public network or have proper systems of consumption hot water preparation		92,00	4,80
3.	Dwellings that have:	- cold water	87,00	11,30
		- sewage	86,00	10,00
4.	Dwellings that have electrical connections for lighting and power outlets		93,00	82,40

On the one hand, this is due to the construction of dwellings for young people and families with modest incomes and the construction of dwellings from the population savings. On the other hand, this increase is due to the rehabilitation of a number of residential buildings from the existing dwellings fund, for the comfort standard improving.

In 2010, there were approximately 389 dwellings per 1000 inhabitants, their percentage depending on rooms number, as shown in Figure 1.

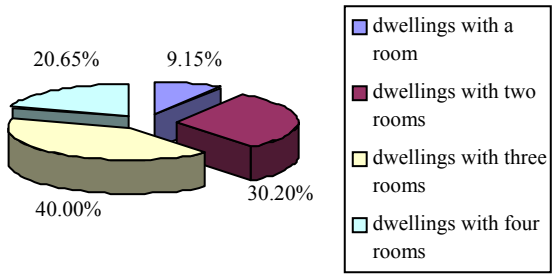

Fig. 1 - Dwellings percentage depending on rooms number in 2010

It is observed that the dwellings with three rooms will be most numerous because they represent a minimum necessary for domestic development, when the purchase of a dwelling will be a problem hard to solve for a good time.

Also the energy consumption in the household sector by 2010 could be divided an classified both fuel type (table 4) and types of dwellings (Figure 2).

Table 4 - Energy consumption in the household sector, by types of fuel

Item	Energy type	U.M.	In the residential sector	
			U.M.	PJ
1.	Solid fuel	10^3· t	6,5	191,6
2.	Liquid fuel	10^3· t	3,8	112,1
3.	Gaseous fuel	10 ·m^3	1,0	34,2
4.	Unconventional energy	PJ	0,7	0,7
	Total	-	-	**338,6**
5.	Electricity	TW·h	7,1	25,6
6.	Centralized heating	PJ	107,3	107,3

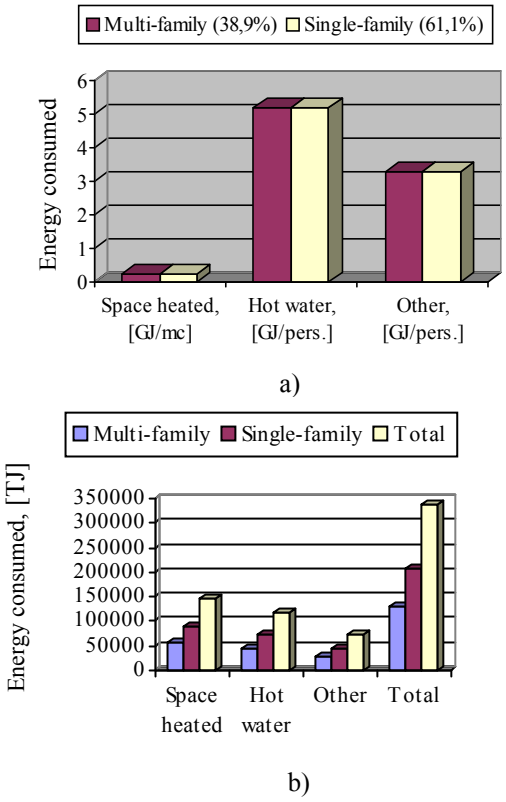

Fig. 2 - Energy consumption by type of housing: a) specific costs expressed in m^3/GJ or GJ/person; b) the total costs, expressed in TJ

3. ENERGY SUPPLY OF BUILDINGS

During cold season, the energy is used for thermal comfort insurance inside. This supposes the realization of a correlation between temperature and humidity. For this, it is necessary a correct heating and ventilation of the house. Otherwise, in the cold season, the dampnes (of walls) and the mildew can form on the walls of bathrooms and massive furniture bodies behind. The humidity can come from outside or onside. The air contains water as vapor. For example, at 0°C the air contains 5g water/m^3, and at 20°C the air can contain can contain 17g water/m^3. The damp air in contact with cold surfaces condenses, leading to gradual walls damping. A damp wall leads of three times more energy towards outside than a dry wall. In addition, the wall material damage appears in time.

Durring warm season, the energy is used for climate maintenance, because it appears the discomfort caused by high temperatures.

To save energy, in both cases it is necessary a correct insulation of the building envelope, both by improving thermal insulation (exterior walls, windows, roof, basement) and by maintaining of the heating and air conditioning installation in the good condition of operating. Lately, the climate maintenance installation number has increased much, and so the electrical consumption afferent to buildings.

It asks the question which is the percentage of the expenses and of the energy costs, in the invoice for the comfort level insurance for diverse buildings types and different energy supply systems (figure 3, 4 and 5) [2], [7].

Apartments (1)	
Heating (blue)	40,47 %
Household hot water (red)	35,48 %
Food preparation (yellow)	15,54 %
Lighting and labour saving devices (violet)	8,51 %
TOTAL	***100,00 %***
Row housing, coupled (2)	
Heating (blue)	41,62 %
Household hot water (red)	35,03 %
Food preparation (yellow)	15,23 %
Lighting and labour saving devices (violet)	8,12 %
TOTAL	***100,00 %***
Individual houses (3)	
Heating (blue)	53,40 %
Household hot water (red)	27,18 %
Food preparation (yellow)	11,89 %
Lighting and labour saving devices (violet)	7,53 %
TOTAL	***100,00 %***

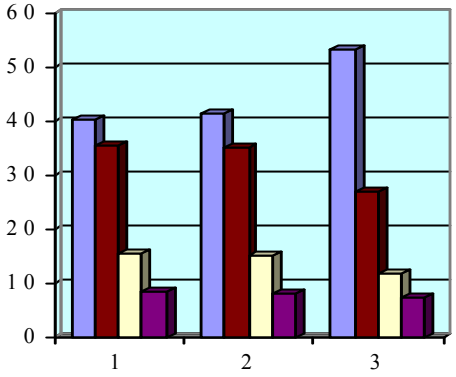

Fig. 3 - The share of activities in the energy invoice for buildings supplied in the centralized system

Apartments (1)	
Heating (blue)	49,82 %
Household hot water (red)	20,58 %
Food preparation (yellow)	19,13 %
Lighting and labour saving devices (orange)	10,47 %
TOTAL	***100,00 %***
Row housing, coupled (2)	
Heating (blue)	50,77 %
Household hot water (red)	20,43 %
Food preparation (yellow)	18,58 %
Lighting and labour saving devices (orange)	10,22 %
TOTAL	***100,00 %***
Individual houses (3)	
Heating (blue)	62,32 %
Household hot water (red)	15,02 %
Food preparation (yellow)	13,88 %
Lighting and labour saving devices (orange)	8,78 %
TOTAL	***100,00 %***

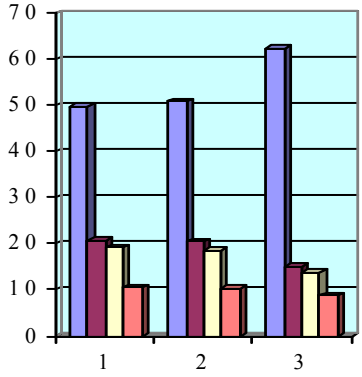

Fig. 4 - The share of activities in the energy bill for buildings equipped with its own thermal power plant

ISSN 2067-5534 © 2012 JSE

Row housing, coupled (1)	
Heating (blue)	61,19 %
Household hot water (red)	4,85 %
Food preparation (yellow)	22,39 %
Lighting and labour saving devices (orange)	11,57 %
TOTAL	***100,00 %***
Individual houses (2)	
Heating (blue)	73,09 %
Household hot water (red)	3,65 %
Food preparation (yellow)	16,28 %
Lighting and labour saving devices (orange)	6,98 %
TOTAL	***100,00 %***

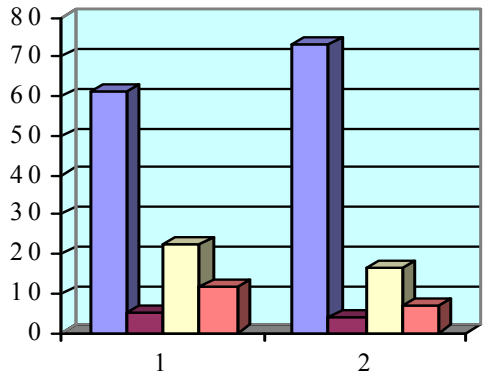

Fig. 5 - The share of activities in the energy bill for buildings equipped with stoves for heating

In all cases, the main percentage of the expances for the energy services of the dwellings is owned by heating costs, irrespective of heat supply system type and of dwellings type (table 5).

Table 5 - Percentage of the expances for the energy services of the dwellings

Energy consumption type	Apartament	Row housing, coupled	Individual house
Dwelling heating	45,15 %	51,18 %	62,94 %
Lighting and labour saving devices	9,49 %	9,97 %	7,74 %
TOTAL	**54,64 %**	**61,15 %**	**70,68 %**

These data are different from one geographical zone to another, from one family to another, being influenced by dwelling endowment and standards of living, implicit by family incomes.

At the national level, the average annual global consumption in Romania has decreased from 2,7 TEP/dweller in 1990, to 1,8 TEP/dweller in 2010, the world average being of 1,76 TEP/dweller. The power consumption is approximately 2000 kWh/(dweller·year), in that domestic consumption is of 340 kWh/(dweller·year) [5]. Comparative with the world level, this represents average value.

4. ENERGY IMPACT ON THE ENVIRONMENT

The correlations that exist between energy and environment are known. In all processes of exploitation, conversion, transport, distribution and utilisation of the all forms of energy, the environment is affected. The substances that result from these processes pollute chemically, visually, electrically, magnetically and sonorously the environment generally, but the living persons too (people, plants, animals). The chemical substances resulted from the fuels combustion (CO_2, CH_4, NO_x, SO_2) are the glass-house effect cause, that leads to the increase temperature environment.

For Romania, the emissions of CO_2 are about 5,2 tonnes/(dweller·year) and at the European Union's level these are of 7,3 tonnes/(dweller·year) [3].

The mode of solving this problem is provided in International Conventions, European Union and national development strategies.

A problem that was given its importance and less attention is given to it, is the problem of the forest that can counterbalance the emissions of CO_2. Both at world level and national, the forests have been cut down mercilessly and without judgment. In addition to climate influences, the forests lack produce soil erosion too. For example, in Dolj district the forests represent less than 45% as compared with the area in 1945 [7]. The forests have been cut before 1990 and after land appropriation. It was not planted and do not plant anything. In these circumstances, the process of desertification of the area south of Oltenia tends to enlarge to Craiova. Urgent measures and programs for reforestation are required, and the population must has an active rol. For this, campaigns of population informing on the effects that feel and see through the severe drought it the zone, in recent years, are necessary. The zones, the areas and the species that will plant, must be identified.

The environment problem must seen through respecting of the following principles [4]: the polluter has responsibility and he pay; the implementation of the environment politics in the main directions of activity (agriculture, industry, energy, transports, tourism, habitat and social life); the increase of the role of participation of the population, of the non-governmental organizations and associations, of local authorities to taking of decisions; the evaluation of the human activity impact on the environment; the subsidiarity principle – the actions undertake by the more efficient persons, in the prior directions and in the places with maximum effects; the development of the information, of the education, of the dialogue and of the transparency.

We will not insist on the known measures that must be followed, but we will insist on the necessity of the urgement and of the application of these measures.

The building as a medium [5]. As how it was mentioned, in the spaces of dwett but in those too in that different activities (education, health, culture, management, industry) are in progress, the realization of a microclimate (thermal, visual, olfactory and auditory comfort) is necessary for the assurance of a good productivity of the activity that is in progress. In an ailing building, a normal activity with healthy people cannot be in progress.

The lack of heating generates low-temperatures, humidity, dampness of walls, mildew, there fore culing buildings. These produces discomfort (stress), but also diseases (rheumatism, cardiovascular ailments, ailments of

the breathing apparatus), leading to the decrease of the intellectual work capacity of the pupils and of the students (in the education spaces and at home), to the decrease of the physical and psychic recovery capacity of the which stay in the ailing buildings. In addition, the diseases lead to the increase of the medicines consumption, of the hospitalization days number, of the sick leaves days number, of the number of those who are pensioned ahead of term. Last but not least, the work capacity and therefore yhe production achieved decrease. The investment made in the educational and professional preparation of the people cannot recover.

It imposes a financial analysis at the macroeconomic level, so at the national level, that to compare the expenses from accounting with the health problems, with the funds that would spend for the improvement of the system of supply with electric energy necessary for the dwellings heating.

It is therefore necessary both a quantization of the supplement ary health expenses, because of the thermal comfort lack (the buildings heating), and their comparison with those for the ailing buildings recovery.

Also, it is imposes an attentive analysis to the use of the actual decentralised systems of climatizing, to the efficiency and the costs of these systems, for a more responsible use of their own, therefore for the electrical energy consumption decrease. Projects for the complex three-generated installations use (electrical energy, thermal energy and cold) at the important buildings (hospitals, space of education, administration, banks) can make.

Also, it is imposes a more attentive analysis of the manner of calculation of the expenses for heating, taking dwelling blocks particularities into account, in the first time. Indifferent by mode of heating of the blocks, to the expenses calculation well must be taken into account the norms of heating requirement calculation, from that the supplementary surfaces of the heating devices result for the flats from the certain positions (the last floor, ground floor, corner, north). These assure the comfort for those which dwell in the rest of the flats. One thing is clearly, simply, knew and that must be taken into account as to the calculation of the repartition of thermal energy consumed for heating.

The manner of assurance of the funds for thermal rehabilitating of ailing buildings is an important problem that must be considered. It is known that a good part of families, which in blocks of flats, are poorly and do not have money to pay for the energy consumption. They unplug and in this way the temperature into buildings decrease, with implications on the health condition. So in the future will must found ways through that the money necessary to the buildings treatment to be assured from the actual funds of subsidization of the heating, for these families.

Also, concrete legislative and financing solutions will must found for the use of the regenerative energy sources, that to cover a part of the electrical and thermal energy requirement. All these will lead to a decrease of the global energy requirement and therefore to the decrease of the reccurency effort for the importation of energy.

5. FACTORS THAT INCLUDE THE IMPACT OF THE ENERGY EFFICIENCY MEASURES

Since 1989, the international organizations have tried to implement the energy efficiency projects in Romania. In spite of the important financial efforts, the energy efficiency measures have not always had the expected social impact.

There are more factors that have contributed to this, of that the most important factors were [3]: the relative decreased price of fuels; the relative decrease price of the energy; until recently, the population was not awarely of the energy saving necessity; energy saving methods are not knew; in the case of the buildings connected to the cogeneration system, a direct connection between the consumed thermal energy (for heating and in the form of householding hot water) and the costs paid for this consumptions was not existed; at the governmental level, a coherent politics of supporting of the energy efficiency measurement was not existed; the beneficiaries dispose not of funds for the energy efficiency measurement application.

An analysis of the view of development of the systems of supply with thermal energy produced centralized in Romania, must take account of the following main factors [2], [6]:

1) Factors of local-zone nature: - The present situation from point of view of the consumer supply with heat; - The technical state, the remanent lifetime and the economical performance of the system of supply with heat; - The type of the consumers from zone from point of view of the electrical energy and heat requirements structure and of the evolution of these requirements in the near, average and long duration perspective; - The social-economic situation of the consumers, under the aspect "of the financial capability" of payment of the energy view; - The present situation and the primary energy resources evolution in perspective, from point of view of the classical fuels used in the perspective, of the industrial energy waste and/or urban reusable energy waste products, of the reusable energy resources available in the zone.

2) Factors of macro-economical nature: - Policy looking to the primary energy resources usable at the level of the country and of the diverse specific geographical zones;- The property forme looking to the existent and perspective sources of supply with heat and possible with electrical energy, at the level of the objective analysed in the present and in perspective; - *The tariff policy looking to: the* fuel consumed by diverse categories of consumers, the electrical energy produced by the power plants belonging to state and the electrical energy produced by the sources of the auto-producers or of the independent producers, the heat produced from point of view of the local tariffs adoption on characteristical types of the consumers; - The legislation and the clear and undiscriminator settlements for the all energy producers (irrespective of their property form) from the energy domain, that refer to the electrical and thermal energy market existence and to the access to this – the consumers

limit in the supplier choise, the transparance at the specific production costs establishment for the all energy producers, the undiscriminator tariffs for the same consumers types and the same conditions of consumption

ISSN 2067-5534 © 2012 JSE

of the fuels and of the sold energy; - The ensemble energy policy of the country, with the emphasizement of the cogeneration domain policy materialized through: the position under the aspect of the cogeneration (keeping into account of hers advantages: the environment pollution decrease in the energy production domain and th total energy invoice decrease at the consumers), the position under the investors aspect (keeping into account of taxes, fees and creating a climate of long – term financial stability by order of 15…20 years, specific to investments in the energy domain).

6. CONCLUSIONS

In life, therefore in the life of a building too, nothing can be concepts without energy. But, the human development generates paradoxes (the life standard improvement requires the energy consumption increase, that in the context of ENERGY – ENVIRONMENT – CONSUMER threatens the human health and the global economy). In addition, the interest for the energy (oil) generates conflicts (1973, 1991, 2003). For that, it is necessary the application of some principles balanced in the energy domain: accessibility, availability (quantity, quality), acceptability.

People must do something, not wait for the disaster. An educated and informed man can have an important contribution to the energy saving. In this action of energy saving, therefore of environmental protection, all people must insolve, especially children on which we must teach them to value the energy and to respect the environment. For this, the projects of information are required for to tell us what we do to save the energy and for to have a clean environment and saving money.

For energy saving, global strategies are required and they must involve the energy and the environmental and must made from to familial level, dweller association, locality, until national and international level.

Acknowledgment

"This work was partially supported by the strategic grant POSDRU/CPP107/DMI1.5/S/78421, Project ID 78421 (2010), co-financed by the European Social Fund – Investing in People, within the Sectoral Operational Programme Human Resources Development 2007-2013."

REFERENCES

[1]. Sârbu, I., Kalmar, F. - *Optimizarea energetică a clădirilor,* Editura MatrixRom, Bucureşti, 2002.

[2]. *** - COM(2002) 415 final – Directive of the European Parlament and of the Council – on the promotion of cogeneration based on a useful heat demand in the internal energy market, Bruxelles, 2002.

[3]. Mircea, I., Ruieneanu, L., Dinu, R.C. - Îndrumar pentru eficiența energetică a clădirilor, Editura Universitaria, Craiova, 2003.

[4]. Cerna, M., ș.a.. - Eficiența energiei în clădiri – situația în România şi acquis-ul comunitar, Masă rotundă - "Eficiența energetică, prioritate națională şi factor de integrare", București 28 august 2003.

[5]. Radu, A., ș.a. - Satisfacerea exigențelor de izolare termică şi conservare a energiei în construcții, Editura Societății Academice Matei-Teiu Botez, Iaşi, 2003.ș.a., Satisfacerea exigențelor de izolare termică şi conservare a energiei în construcții, Editura Societății Academice Matei-Teiu Botez, Iaşi, 2003.

[6]. *** - Foaie de parcurs în domeniul energetic din România, aprobată prin HG nr.890/29.07.2003.

[7]. Mircea, I., Dinu, R.C. - Locul clădirilor în contextul interacțiunii energie-mediu-consumator, Conferința „Instruire în utilizarea noilor tehnologii de informații şi comunicații cu aplicații în domeniul energetic", Craiova, 25 noiembrie, 2005.